



Australian Government

Geoscience Australia

Post-cruise Report

NSW Continental Slope Survey

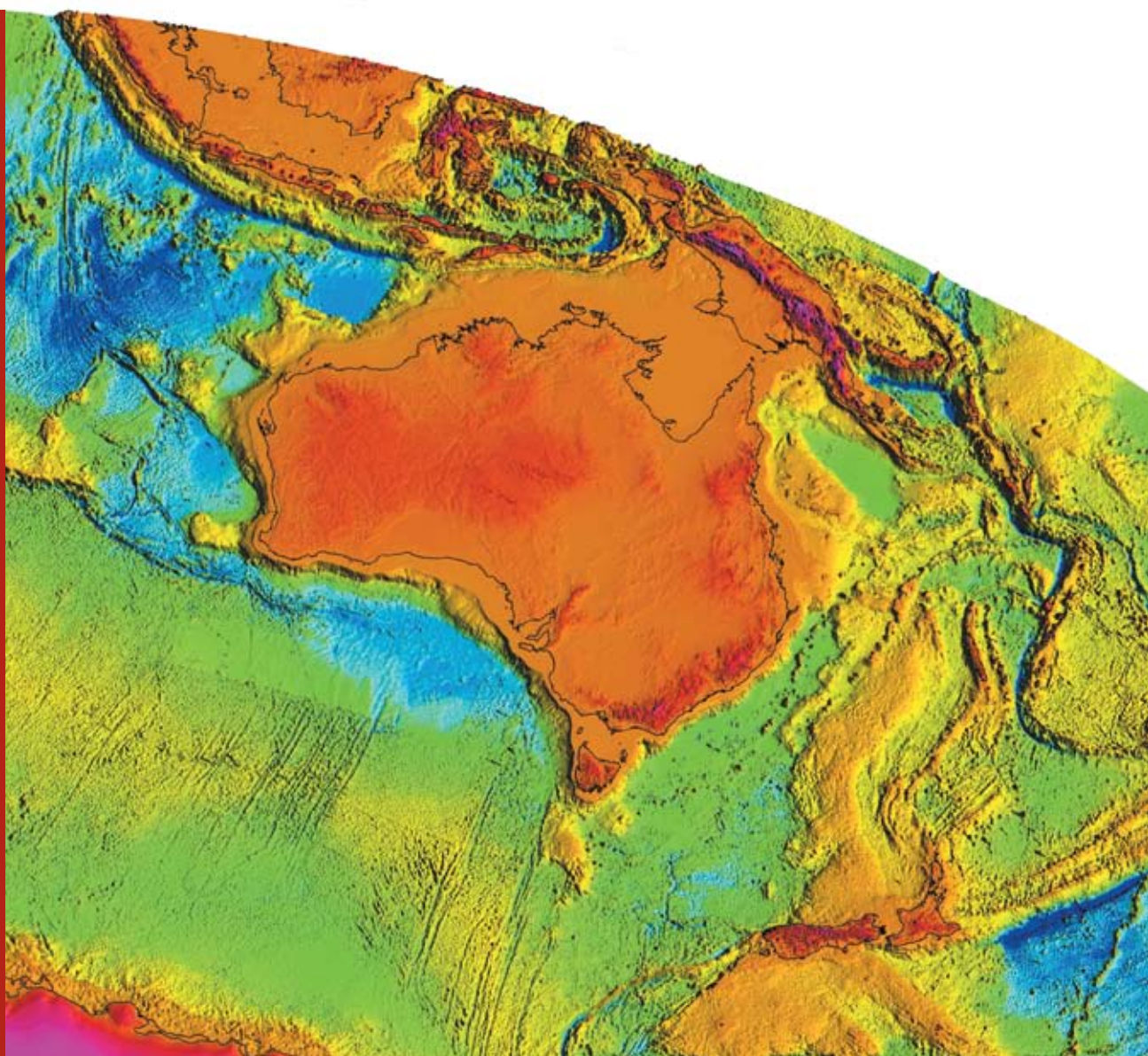
RV Southern Surveyor 10/2006

October 2006

*Kriton Glenn, Alix Post, Jock Keene, Ron Boyd, Leharne Fountain,
Anna Potter, Monica Osuchowski, Nicholas Dando, and Shipboard Party*

Record

2008/14



Post-cruise Report

NSW Continental Slope Survey

RV Southern Surveyor 10/2006

October 2006

Glenn, K. C.¹, Post, A.¹, Keene, J.² Boyd, R.³, Fountain, L.¹, Potter, A.¹,
Osuchowski, M.¹, Dando, N.¹, and Shipboard Party

¹*Geoscience Australia, GPO Box 378, Canberra, ACT 2601*

²*The University of Sydney, NSW 2006*

³*University of Newcastle, University Drive, Callaghan NSW 2308*



Australian Government

Geoscience Australia

Department of Resources Energy and Tourism

Minister for Resources Energy and Tourism:

The Hon Martin Ferguson, AM MP

Secretary: Dr Peter Boxall, AO

Geoscience Australia

Chief Executive Officer: Dr Neil Williams, PSM

© Commonwealth of Australia 2008. This work is copyright. You may download, display, print and reproduce this material in unaltered form only (retaining this notice) for your personal, non-commercial use or use within your organisation. Apart from any use as permitted under the Copyright Act 1968, all other rights are reserved.

DISCLAIMER

The views and opinions expressed in this publication are those of the authors and do not necessarily reflect those of the Australian Government.

While reasonable efforts have been made to ensure that the contents of this publication are factually correct, the Commonwealth does not accept responsibility for the accuracy or completeness of the contents, and shall not be liable for any loss or damage that may be occasioned directly or indirectly through the use of, or reliance on, the contents of this publication.

ISSN: 1448 - 2177

ISBN: 978 – 1 – 921498 – 02 – 2 (Hardcopy)

978 – 1 – 921498 – 01 – 5 (CD-ROM)

GeoCat No. 65699

Bibliographic reference: Glenn, K.C., Post, A., Keene, J., Boyd, R., Fountain, L., Potter, A., Osuchowski, M., and Dando, N. (2008). *NSW Continental Slope Survey – Post Cruise Report*. Geoscience Australia, Record 2008/14, 160pp.

Correspondence for feedback:

Sales Centre

Geoscience Australia

GPO Box 378

Canberra

ACT 2601

Sales@ga.gov.au

Table of Contents

List of Figures	vi
List of Tables	vii
Executive Summary.....	viii
1. Introduction.....	1
1.1. Background	1
1.1.1. Study Area	1
1.1.2. Survey Objectives	1
1.1.3. Previous Studies	2
1.1.4. Regional Setting	4
1.1.5. Submarine Slope Failure and Tsunami Hazard	9
1.2. Survey Participants and Vessel	12
1.2.1. Vessel Description	12
1.2.2. Scientific Personnel	12
1.2.3. Ship's Crew	13
2. Methods.....	14
2.1. Equipment and Processing.....	14
2.1.1. Swath (multi-beam) Sonar	14
2.1.2. Oceanography and Meteorology	14
2.1.3. Sub-bottom Profiling	14
2.1.4. Echo-Sounder	17
2.1.5. Seismic.....	17
3. Sedimentology.....	18
3.1. Sample Acquisition	18
3.1.1. Sub-Surface Sediment Samples	18
3.2. Sample Preparation, Measurement and Results	18
3.2.1. Grainsize	18
3.2.2. Density	19
3.2.3. Multi Sensor Core Logger (MSCL)	20
3.2.4. Geotechnical Testing.....	20
3.2.5. Composition	21
3.2.6. Digital Video Footage	22

4. Results and Analysis	24
4.1. Introduction	24
4.1.1. Seismic Reflection Profiles.....	25
4.1.2. Sub-bottom profiles	26
4.1.3. Geomorphology.....	26
4.1.4. Sediment cores	27
4.1.5. Biology	29
4.1.6. Underwater video tow	29
4.2. Jervis Bay Region	29
4.2.1. Results from geomorphic interpretation	30
4.2.2. Discussion of geomorphic interpretation	32
4.3. Sydney / Illawarra region.....	32
4.3.1. Seismic Profiles.....	33
4.3.2. Analysis of High Resolution TOPAS Data	46
4.3.3. Geomorphology.....	50
4.3.4. Sediment Cores	59
4.4. Hunter Region	60
4.4.1. Seismic Analysis	63
4.4.2. Analysis of High Resolution TOPAS Data	68
4.4.3. Geomorphology.....	70
4.4.4. Sediment Cores	75
4.5. Myall Region	77
4.5.1. Seismic reflection profiles	80
4.5.2. Analysis of High Resolution TOPAS Data	86
4.5.3. Geomorphology.....	91
4.5.4. Sediment Cores	93
4.6. Manning Region	95
4.6.1. Geomorphology.....	95
5. Discussion	98
5.1. Regional Synthesis.....	98
5.1.1. Seismic Data from the Central NSW Slope	98
5.1.2. Sedimentation and Stability on the Central NSW Slope	102
5.2. High Risk Areas for Future Submarine Landslides.....	106
6. Conclusions	108
7. Acknowledgements.....	110
8. References	111

9. Appendices	117
9.1. Appendix A: Availability of Survey Digital Data.....	117
9.1.1. Sub-bottom Profile Data	117
9.1.2. Multi-beam Data	117
9.2. Appendix B: Video Commentary	118
9.3. Appendix C: Visual core logs.....	121
9.4. Appendix D: XRD and PIMA Results.....	135
9.5. Appendix E: Geotechnical Data.....	139
9.6. Appendix F: Radiometric Data.....	154
9.7. Appendix G: Seismic Data.....	156

List of Figures

Figure 1.1 Regional map of survey location zones	2
Figure 1.2 Previous seismic surveys within the study area.....	3
Figure 1.3 Distribution and magnitude of earthquakes in study area.....	8
Figure 1.4 Interpreted slumps on the continental margin in the study area.	11
Figure 4.1 The five regions of the study area	24
Figure 4.2 Location of seismic lines acquired in the survey area.....	25
Figure 4.3 Location of sub-bottom profile (TOPAS) lines	26
Figure 4.4 Location of sediment core sites and video transect of the survey	27
Figure 4.5 Jervis Bay Region.....	30
Figure 4.6 Sydney / Illawarra Region.....	33
Figure 4.7 Seismic Line 1	34
Figure 4.8 Seismic Line 2	38
Figure 4.9 Seismic Line 3	38
Figure 4.10 Seismic Line 4	41
Figure 4.11 Seismic Line 5	42
Figure 4.12 Seismic Line 6	44
Figure 4.13 Location of TOPAS transect across the Bulli and Shovel slides	47
Figure 4.14 TOPAS profile across the shovel slide	49
Figure 4.15 Overview location of the Shovel slide and Bulli slide	50
Figure 4.16 Location of Bulli basement block, and the Shovel and Bulli slides.....	51
Figure 4.17 Hunter Region	61
Figure 4.18 Zoom extent of 'Figure 5' within Figure 4.17.....	62
Figure 4.19 Zoom extent of 'Figure 6' within Figure 4.17.....	62
Figure 4.20 Core sites within the Hunter Region	63
Figure 4.21 Seismic Line 11	64
Figure 4.22 Seismic Line 10	67
Figure 4.23 Seismic Line 9	67
Figure 4.24 Location of TOPAS transect in the Hunter Region	69
Figure 4.25 Profile across two of the dewatering channels	70
Figure 4.26 Myall Region.....	77
Figure 4.27 Location of TOPAS line transects.....	78
Figure 4.28 Location of seismic lines in the Myall Region	78
Figure 4.29 Bathymetry contours and seismic line in the Myall Region.....	79
Figure 4.30 Location of core sites in the Myall Region	80
Figure 4.31 Seismic Line 8	80
Figure 4.32 Seismic Line 7	82
Figure 4.33 Buried slump features upslope from the Yacaaba Slide	88
Figure 4.34 Profile across the Yacaaba Slide.....	88

Figure 4.35 Strong basement reflection extends beneath the Yacaaba Slide89

Figure 4.36 Basement reflection downslope of the Yacaaba Slide89

Figure 4.37 Profile across Birubi Slide90

Figure 4.38 Location of the Manning Region96

List of Tables

Table 4.1 Overview of Core Data Results.....28

Executive Summary

The October 2006 Continental Slope Survey was completed on behalf of Geospatial & Earth Monitoring Division by the Marine and Coastal Environment Group, Geoscience Australia on RV Southern Surveyor. This survey forms part of an ongoing cross agency project that is assessing high risk areas along the Australian continental slope which have the potential to generate tsunamigenic submarine slides. Its primary regions of interest were adjacent to coastal population centres and critical infrastructure.

The data sets from this survey indicate that significant areas of the central NSW continental slope have been prone to sediment mass wasting over time. Critical factors which contribute to slope failure include basement geometry, angle of slope and thickness of overlying sediment. Evidence of slope failure are observed through: surficial tension cracks; creep features; faulting; redistribution of sediments, multiple relict slides buried on the sea floor and erosional surface scars of slides such as the Bulli (~20 km³), Shovel (7.97 km³), Birubi (2.31 km³) and Yacaaba (0.24 km³).

Radiometric dating of the slides proved challenging as none of the cores acquired appeared to penetrate the un-failed surface. Therefore, exact failure dates could not be determined. The youngest date recorded was 3700 years BP.

The preliminary findings in this report are based on 23 200 km² high resolution bathymetry (~9200 km² acquired from this survey), 3414 line kms of sub-bottom profiles, 340 line kms of seismic and 14 gravity cores. Based on the seismic data there are two distinct types of gravity slides on this margin: those related to the sediment bedding planes in the Cainozoic sediment wedge and those that are related to the critical dynamics of the seaward face of volcanic highs, basement slope and sediment thickness. Future failures may also exhibit these relationships and be characterised by sections of relatively steep unsupported Cretaceous / Cainozoic sediments.

Taking these factors into consideration and assessing the location of significant un-failed sediment accumulations, a preliminary prediction can be made about the location of high risk areas for future slides. These high risk areas contain complex features that often have a composite, multiphase history which can be divided into two types:

Sediment seaward of basement highs:

- Two sedimentary blocks, seaward of Sydney.
- The unfailed sediment on seaward face of volcanic high immediately south of Bulli slide.

- The unfailed sediment on seaward face of inferred volcanic/plutonic high in Jervis Bay region.

Sediment wedge:

- Existing sites in the Hunter region
- The unfailed section of sediment wedge immediately south of the Shovel Slide
- The undercut, unfailed area on the boundary of the Myall and Manning regions

This survey provides valuable information that computer modellers and software engineers within the Risk and Impact Analysis Group can use to assess the tsunamigenic potential of pre-existing and potential submarine slides and their implications for coastal communities and infrastructure. Upon completion of this modelling work, priorities for future surveys that assess the stability of other continental slope areas along the Australian continent will be assessed.

1. Introduction

This report contains the preliminary results of Geoscience Australia survey in the Pacific Ocean off the New South Wales coast in water depths of 150 to 4000 metres. The survey focused on an area between 31°50'S and 35°20'S and 150°55'E to 153°20'E.

1.1. BACKGROUND

Historically, there have been few research surveys undertaken along the NSW continental slope. The disparate existing datasets from these surveys focus primarily on the shelf, with limited data capture across the continental slope. The seismic and sedimentary data collected from the shelf and slope environments provides a geological framework within which the seismic and sedimentary data from the current survey can be interpreted. This context, including the structure and evolution of the margin and its subsequent sedimentary regimes, are summarised in this chapter. These datasets also provide some insight into the nature of mass wasting on the slope. Jenkins and Keene (1992) showed that the Cainozoic sedimentary sequence has undergone slumping or mass wasting geologically recently (possibly Quaternary).

1.1.1. Study Area

The survey was carried out along the New South Wales continental slope. The southern extent of this survey is adjacent to Jervis Bay and the most northern extent is at the Manning River east of Taree. Data was collected in water depths ranging from 150 m to over 4000 m and between 20 and 100 km off shore from Jervis Bay and Newcastle respectively ([Figure 1.1](#))

1.1.2. Survey Objectives

The scientific survey objectives were to assess the physical nature of the NSW continental slope, to improve the understanding of the surficial and subsurface structure of the slope and to investigate the history of sediment movement along and down the continental slope.

Several specific tasks were adopted to fulfil the objectives of the survey and were designed in order to reveal the timing and extent of sediment movement. Each survey area was first imaged utilising swath and sub bottom profiles. Once this data was acquired, it aided the selection of sampling sites for side scan, seismic acquisition and physical sampling that included gravity cores.

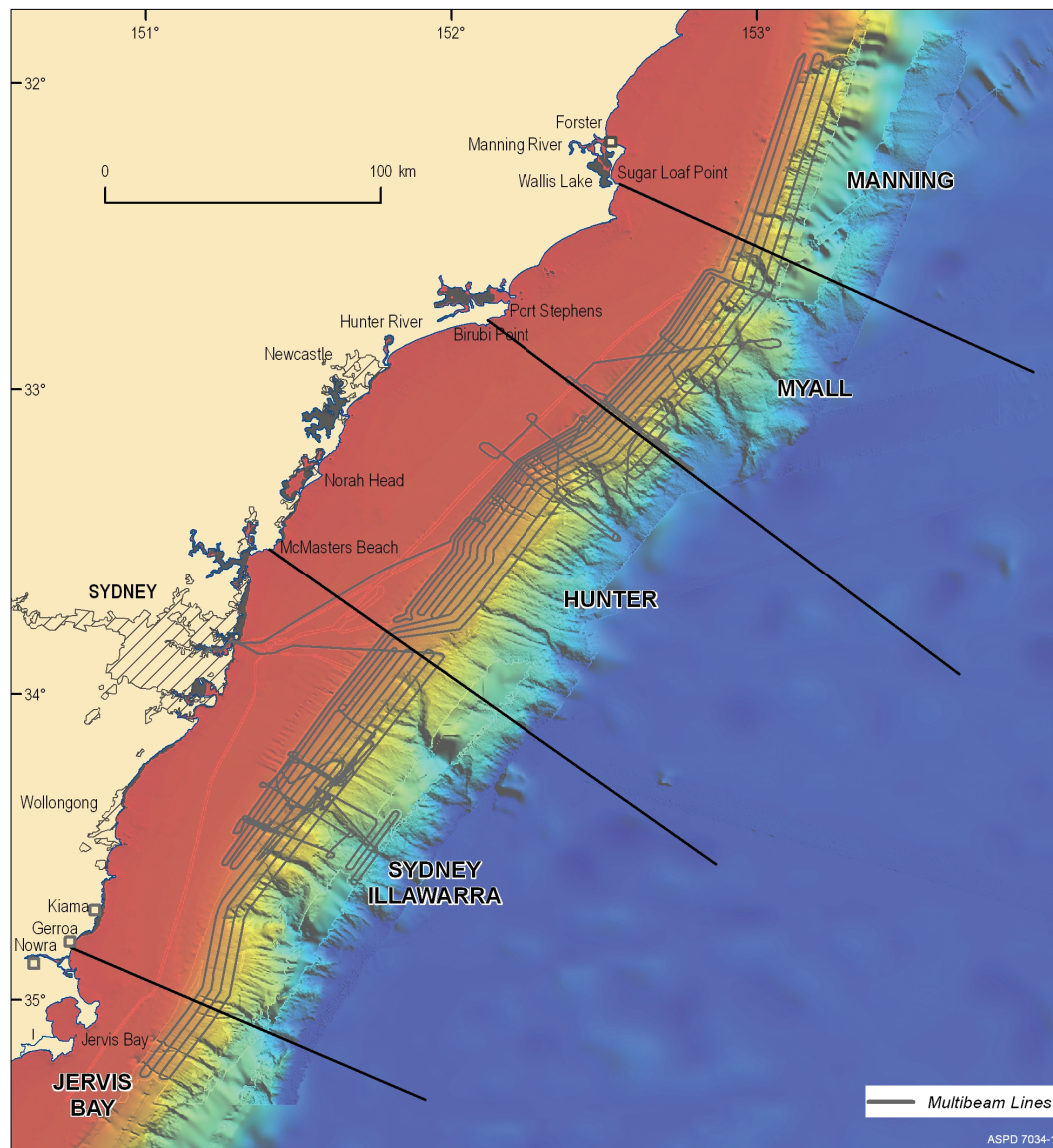


Figure 1.1 Regional map of survey location zones

1.1.3. Previous Studies

Several seismic surveys have acquired data offshore of the central NSW coast (Figure 1.2). Detailed surveys include the 1991 Seaspray survey and the Offshore Sydney Basin 1981 seismic survey. These two surveys have been reprocessed by Bounty Oil and Gas (Daytona Energy and Bounty Oil and Gas, 2001). The average line spacing for these surveys is 8-10 km E-W and ~5 km N-S. Additionally, an extensive survey along the entire NSW coast was conducted by the Bureau of Mineral Resources (BMR) in 1972. This survey (BMR Continental Survey 12) has an average N-S line spacing of 37 km, but data quality was often poor, and no digital seismic records exist. The seismic lines in the southern section of BMR Survey 12 do not reach the abyssal plain, as a result, no displaced sediment masses are observed on the southern section of

the margin. The northern seismic lines that reach the abyssal plain cross the margin where no significant upper wedge failure has occurred. Lines 1 and 2 of BMR Survey 68 (Gippsland Basin Survey) also provide some coverage at the southern end of the study area, extending onto the abyssal plain. In the northern part of the study area Australian Geological Survey Organisation (AGSO) Survey 112 was conducted by AGSO, Sydney University and NSW Department of Mineral Resources in 1992 (Bickford et al., 1992). Boomer and airgun data were obtained across the shelf. The boomer data were of poor quality with a typical vertical resolution of ~ 6 m and a maximum penetration of only 50 m. The airgun results gave good penetration (150 m) with a vertical resolution of 6-8 m. Thirteen airgun lines were collected between Wollongong and Foster in water depths ranging from 27 to 3000 m.

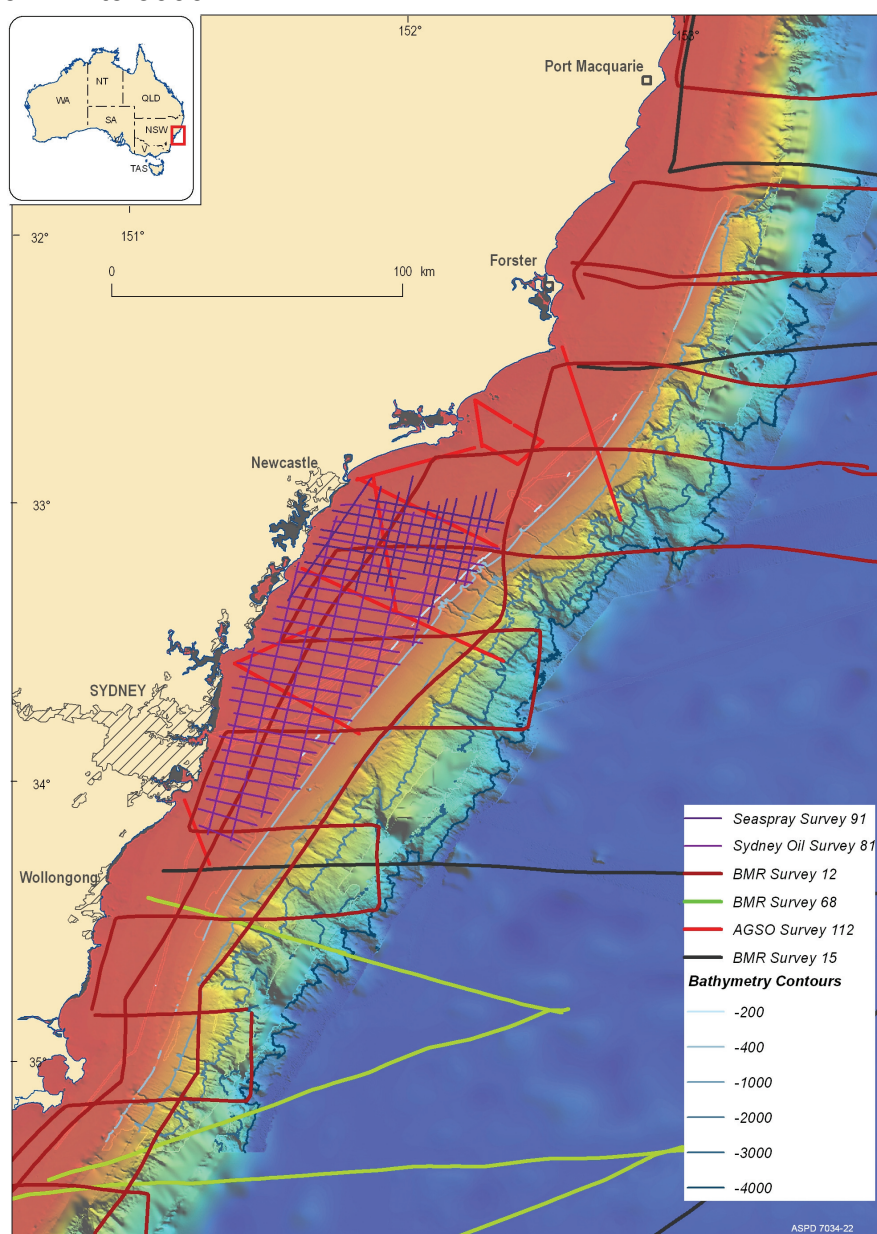


Figure 1.2 Previous seismic surveys within the study area

Sampling and dredging has also been conducted to: investigate the development of the eastern Australian continental margin (Hubble et al., 1992); to determine the nature of sediments along the continental margin (Davies, 1979; Marshall, 1980; Hubble and Jenkins, 1984; Lane and Heggie, 1993; Troedson and Davies, 2001; Boyd et al., 2004); to reconstruct the Quaternary history of this region (Colwell and Roy, 1983; Bickford et al., 1993; Ferland et al., 1995); to determine the nature and origin of sediment masses associated with slope failures (Jenkins and Keene, 1992); to explore for heavy mineral sands (Colwell and Roy, 1983; Bickford et al., 1993; Browne, 1994); to investigate the distribution and dispersal of metallic and organic contaminants (Bickford et al., 1993); and, to understand the formation of Quaternary phosphorites on the NSW upper slope (O'Brien and Heggie, 1990). The key findings of these studies are summarised below.

1.1.4. Regional Setting

The NSW continental margin has been previously described as a typical 'passive' margin which developed in the Late Cretaceous and Paleogene due to rifting and break-up between Australia and the Lord Howe Rise / Dampier Ridge (Hayes and Ringis, 1973; Weissel and Hayes, 1977; Shaw, 1978). For the central NSW margin, spreading appears to have been in a northeast-southwest direction, which is oblique to the present-day shelf and slope (Shaw, 1978). The basement structure appears to largely control the location of the shelf break, which tends to vary between water depths of 130 to 170 m (Jones et al., 1975; Davies, 1979). The nature and age of these basement rocks are largely unknown, with a limited number of dredge and core sites.

Rocks dredged from the continental slope off Sydney yielded Palaeozoic basement rocks consisting of argillites and metavolcanics which represent thin-bedded turbidite and volcanogenic facies (Bickford et al., 1992). Additional insight into the nature of the basement can be gained from coastal outcrops. Coastal outcrops of the Lachlan Fold Belt along the NSW coast south of the Sydney Basin, consist of Devonian and Ordovician conglomerates, quartzites, greywackes, slates and volcanics (Hubble et al., 1992). Dredge samples from the continental slope off southern NSW indicate that the Late Silurian or Early Devonian lithologies extend offshore.

Sediments of the Sydney Basin appear to extend beneath the shelf between 32° and 35°S. These sediments consist of at least 6 km (and possibly up to 9 km) of Permo-Triassic marine and non-marine sequences of sandstone, mudstone, shale, coal and basalt (Stewart and Alder, 2001). Deposition in the Sydney Basin was largely driven by foreland thrust loading initially directed from

the east and later from the north to north-east (Maung et al., 1997). The Early Permian sequences are derived from marine sedimentation, with fluvial sediments and coal measures thereafter. It is generally agreed that sedimentation continued through the Jurassic and Early Cretaceous, but uplift in the Late Cretaceous associated with the opening of the Tasman Sea led to massive erosion which removed these sequences from the onshore sections (Alder et al., 1998). Post-rift rocks contained in dredge samples from the continental slope are dominated by non-calcareous shallow marine mudstones of Late Cretaceous age and calcareous marine greensands which are Paleocene in age (Bickford et al., 1992). A dredge sample collected from ~3300 m on the continental slope off Sydney provides further evidence for continued marine sedimentation in a shallow (<20 m) warm temperate marine setting during the Early Paleocene (Quilty et al., 1997). During Tasman Sea rifting, extensional normal faulting was superimposed on pre-existing structures in the Basin.

The New England Fold Belt outcrops on the coast north of Newcastle and consists of Carboniferous sandstone, conglomerates and lavas (Davies, 1979). Echo-sounder data collected in 1100 m water offshore Newcastle reveal a series of seafloor structures up to 30 m high (Bickford et al., 1992). The pinnacles overlie two inferred igneous bodies suggesting that the structures represent igneous dykes.

1.1.4.1. Margin sedimentology

The margin along southeastern Australia is characterised by very slow sedimentation. Sedimentary deposits are generally no more than 0.5 s TWT, or ~500 m (Conolly, 1969; Ringis, 1972). This thin cover reflects the low terrigenous input, lack of suitable accommodation space, strong reworking by the northward longshore drift and southward sediment transport by the East Australian Current (EAC). Longshore drift is thought to have a greater effect on sediment transport than the EAC (Short and Trenaman, 1992). As a result of this low sedimentation, basement is exposed over 30% of the lower continental slope on the margin (Bickford et al., 1992).

Thicker Quaternary sedimentary sequences (> 15 m thick) are preserved in isolated patches along the inner shelf as shelf sand bodies, flood tidal deltas, valley-fill sequences and drowned barrier complexes (Bickford et al., 1992). These sequences overlie a sedimentary wedge that thickens towards the shelf break (Davies, 1979). The thickness of this wedge ranges from 0.3 s TWT (~270 m) at the shelf break off Wollongong to 1.0 s TWT (~900 m) off Eden (Colwell et al., 1993). Dredging and coring at sites on the southern NSW margin suggest that most of the wedge consists of Neogene deposits (Packham, 1983; Hubble and Jenkins, 1984).

The physiography of the east Australian margin is largely controlled by the original shape of the basement due to the low sediment input (Colwell et al., 1993). The basement shape is dominated by the distribution of syn-rift and post break-up sediments, grabens, half-grabens and ridges. Mid-slope graben and half-graben occur along the continental slope, with most pronounced development towards the central NSW margin with thicknesses of up to 2.2 s TWT (~2500 m) thick (Colwell et al., 1993). None of these half-graben sediments have been directly dated, but correlation to the Bass Strait rift basins suggest they may be Late Jurassic in age. Synrift sediments are also well-developed off the Clarence-Morton Basin at depths of ~3000 m, but are only known from seismic sections.

Sedimentary processes along the margin are controlled by a range of factors, namely: sediment supply, accommodation space, shelf morphology; eustatic sea level change; climate; and oceanographic setting.

The continental margin offshore Sydney is narrow (~35 km wide) and relatively steep (Troedson and Davies, 2001). This morphology results in the accumulation of muddy sediments on the mid-shelf during high stands, with subsequent scouring and redeposition of the material off the shelf during low stands. There is little off shelf transportation during high stands due to the effective low stand scouring of shelf sediments.

Seismic profiles from transects along and across the NSW continental shelf also reveal the influence of eustatic sea level change on margin sedimentation. This is seen in a range of depositional morphologies and regional unconformities. One unconformity forms a prominent reflection at about 100 to 200 m below the sea floor beneath the outer shelf and upper slope (Davies, 1979; Marshall, 1979). The surface has morphological characteristics of a previous sea floor, and it is suggested that it forms the boundary between a transgressive and prolonged regressive phase associated with a long hiatus above sea level. The unconformity may be related to the Late Miocene eustatic sea level low (Jones et al., 1982). In the Sydney Basin the position of the shelf break for this sequence varies laterally between seismic lines, suggesting that sediment supply varied along the margin during deposition (Bickford et al., 1992). Several sequences are also observed beneath this regional unconformity along parts of the margin.

In the Newcastle region, a seaward thickening sequence (Sequence 2 in Jones et al., 1982) occurs below the unconformity, and this is bounded by a lower unconformity representing an erosional surface. This sequence is also clearly identified on the inner shelf in the Sydney region with data from AGSO Survey 112, but becomes highly irregular on the mid and outer shelf due to outcropping of the surface by large rotated fault blocks (Bickford et al., 1992). A third sequence is observed overlying basement in the Newcastle Bight region. The

thickness of this sequence varies according to the bedrock relief, but reaches up to 100 ms in Newcastle Bight. The lower parts of the sequence onlap basement landwards, therefore representing a transgressive phase.

Modern sediment distributions along the NSW shelf fall into three zones parallel to the shelf: Inner Shelf sands; Mid Shelf muddy sands; and Outer Shelf calcareous sands (Shirley, 1964; Davies, 1979; Roy and Thom, 1981). The Inner Shelf sands are predominantly reworked terrigenous quartzose sands with minor lithics, heavy minerals and carbonate components (Roy and Thom, 1981). Mid Shelf muddy sands are concentrated offshore from major rivers (eg. the Hunter), with poorly sorted quartz and clays deposited from suspended load during floods. These muds also contain significant carbonate content, composed primarily of foraminifera. Outer Shelf carbonate sands are bioclastic, containing up to 100% carbonate composed of fresh and abraded bivalves, bryozoa and foraminifera.

1.1.4.2. Regional oceanography

The East Australian Current (EAC) begins in the Coral Sea and extends along the east coast of Australia from 18° to about 35°S (Boland and Church, 1981; Ridgway and Godfrey, 1994). The upper layers of the current diverge from the coast north of Sydney (north of 33°S) and flow eastward across the Tasman Sea (Andrews et al., 1980; Boland and Church, 1981), while the deep layers of the EAC continue south to Tasmania (Wyrki, 1962; Reid, 1986; Ridgway and Godfrey, 1994). North of 33°S, large asymmetric anticyclonic eddies occur which are connected by the EAC, while to the south there are no cyclonic features and the anticyclonic features are not connected to the core of the current (Boland and Church, 1981). Flow calculations indicate that southward flow along the shelf-slope is approximately 30 Sverdrups (Sv, $1 \text{ Sv} = 10^6 \text{ m}^3 \text{ s}^{-1}$), however strong northward flows can lead to much lower mean flow. Across 28°S, for instance, the mean flow is only 9.5 Sv, consisting of 27 Sv of southward flow near the coast and approximately 17 Sv of northward return flow (Ridgway and Godfrey, 1997).

1.1.4.3. Regional seismicity

There have been relatively few earthquakes recorded in the offshore part of the NSW margin, with more activity documented onshore. Within the offshore part of the survey area 63 earthquakes have been recorded between 1962 and 2002, with magnitudes ranging from ML 2 to 4.3 and averaging ML 2.7 ([Figure 1.3](#)). The largest earthquake (ML 4.3) to have occurred in the offshore region was directly east of Palm Beach beneath the upper continental slope, at a depth of 15 km.

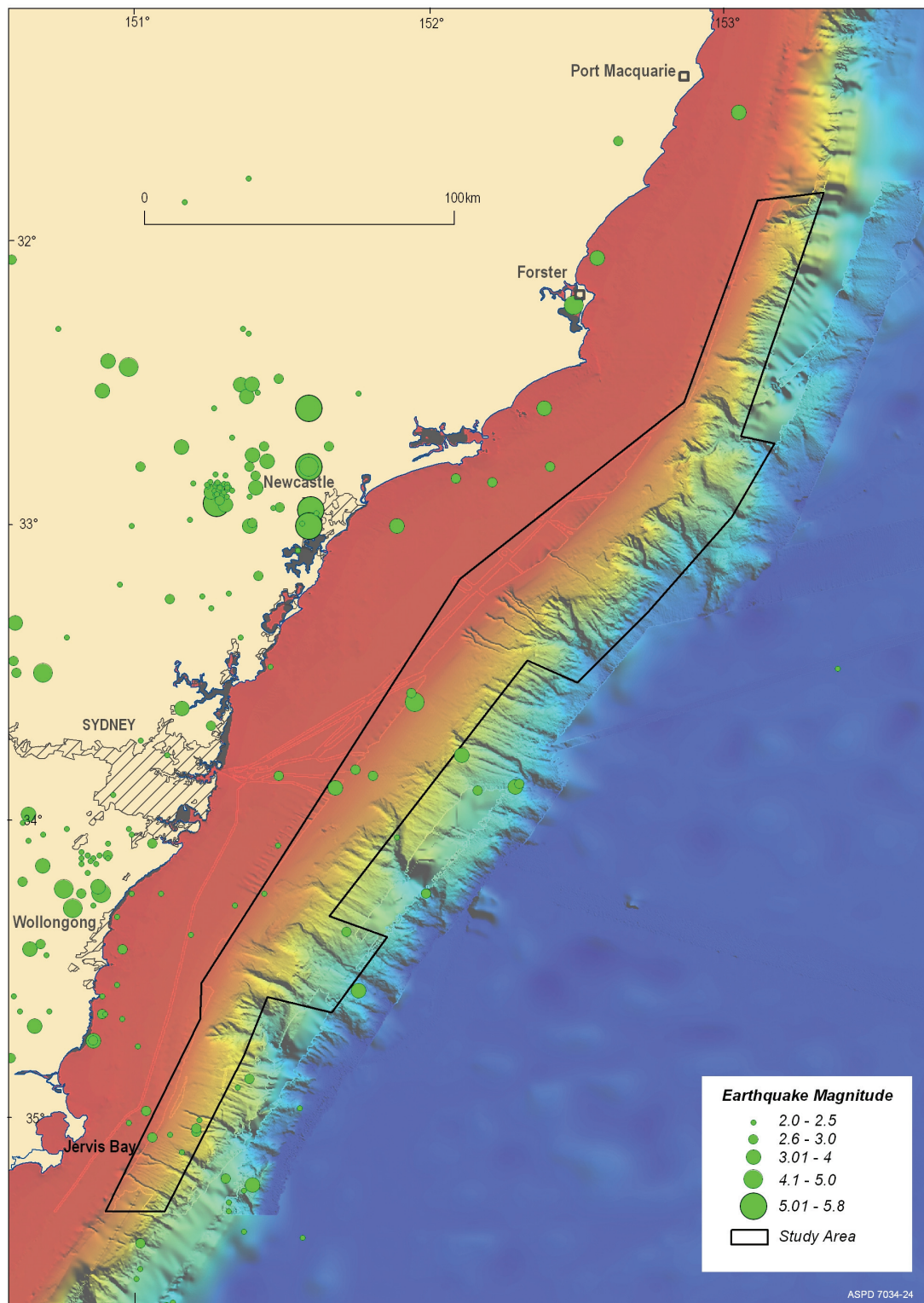


Figure 1.3 Distribution and magnitude of earthquakes in study area.

The largest onshore earthquake to have occurred along this part of the NSW margin was the 1989 Newcastle earthquake (ML 5.7). Based on the analysis of all onshore and offshore seismic data, Chaytor and Huftile (2000) conclude that there is only one fault in the Newcastle / Hunter Valley region in which Quaternary sediments have been deformed. They suggest that this Newcastle

fault is the most likely source of the 1989 earthquake, although Huftile et al. (1999) state that it does not extend far enough north to have caused the 1989 earthquake, but it may be related to the fault that was responsible. The Newcastle fault is northwest-striking and is located ~20 km southeast and offshore of Newcastle (Huftile et al., 1999). It is not clear how far the fault extends offshore. The fault has not completely ruptured in recorded history, and future events are most likely to occur to the south of Newcastle (Chaytor and Huftile, 2000).

1.1.4.4. Regional overview

The NSW continental margin has developed under a range of large scale geological processes. The Late Cretaceous rifting associated with the forming of the Tasman Sea and subsequent subsidence still defines the modern shape of the continental slope. Sedimentation in the Cainozoic has been relatively slow due to low terrigenous input and strong reworking. During high stands, sediments tend to accumulate on the mid-shelf, while during low stands sediments are scoured and redeposited off the shelf. A regional unconformity forms a prominent reflector at 100-200 m below the seafloor, and may relate to the Late Miocene eustatic sea level low. Another unconformity has been identified below this surface in the Newcastle region and the inner shelf in the Sydney region, and represents the basement surface on which the shelf sediment sequence has been built.

1.1.5. Submarine Slope Failure and Tsunami Hazard

Tsunamis are most often thought of as being caused by large earthquakes, and historically tsunamis affecting the east coast of Australia have been caused either by massive earthquakes in the South American subduction zone, or smaller earthquakes in the SW Pacific region. However, worldwide, increasing attention is being drawn to submarine slope failure as a possible source of a hazardous tsunami. A submarine slump of a few cubic kilometres volume is sufficient to cause a locally devastating tsunami, as appears to have been the case with the 1998 Sissano tsunami in Papua New Guinea (Tappin et al., 1999), and the 1741 Oshima-Oshima tsunami in the Japan Sea (Satake and Kato, 2001), each of which killed ~2000 people. Although these submarine slumps were triggered by an earthquake and a volcano, respectively, it seems likely that spontaneous slumps can also occur due to thawing of frozen methane gas in the sea floor or over-pressuring of sediments on the continental slope (Dugan and Flemings, 2000).

Evidence for the occurrence of a large prehistoric tsunami on the eastern Australian coast remains controversial and is not widely accepted. Young et al. (1996) have documented deposits of large boulders above modern limits of storm lines along the coast of southeastern Australia, and Bryant et al. (1992) have also reported Holocene deposits of marine sediments well above the storm line. The conclusion of these authors is that most of these deposits were left by “megatsunami” of some 10’s of meters height, which may have been generated by meteor impacts. Some of them, however, may have been deposited by local tsunami, and one potential mechanism for generating these is via submarine landslides on the continental shelf.

The previous Jenkins and Keene’s (1992) study of marine seismic profiles have shown that submarine landslide scarps are evident on the continental slope off Australia’s southeast coast. Although geologically recent (probably Quaternary), no minimum ages for these scarps were identified in their work. Due to the rugged topography of the margin, existing swath and bathymetric data prior to the survey was insufficient to confidently identify even the scarps studied by Jenkins and Keene (1992). The 2006 Geoscience Australia survey resolved this by estimating the volumes of material involved in each slope failure and obtaining material for radiometric dating.

There is evidence for significant failures of the slope sediments between Newcastle and Jervis Bay, however, the existing swath and bathymetry data is not sufficient to fully constrain the extent and scale of these features. The age of these failures can also not be determined from the current data sets. The uncertainty in the timing, frequency and causes of these illustrates a potential risk. This is due to the proximity to the coast, and the subsequent short warning times to settlements and developments on low lying coastal areas.

1.1.5.1. Nature of slope failures

The predominant failures on the margin occur in the lower part of the Cainozoic sediment wedge. The Cainozoic sediment wedge, as described by Davies (1979), varies in thickness and width along the shelf. Data collected prior to this survey indicated that the sediment wedge contains significant failures between Newcastle and Jervis Bay (Jenkins and Keene, 1992) where the sediment wedge is relatively thick and wide, pinching out at depths of 1500-2000 m (see Figure 1.4). At this depth, the slope is relatively steep which likely contributes to the consistency of failures across this part of the margin. In [Figure 1.4](#), regional seismic lines from previous surveys were assessed. Contours infer the thickness of the Cainozoic sediment wedge, blue lines indicate the interpreted wedge distribution, brown lines indicate the interpreted slump material and green lines indicate possible slump material.

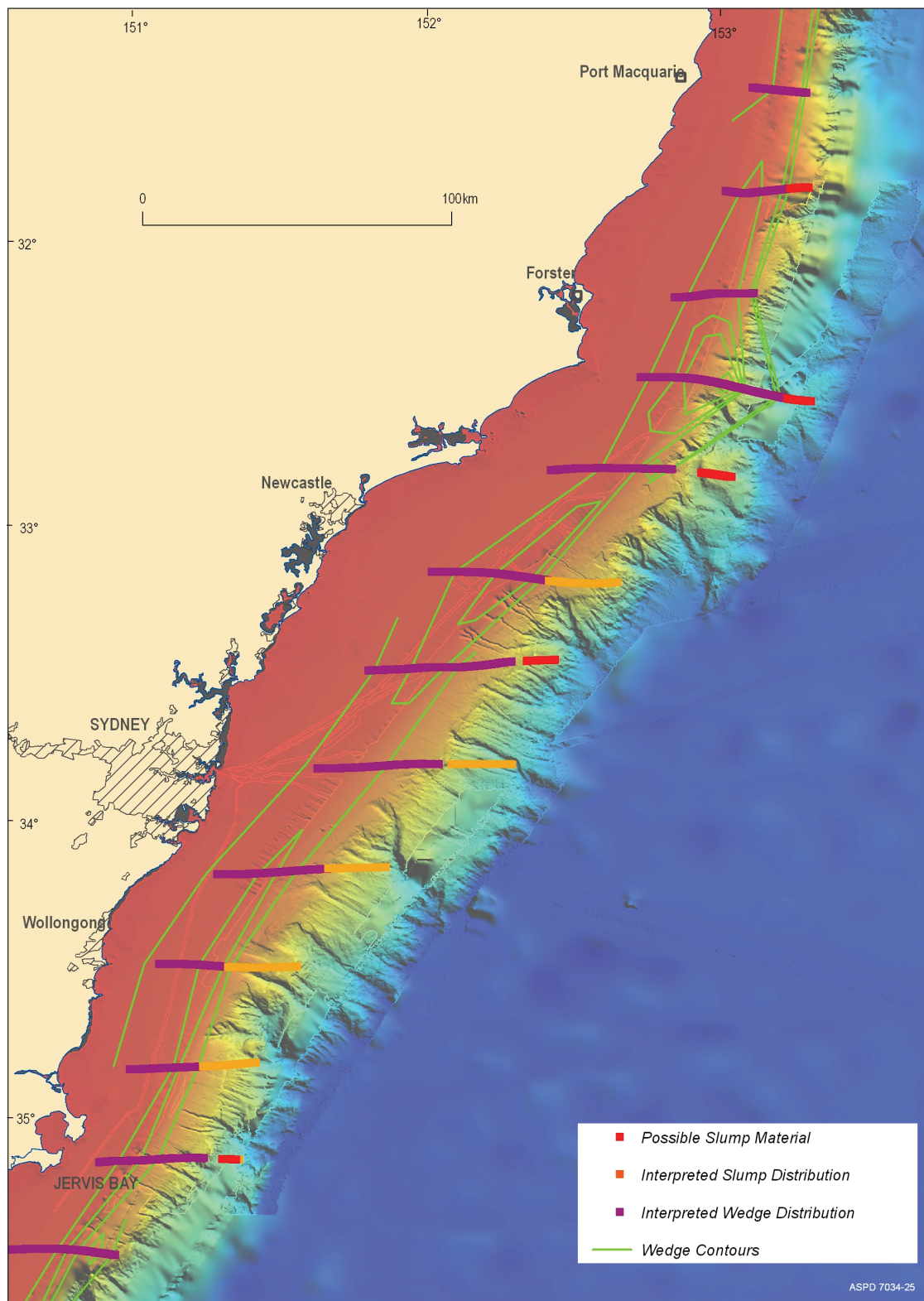


Figure 1.4 Interpreted slumps on the continental margin in the study area.

1.2. SURVEY PARTICIPANTS AND VESSEL

1.2.1. Vessel Description

The vessel used for the survey was the National Facility Research Vessel *Southern Surveyor*. The RV *Southern Surveyor* is a converted trawler, with accommodation for 24 participants (including 12 crew), Auxiliaries: 3 Deutz diesel engines driving Stamford generators, generating 3500 kVA: Fuel oil 260 tonnes, fresh water 72 tonnes, fresh water evaporator and reverse osmosis up to 10 t/day. The endurance is 26 days at 11 knots, Electrical supply: 415/240 V AC 50 cycle and a partial uninterruptible power supply. Propulsion: Kort nozzle, controllable pitch propeller, maximum speed 14 knots. Bow and Stern thrusters: Each with two 403 kW Brunvoll SPX-VP units Azimuth thruster: One 552 kW retractable Azimuth unit. Moonpool: 1.2 m x 1.0 m with a vertical instrument carriage Winches: Main fishing winches (up to 30 t each winch), net drum winch, coring winch, hydrographic, towed body and scientific winches, electro-hydraulic with low pressure hydraulic transmission supplied by A/S Hydraulic Brattvaag, Norway. The vessel is equipped to fish demersal and pelagic commercial trawls to 2000 m and to make hydrographic observations to 6000 m. Navigational equipment: Trimble GPS Nav Trac XL and Ashtech 12 channel DGPS (both with DGPS capability); Furuno GD 180 course plotter, Oceantech Seaplot Chart System, two Sperry gyro compasses Mk 37. Radar equipment: Furuno FR2010 (No. 1) Furuno FR1011 (No. 2). Echo sounder: Furuno TE 881 50 kHz, Furuno FCV 140 28/200 kHz colour sounder.

1.2.2. Scientific Personnel

Kriton Glenn	Chief Scientist
Alix Post	Co Chief Scientist
Jock Keene	Scientist
Ron Boyd	Scientist
Monica Osuchowski	Scientist
Leharne Fountain	Scientist
Anna Potter	Scientist
Michele Spinoccia	Swath processing
BB	Science technician
Craig Wintle	Mechanical technician
Andrew Hislop	Mechanical technician
Franz Viligranz	Electronic technician

Lindsay Pender
Drew Mills

Voyage manager
Electronics support

1.2.3. Ship's Crew

Ian Taylor

Master
2nd Officer
Chief Engineer

Rinaldo Di Vitis

1st Engineer

Chris Heap

2nd Engineer

Malcolm McDougall

Bosun

Tony Hearne

IR

Tony Van Rooy

IR

John Baker

IR

Paul O'Grady

Greaser

Charmayne Aylett

Chief Steward

Pat Wainwright

Chief Cook

Angela Zutt

2nd Cook

2.Methods

A geophysical survey was conducted to determine sea bed characteristics and sub-surface geology to allow the selection of sample sites and also link to previously recorded regional 2D seismic data.

2.1. EQUIPMENT AND PROCESSING

A range of different data sets were recorded during the survey. The acquisition and processing parameters are outlined below.

2.1.1. Swath (multi-beam) Sonar

Swath bathymetric data collected using a Kongsberg Simrad EM 300 multi-beam echo-sounder fitted on a gondola beneath the vessel hull. The nominal sonar frequency is 30 kHz with 135 beams, each with a 1° beam width, giving a total angular coverage of 135°. The system provides roll and pitch stabilisation, with optional yaw compensation.

2.1.2. Oceanography and Meteorology

Onboard measurements of surface salinity, temperature and fluorescence were taken throughout the survey using the ship's thermosalinograph and fluorometer. In addition, the onboard meteorological log recorded atmospheric temperature, relative humidity, wind speed and direction, and atmospheric pressure. Expendable Bathythermograph (XBT) deployments were undertaken at regular intervals throughout the survey to calibrate the sound velocity profiles for the multibeam sonar system. These data are available via: <http://www.cmar.csiro.au/marlin/> and are listed under SS 10/2006.

2.1.3. Sub-bottom Profiling

A TOPAS PS18 Parametric Sub-bottom Profiler fitted on a gondola below the hull was used to collect sub-bottom profile data. Acquisition generally involved 'normal' transmit with either an 'internal' and 'external' trigger mode. The TOPAS transmission pulse varied between the Ricker and Chirp wavelet form. The Ricker was employed with 1.5 kHz frequency and the Chirp pulse was adopted with 1-5 kHz frequency. Pitch, roll, and heave were internally corrected. Manual beam steering was activated in both pitch and roll directions as appropriate. These settings enabled beam penetrations of up to 100 ms (i.e. ~75 m) in good sea conditions, depending on the sea bed morphology, sediment type and water depth.

Data were saved in the RAW TOPAS format, while processed data was output in the IEEE 32 bit SEG-Y format and file sizes were limited to 200 Mb.

Navigation data were extracted from the SEG-Y headers using the seismic viewing program SeiSee, a freeware package produced by the Russian geophysical company, DMNG. The navigation data and SEG-Y data were subsequently loaded into the PC-based seismic interpretation package, Kingdom Suite, along with georeferenced images of the processed swath bathymetry, to aid the selection of sampling sites.

2.1.3.1. General Operating Procedure

The acquisition parameters were modified frequently throughout the survey due to the highly variable water depths and seabed morphology of the survey area. The parameters were modified based on water depth, direction of travel, angle of slope and the level of interference TOPAS created in the collection of bathymetric multi-beam data.

The TOPAS sub-bottom profiler has two main waveforms that can be used to achieve maximum sub-bottom penetration and bottom tracking for different water depths and for different sediment types and/or variable terrain. The Chirp pulse was regularly adopted throughout the survey in depths that ranged from 150 m to 2300 m. The chirp length was adjusted depending on the water depth and required power level, and ranged between 2 ms and 30 ms. The Ricker pulse was employed in water depths less than 200 m. The ping trigger varied between external and internal modes for both of the transmission pulses. The internal trigger mode was used in combination with a manually adjusted ping interval. The 'external' trigger mode was employed when simultaneously collecting the swath bathymetric data to reduce interference noise. The transmitted power level remained on 0 dB (maximum power) where possible, however this was reduced as required.

Manual beam steering was activated throughout the survey to increase the signal received over the changing slope of the subsurface. The beam offsets for pitch and roll ranged between -6 and 6 degrees. Offsets were targeted based on the direction of travel in relation to the angle of the slope, and the angle of subsurface features. Combination offsets in pitch and roll directions were frequently utilised. The following acquisition parameters were maintained throughout the survey:

- transmit mode: normal
- sample rate: 40°S (i.e. 25 kHz)
- ping interval: dependant on speed but generally 450 ms
- transmitted pulse frequency: Chirp 1-5 kHz, Ricker 1.5kHz
- beam stabilisation for ship movement: always on
- sound velocity in water: 1500 m/s

- trace length: between 100 ms and 600 ms depending on sub-bottom visual penetration and ping interval
- receiver gain: 15-24 dB depending on bottom hardness and sub-bottom penetration (average: 19 dB).

2.1.3.2. *General Processing Procedure*

The processing procedure for TOPAS refers to the processing chain applied to the incoming ping data in real-time for on-screen display purposes. The parameters used dictate the appearance and what is seen on-screen is written to the associated SEG-Y file – the ‘RAW’ file format is unaffected by the processing stream. Apart from the occasional modification for experimental purposes the following processing parameters were maintained throughout the survey:

- filters: Ricker – band pass 1000-5000 Hz with roll-on and roll-off; Chirp - matched filter
- bottom-tracker: mostly enabled in auto-mode
- time-variable gain: on
- stacking: a 2-trace mix was applied for the Ricker pulse in shallow water.

During acquisition, the instantaneous amplitude was enabled which significantly improved the quality and appearance of the data. The lower colour threshold level (in the ‘display’ tab) was reduced to enhance the visual outputs. The time variable gain was selected to ‘tracking’ and adjusted manually as necessary.

Areas of highly rugose sea bed occasionally interfered with the ability of the bottom-tracker to correctly track the sea bed, however employing manual beam steering significantly relieved this difficulty at times. The bottom tracker had greater difficulty once water depths began exceeding 2300 m, particularly where the subsurface was also highly rugose. Therefore, in these areas the operator disabled the tool.

2.1.3.3. *Data Quality*

Data quality was very good with low noise levels and good sub-bottom penetration. Low to moderate sea conditions produced noise levels and ship-roll/heave/pitch movements which were effectively handled by appropriate choices of filtering and compensating parameters. Data quality was significantly reduced at times when the TOPAS began interfering with the collection of swath bathymetric data, as the power level needed to be reduced until the interference was removed.

2.1.4. Echo-Sounder

A Simrad EK 500 echo-sounder (12, 38 and 120 kHz transmission frequencies) was used to provide water column and water depth information. The 38 kHz frequency was continuously recorded, while the 120 kHz frequency was only used when water column targets were observed to be abundant.

2.1.5. Seismic

The aim was to collect high resolution seismic over a range of water depths from 150 m to 1900 m water depth. The seismic source was provided by 2 GI airguns, each with 45/105 cubic inch volume with compressed air at 1900 psi supplied from the Price air compressor with 2000 psi capacity. A 450 m *Stealtharray* solid seismic cable with 300 m of active section and 48 channels was used for acquisition at a speed of 5 to 6 kts. The sampling rate was set at 0.5 ms with a record length of 4 seconds. The filters used were a 50Hz notch filter and a 500 Hz high filter.

Cainozoic sediment thickness maps were produced from the seismic interpretations based on the thickness of units 1 to 3. A sediment velocity of 1.8 km/s was assumed for conversion to meters. The results from the seismic lines collected during this survey were combined with those from BMR Survey 12 to obtain greater coverage of sediment thickness information.

3.Sedimentology

3.1. SAMPLE ACQUISITION

3.1.1. Sub-Surface Sediment Samples

Cores were collected using a gravity corer with a 1 tonne core head and a PVC core barrel liner deployed from the stern A-frame. The length of the core barrel was varied depending on the sediment type; typically a 6 m barrel was used as penetration generally varied between 3 and 5 m. The corer was deployed and retrieved using a hydraulically-operated cradle and the ship's coring winch.

3.1.1.1. Sediment Core Sampling and Handling During Survey

The gravity cores were collected during the survey for stratigraphic and geochemical analysis. A total of 15 gravity cores were attempted and > 48.8 m of core was obtained from the 11 successful returns, the data from these cores is available at (<http://www.ga.gov.au/oracle/mars/>).

Once the core barrel had acquired a successful sample, it was secured on deck and safety procedures were adhered to. The stratigraphic cores were cut into various sections for a range of analysis. Starting at the base of the core a ~30 cm section was removed and capped followed by another 20 cm section acquired for triaxial testing and stored vertically. The rest of the core was cut into 1 m sections. Each section was tape sealed with PVC end caps, labelled and stored horizontally at 3 - 4°C.

3.1.1.2. Variation in Sampling for Geotechnical Testing

Variations in the typical marine geological coring method allowed geotechnical samples to be taken. In particular, selected cores (07GC06, 10GC09, 11GC10 and 04GC03) had the bottom sections extensively sub-sampled for several geotechnical tests including triaxial and shear box tests. These geotechnical tests are important for determining the physical behaviour of the sediments under load, such as experienced from its own internal self weight, earthquake ground accelerations and changes in pore water pressures.

3.2. SAMPLE PREPARATION, MEASUREMENT AND RESULTS

3.2.1. Grainsize

Access to these data sets is explained in [Appendix A](#).

3.2.1.1. *Sieve Method*

Each sample was dried at 40°C for 24 hrs and disaggregated by adding deionised water. Samples were then sieved into separate gravel (>2 mm), sand (63 µm - 2 mm) and mud (<63 µm) fractions using a wet sieve method. Sand and gravel fractions were dried by placing in a warm oven for 48 hrs. The mud fraction was spun down in centrifuge, excess water removed, and mud placed in a freeze drier for 24 hrs. The mud samples were kept in sealed vial up until point of weighing to prevent sediment absorbing moisture. Fractions were then weighed and weight percentage of each fraction in bulk sample calculated.

3.2.1.2. *Laser Particle Size Analyser Method*

A representative sub sample was weighed then immersed in 10% hydrochloric acid to remove carbonate. Samples were washed free of acid and placed in an ultrasonic bath for 2 minute prior to analysis (Watson et al., 2003; McLachlan, 2005). Malvern Laser Particle Size Analyser was calibrated using 800 ml of water in a 1L beaker. The sample was then added to the system and analysis performed using ultrasonic setting.

Mud was the dominant fraction in the majority of samples with content varying from 30-90 weight %. Sand was present in all samples and formed 10-70 weight %. Gravel was present but formed a minor component (<1%) in around 30% of samples.

3.2.2. **Density**

3.2.2.1. *Density Cubes Method*

Measurements were taken to establish wet and dry bulk densities from the gravity core sediments. In preparation, plastic cubes (~2cm³) were numbered and their individual weights recorded prior to survey departure. Samples were collected by pressing cubes into the centre of fresh core, and carefully extracting the sediment. Once extracted, full plastic cubes were sealed immediately and refrigerated until time of analysis (4 weeks after sampling).

At time of analysis, the seal was removed and the cube sample weighed. The wet weight of sediment was determined by comparison to its empty cube weight. Cube lids were then removed, and the cube and sediment were placed in an oven at 40°C for 12 hours. Cubes were then placed in a desiccator until they returned to room temperature. The lid was returned to cube and entire cube was reweighed. The dry weight of sediment was determined by comparison to empty cube measurement. Results for this are shown in the core logs in [Appendix C](#).

3.2.3. Multi Sensor Core Logger (MSCL)

A single unsplit core, SS102006/14GC13, was run through the GEOTEK Multi-Sensor Core Logger (Watson, 2007; *GEOTEK Multi-Sensor Core Logger Manual*, 2000: <http://www.geotek.co.uk/ftp/manual.pdf>)

Core diameter, density, magnetic susceptibility, P-wave travel time, and temperature were measured using GEOTEK MSCL software. The plotted results of this process are in [Appendix C](#).

3.2.4. Geotechnical Testing

3.2.4.1. *Triaxial Tests*

Triaxial samples were taken from the bottom 30-60cm sections of cores before being split on the vessel. Triaxial samples were immediately capped to prevent moisture loss and volume change. Samples were stored upright and separately to minimise vibration interference to help prevent potential degradation on soil skeletal structure. Samples were kept refrigerated between retrieval of core and testing. Cores were sub-sampled to around a 50mm diameter by 100mm tall triaxial specimen, excess material inside the cores was used as samples for shear box tests.

Samples were placed in a pressurised cell that emulates stresses corresponding to the target overburden. The soil was then brought to, and through, the point of failure as well as through the introduction of a change in vertical load. Test parameters were recorded that allowed the calculation of the internal effective friction angle ϕ' (measured in $^{\circ}$) and undrained strength s_u (in kPa). (Refer to pp. 74-80 in Atkinson and Bransy, 1978. These values will represent the assumed strength of the soil at the pre-failure conditions under the stress environment inferred from the geometry of the slide scar. The results of these tests are in [Appendix E](#).

3.2.4.2. *Shear box tests*

Some of the slides have shown creep or incipient movement, which can indicate the development of a failure plane at depth within the soil. Some soils can develop lower shear strengths to a residual value as the shearing distance increases. A shear box test replicates these conditions by measuring the forces needed to shear a sample over increasing distances until a residual value has been reached (Refer to pp. 81-85 in Atkinson and Bransy, 1978). The results of these tests are in [Appendix E](#).

3.2.4.3. *Radiocarbon dates*

Radiocarbon dating was conducted on down-core sub-samples from seven gravity cores. Dates were obtained from mixed planktonic foraminiferal assemblages, and were run at the Rafter Radiocarbon Laboratory. Calibrated ages were obtained using a reservoir correction of 403 ± 17 (the average for eastern Australia; see <http://calib.qub.ac.uk/marine/>) and the calibration curve of Fairbanks (<http://radiocarbon.ldeo.columbia.edu/research/radiocarbon.htm>). Some dates could not be calibrated as they fell outside the calibration range (0-55,000 years). Results are shown in [Table 4.1](#) and [Appendix F](#).

3.2.5. **Composition**

3.2.5.1. *Carbonate Content: Carbonate Bomb Method*

Each sample was ground to a fine powder. For mud, gravel and bulk samples, the original sample was used. To determine the sand fraction, 150-2000µm was sieved out and around 10 gm of carbonate was picked from the samples. Sediment was then recombined before carbonate analysis was performed whereby 0.8 grams of each sample was combined with 10 ml of orthophosphoric acid (H_3PO_4) in a sealed cylinder. When the entire sample was dissolved, the CO_2 gas pressure in the cylinder was measured. CO_2 gas pressure (kpa) was converted to % $CaCO_3$ by comparison to a calibration graph.

Bulk carbonate for samples varied from approximately 15-50 weight %. Where present, gravel was composed of 100% carbonate grains. The carbonate content of sand and mud fractions varied in a similar range to bulk carbonate measurements.

3.2.5.2. *PIMA-IITM (Portable Infrared Mineral Analyser)*

Fifteen 10 g wet samples were dried for 1 week in an oven at 40°C then air dried for 2 weeks. Although samples appear homogeneous, dried material was ground to a consistent coarse powder and placed in a glass dish.

PIMA was calibrated using settings for analysis through glass. Samples absorption/reflectance was measured in the wavelength range 1300-2500 nanometres at integration 8 (long exposure to light source). Each sample was agitated and remeasured at the same settings. The resulting absorption spectra was analysed in TSG (The Spectral Geologist) software. The most abundant mineral, second most abundant mineral, their mineral group, and % composition were identified using the software's standard methods.

Spectra were generally good (TSG error 122-346). The minerals identified by TSG from PIMA spectra included kaolin group minerals (halloysite), carbonate

group minerals (calcite, siderite) and minor Al (OH)-1 group minerals (illite). A significant organic component identified as “wood” by TSG was recorded for one sample, although error on measurements for this sample was very high (>1000). TSG results for minerals with characteristic absorption features in infrared wavelengths suggest that by volume, Kaolin group minerals generally dominated over Carbonate minerals in samples analysed. This agrees with lab results (Carbonate Bomb method) which record carbonate contents for these samples at <40%. The data is presented in [Appendix D](#).

3.2.5.3. *XRD (X-ray Diffraction)*

Samples used for PIMA analysis were ground with a mortar and pestle to a fine powder, then packed into an XRD powder holder and ground with SVR or methylated spirits. Each sample was poured onto a glass slide and allowed to dry out prior to analysis as per Mernagh et al (2007). Analysis and interpretation were performed using the Siemens D500 Diffractometer; Eva Diffrac^{plus}™, search/match software and Siroquant™ quantification software.

XRD identified quartz, halloysite and calcite as the dominant minerals present in all samples. Results suggest aragonite, albite, and halite (sodium chloride) are present in lesser amounts in all samples. Muscovite was identified in one sample. The data is presented in [Appendix D](#).

3.2.6. **Digital Video Footage**

Video footage of the sea bed was collected to provide a continuous visual recording of the substrate, morphology, habitats, and benthic biota in the survey area. The digital video camera was contained in a watertight housing attached to a steel frame. Four battery-powered 25W halogen lights were used to illuminate the sea bed. The underwater camera recorded on digital videotape in the camera housing and was also fed to VHS tape and a monitor on board the vessel. This “live” video feed enabled the winch control operator to raise and lower the camera in order to image a representative area of the sea bed and specific features while the vessel drifted beam on to the swell. A total of 40 minutes of benthic video footage was acquired at one transect.

Scenes were recorded in water depths of 1620 – 1372 m. The biota observed at the single site was limited in population size and overall diversity. The view from the video is limited (approximately 1 m x 1 m), due to the overall capability of underwater imagery, lighting and water clarity. Therefore large scale features are not able to be observed in totality.

3.2.6.1. *Digital Video Footage Results*

General observations revealed a substrate that was usually uniform with limited variation from unconsolidated soft muddy sands and sandy muds. The extensive areas of soft substrate commonly exhibited small scale low relief morphology. Interestingly no sediment ripples were observed across the site. The epibenthos produced burrows and small scale (5cm) mounds in soft muddy sea bed sediments. The surficial benthos covered < 1% of the seabed. Visibility over the site was generally good, restricted by the strength of the video lights.

Overall, there were few epifaunal species (fixed or sessile) and those observed were solitary. The nektonic/planktonic species were seen only sporadically (see [Appendix B](#)).

4. Results and Analysis

4.1. INTRODUCTION

The survey descriptions are organised into five regions (Figure 4.1.)

- Jervis Bay, southern extent of the data, north to Black Head, Gerroa.
- Sydney / Illawarra, between Black Head and McMasters Beach
- Hunter, from McMasters Beach to Birubi Point near Port Stephens.
- Myall, extending north from Birubi Point to Sugarloaf Point near Seal Rocks (southern edge of Wallis Lake)
- Manning, north from Sugarloaf Point to the limit of the voyage study area.

Within each region, the results are presented and discussed from south to north. First, the seismic airgun results are presented and discussed. These are followed by the sub-bottom profile results, the geomorphic features interpreted from the multibeam bathymetry, the sedimentary results from the cores, the video observations from one underwater tow, and finally a brief description of the oceanographic and meteorological results. A summary of each of these datasets is given briefly in the following section.

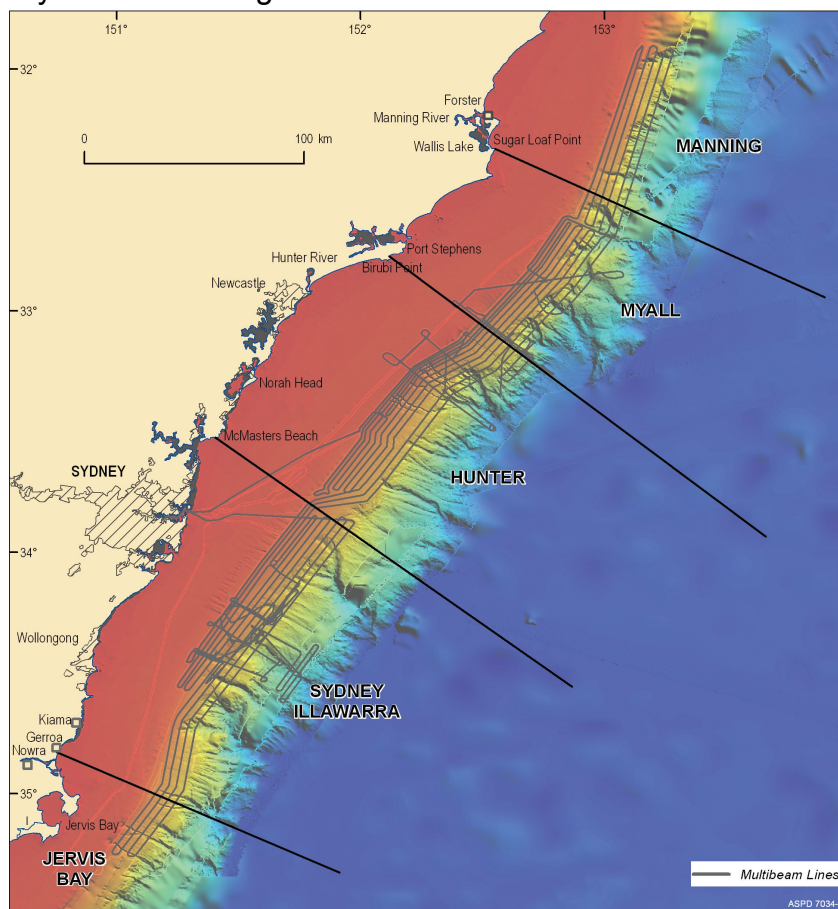


Figure 4.1 The five regions of the study area

4.1.1. Seismic Reflection Profiles

Approximately 340 line kms of seismic reflection data were collected during the survey. The 11 seismic reflection lines focused on three areas: the slides in the Sydney/Illawarra region, the canyons and slides in the Hunter region and the slides in the Myall region ([Figure 4.2](#)). Sequence stratigraphic principles (Vail and Mitchum, 1977) were used to interpret the lines for the post rift sedimentary history of this passive continental margin. Interpretation of the basement was based on seismic volcanostratigraphy as defined by Planke et al. (2000) for rifted margins. Migrated data was used to establish the different seismic units.

The regional nature of the seismic units is confirmed by the seismic data collected. There are five sedimentary units on this margin. They are defined in Line SS102006/01 and can be clearly recognised in other lines. Similarly, three types of basement are recognised along this passive margin and they are also defined in Line SS102006/01. Where the lines are on the shelf, multiples make detailed interpretation difficult. The quality of the seismic also deteriorates below 2000 m water depth, particularly where the sea floor is rough (see [Appendix G](#)).

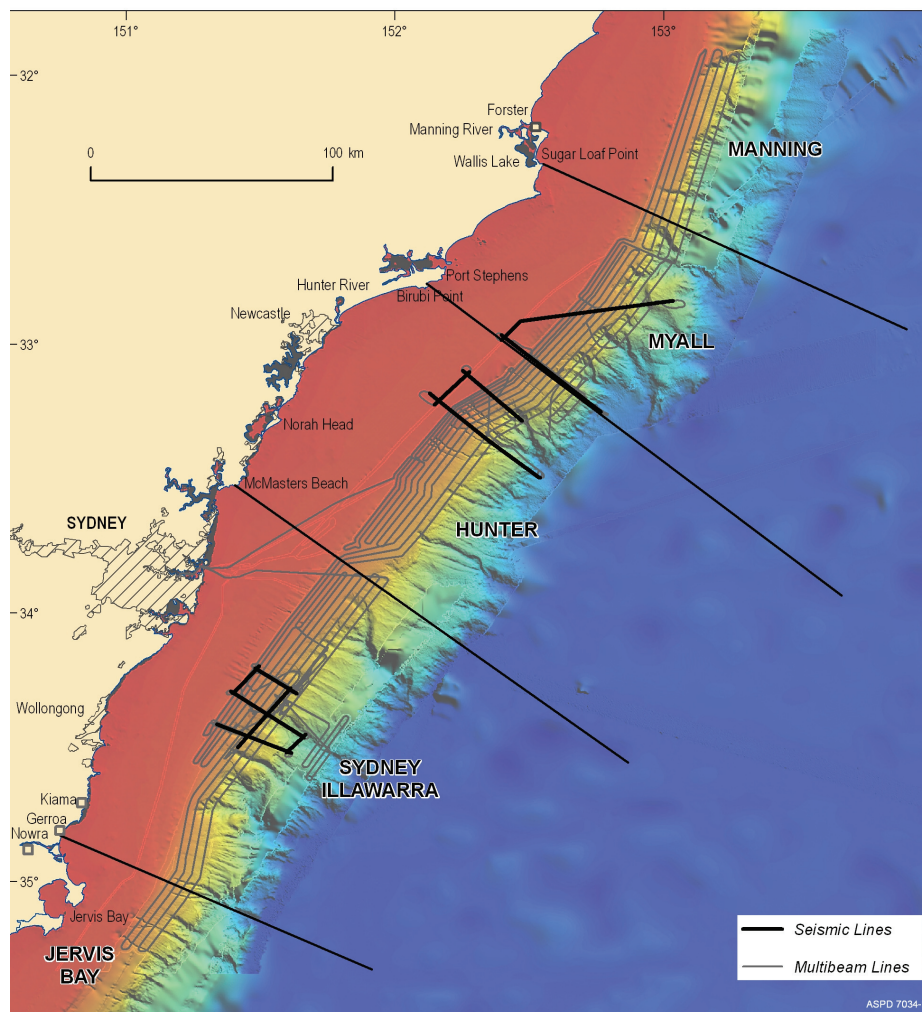


Figure 4.2 Location of seismic lines acquired in the survey area

4.1.2. Sub-bottom profiles

During this survey, 3414 line kms of sub-bottom profiles were acquired using a TOPAS PS18 Parametric Sub-bottom Profiler according to the methodology outlined in [Chapter 2](#) (Figure 4.3). The TOPAS data was acquired in the three central areas: the Sydney / Illawarra, Hunter and Myall. No TOPAS was collected over the Manning area in the far north, or Jervis Bay in the south.

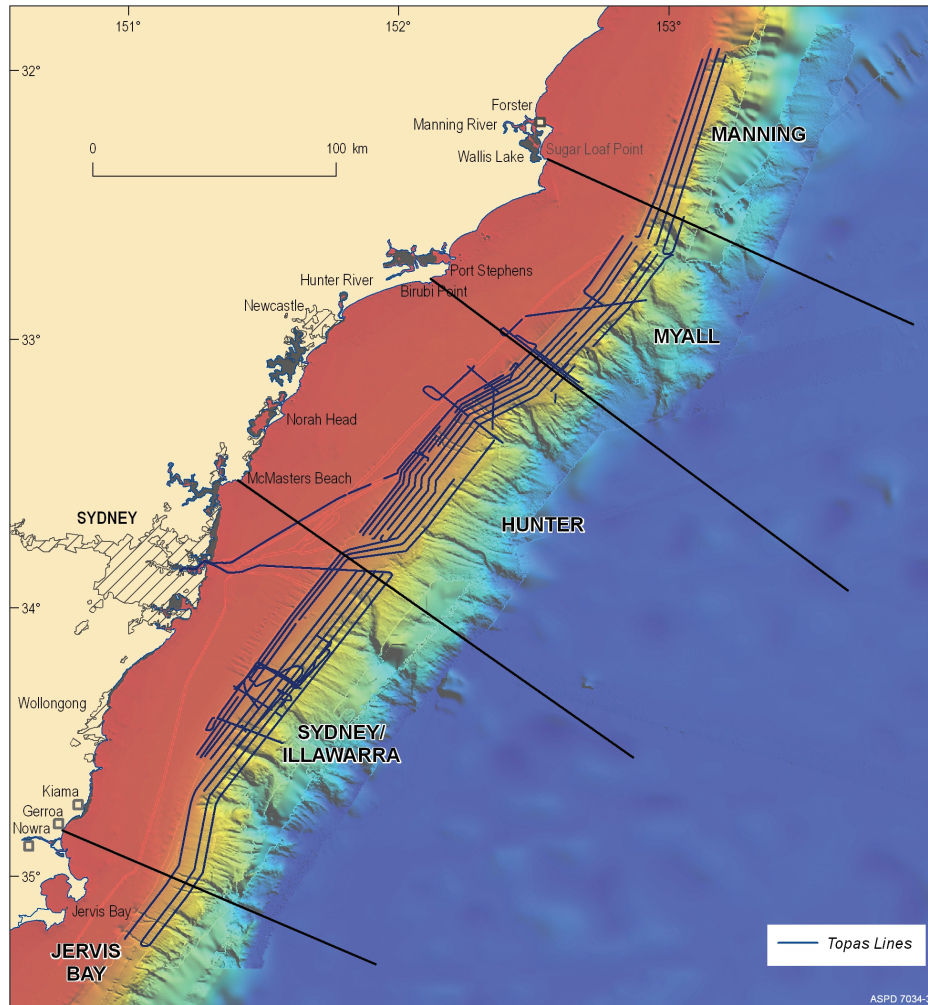


Figure 4.3 Location of sub-bottom profile (TOPAS) lines

4.1.3. Geomorphology

Geomorphic interpretations are based on 23 200 km² of high resolution bathymetric data (9200 km² from this survey) collected with multibeam sonar systems. Almost complete coverage of the seafloor was obtained across the five regions from these combined high resolution data sets over a depth range from 140 to 5000 m. Some data gaps occur between 2400 and 3600 m depth in the Jervis Bay, Sydney / Illawarra and Manning regions.

4.1.4. Sediment cores

Fifteen cores were attempted and fourteen gravity cores were collected within the Sydney / Illawarra, Hunter and Myall regions (Figure 4.4). The cores range in length from 1.17 m to 5.32 m, and the ages ranges are described in [Table 4.1](#). The cores were targeted on the basis of the sub-bottom profile and multibeam data to sample sediments within the failure scars, areas adjacent to the scars which appeared to contain unfailed sediment, parts of the upper continental slope, and a large depression in the Hunter region. Radiocarbon dating was undertaken on cores within the Sydney / Illawarra and Myall regions (see [Appendix F](#)).

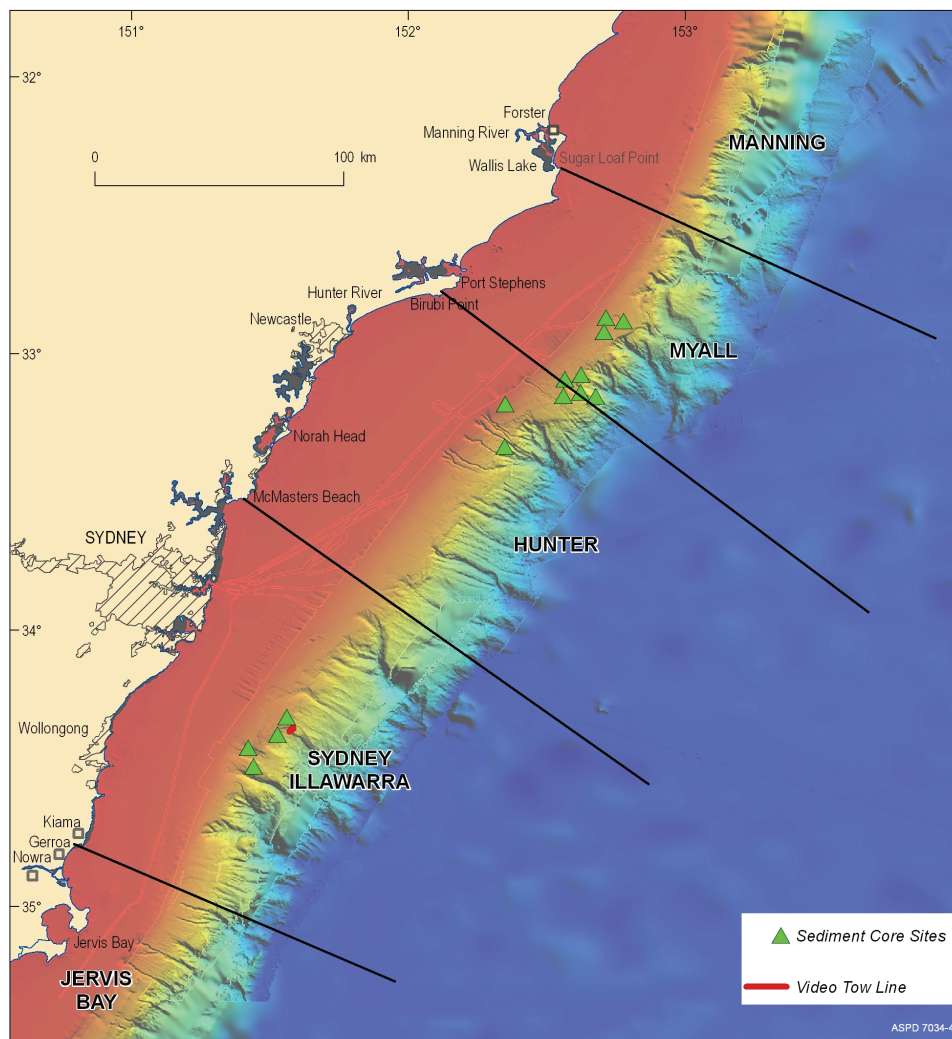


Figure 4.4 Location of sediment core sites and video transect of the survey

Table 4.1 Core data overview

Sample Name	lat	long	water depth	core length (m)	Cal age range (BP)	% mud range	% sand range	Variation in Wet density (gm/cm ³)	% carbonate mud range	% carbonate sand range
GC01	-34.317	151.578	1214	4.5	§	47-82	17-52		21-49	42-69
GC02	-34.461	151.435	1194	3	1359 / 15183	40-81	19-60	0.26	27-54	42-59
GC03	-34.428	151.422	947	4.04	2156 / 45048	43-74	26-57	0.26	28-52	41-67
GC04	-34.378	151.546	1518	5.015	§	65-88	12-35	0.15	21-48	41-51
GC05	-32.871	152.753	922	4.65	1995 / 28663	50-90	10-50	0.01	12-38	40-48
GC06	-32.876	152.751	934	4.31	674 / 27275	53-82	18-47	0.13	20-38	38-45
GC07	-32.920	152.707	828	5.05	3198 / 12820	36-78	22-64	0.06	13-38	22-45
GC08	-33.140	152.621	1424	4.83	1428 / 19794	52-83	17-48	0.14	14-41	33-62
GC09	-33.122	152.599	1329	3.72	§	60-89	11-40	0.23	18-40	50.5 - *
GC10	-33.095	152.621	1183	5.32	§	50-88	12-50	0.07	18-41	34-51
GC11	-33.109	152.599	1257	4.27	§	71-84	16-29	0.13	24-42	#
GC12	-33.140	152.622	1420	4.6	1499 / 28203	60-91	9-40	0.17	17-43	36-60
GC15	-33.201	152.374	648	1.17	§	28-78	22-72	§	32-42	40-44

X = dated sediment

* =single measurement

= insufficient volumes

§ = not analysed

This chapter includes descriptions from these sediment cores. These descriptions assist in the overall understanding of the depositional processes and systems present on the NSW continental slope. Future work on these data will investigate the relationships between the delivery of sediment the erosional regimes and the amount of mass wasting experienced on the continental slope.

The implications of these sediment descriptions and core observations are outside the scope of the post survey report and will be discussed in future publications. The more detailed supporting data and imagery from these cores are attached in Appendix C or, the details of the sedimentology can be accessed in MARS: Go to <http://www.ga.gov.au/oracle/mars/>, click on both the simple or advanced version, and typing in 'SS 10/2006' into survey ID.

While this information provide insights into sediment accumulation rates over the survey area, more detailed dating is needed to provide further information on the Holocene (and older) evolution of Australia's central eastern margin.

4.1.5. Biology

In prioritising of the work program, video and sediment grabs were low graded and subsequently only one camera station was undertaken. These two methods are the ones usually used to assist in establishing the benthic biodiversity. At this short transect, 40 minutes of video was taken and the results of this are listed in [Appendix B](#).

4.1.6. Underwater video tow

An underwater video tow was obtained in the Sydney / Illawarra region across the side scarp of the upper Bulli Slide in water depths ranging from 1370 to 1620 m ([Figure 4.4](#)). A total of 40 minutes of footage was recorded with variable quality, depending on the distance from the seabed. The video was analysed to characterise the seabed biota and sediment types along the transect. A transcript of observations is available in [Appendix B](#).

4.2. JERVIS BAY REGION

The Jervis Bay region ([Figure 4.5](#)) occurs at the southern extent of the

survey zone, extending for 50 km offshore from the Shoalhaven River and Jervis Bay in the area south of Gerroa. No seismic or sub-bottom profile lines were acquired in this region, and no gravity cores were collected. New multibeam swath data was collected across a depth range of 400 to 3000 m.

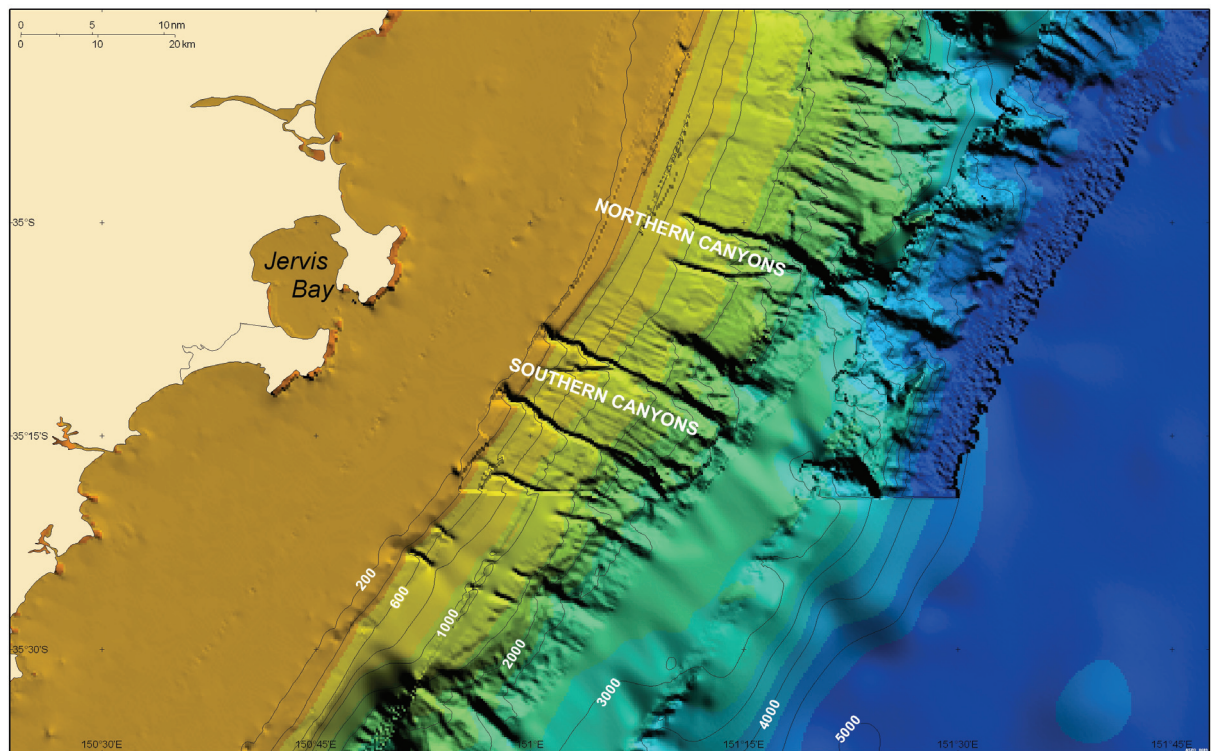


Figure 4.5 Jervis Bay Region

4.2.1. Results from geomorphic interpretation

Prominent features on the upper slope in the Jervis Bay region are six narrow canyons and many smaller, slope gullies. There are also small ridges and depressions in the sea floor that are sub-parallel to the isobaths above 650 m.

The Jervis Bay region has a very steep slope of 8 to 9° between the 400 and 600 m isobath and 7 to 8° down to approximately 1500 m where it again steepens. Between 1500 and 2500 m the continental slope is up to 18° and there are numerous retrogressive slides. Below this is a 15 km wide terrace, largely un-surveyed, with a prominent linear ridge forming its outer margin. This ridge rises to 2800 m and descends on its eastern side

by a spectacular 2000 m scarp (average gradient 25°) to the abyssal plain at 4800 m. The overall width of the continental slope from 400 m to 4800 m is 41 km. The isobaths on the upper slope trend 030° whereas the structural feature (fault) at the base of the slope strikes 020° .

The heads of the southern four canyons were not surveyed as they cut into the relatively steep upper slope sediment wedge and extend above the 400 m isobath. Only a short length of the southernmost canyon was surveyed. In their upper reaches for 15 to 25 km down to 1100 m these canyons are 200 m deep, meander and are V-shaped. The two northern canyons join at 1100 m water depth. Below this depth the canyons erode into the lower part of the sediment wedge and are flat-bottomed, 200-400 m wide and only 100 m deep. The slope of their thalweg becomes abruptly steeper below 1500 m (doubles from 4.3° to 9°).

Between the canyons on the upper slope, ridge and gully topography occurs along with incipient slumps. Some gullies merge and some diverge down slope. The ridges and gullies are linear and run down slope with a typical spacing of 200-400 m and relief of 30 m. This ridge and gully topography is particularly common immediately north of the southern four canyons on the slope between 700 and 1100 m. This particular group of gullies feeds into crown slump scarps at the head of a box canyon at 1300 m. north of this box canyon is a 7 x 7 km block of slope material before the next canyon. Chevron-shaped sediment slides occur on the down-slope margin of the block where the slope is 17° from 1800 to 2600 m. Upslope of this block is a broad dome at 1320 m water depth (35.1140° S; 151.2045° E) with incipient failure scarps on its down-slope side. Defining the shape of this dome is difficult because of a velocity offset between swaths across it.

The two northernmost canyons in the upper slope within the Jarvis region are relatively straight and shorter than the southern four. They have their heads (possibly filled by sediment) at 900 m. They are 100-200 m deep and 200-400 m wide and run straight down slope for 8 km with a 5.5° slope to 1700 m water depth. Their floors descend in several steps of 60 m, and at 1700 m there is a major change in floor gradient (a 200 m step down) coinciding with the scarp on the slope. The two canyons join at 2500 m to form a wider and deeper canyon.

4.2.2. Discussion of geomorphic interpretation

The shelf offshore of Jervis Bay is narrower than at any other part of the survey and this enables the East Australia Current (EAC) to sweep sediments from the shelf onto the slope. This results in a higher sediment deposition rate on the slope compared with adjacent areas. The higher sediment supply and subsequent steeper depositional slope of 9° has caused sediment failure to generate turbidity currents that flow down slope. Smaller flows have eroded gullies and others have cut canyons.

The narrow and relatively straight canyons extending up the slope in the Jervis Bay region are likely related to the Shoalhaven River drainage and its deposition of sediment at or near the heads of these canyons on the shelf and slope during the Cainozoic. This implies that they were incised into the sediment wedge above the 1500 m isobath by turbidity currents carrying the terrigenous sediment down slope. Meanders in the canyons are caused by deflection by more resistant strata in the sediment wedge, which have also led to the development of steps in their otherwise flat floors. The particularly large step down in the floor of the canyons at 1500 m is caused by a change to a more resistant basement lithology.

Bedrock appears to control the extent and type of failure in the 1500 to 2000 m depth range. For example, near the southern margin of the survey (centred on 35.2967S; 151.0746E) there is a 28° scarp from 1500 to 1800 m which is an exposed bedrock failure surface. The surface dome described at 1300 m water depth may be sediment draped over a subsurface bedrock intrusion and could provide a potential failure surface for the sediment block on its seaward side.

4.3. SYDNEY / ILLAWARRA REGION

The Sydney / Illawarra region lies offshore from the Sydney and Wollongong urban areas and the Royal National Park. Six seismic lines were acquired in the central part of this region, focussing on the areas near the Bulli and Shovel Slides ([Figure 4.6](#)). Multiple TOPAS profiles were also acquired on the mid to upper slope, and four gravity cores were collected within the slide scars and on an unfailed section.

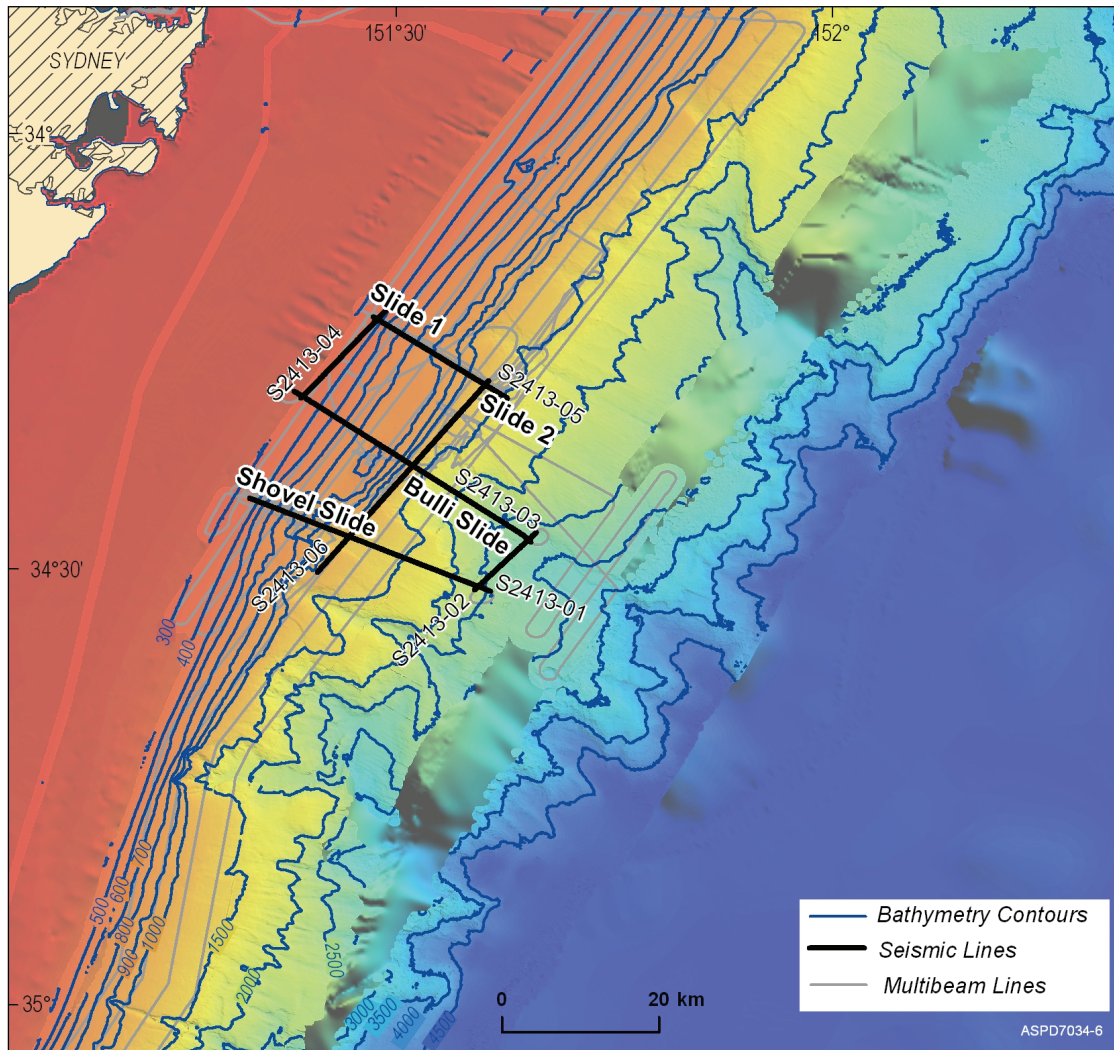


Figure 4.6 Sydney / Illawarra region

4.3.1. Seismic Profiles

4.3.1.1. Analysis of Line SS 10 2006/01

Line 1 is the most southern line in the Sydney/Illawarra region. It starts on the upper continental slope in 330 m of water, goes down slope and ends at a water depth of 2500 m (Figure 4.7). It is 28 km in length. The aim of this line was to determine the failure characteristics in the sediment wedge by following the axis of a major slide, known as the Shovel Slide.

The seismic profile defines a sediment wedge overlying 'basement' on the upper slope. This wedge is thickest (370 ms) at the start of the line and can be divided into three units based on acoustic properties:

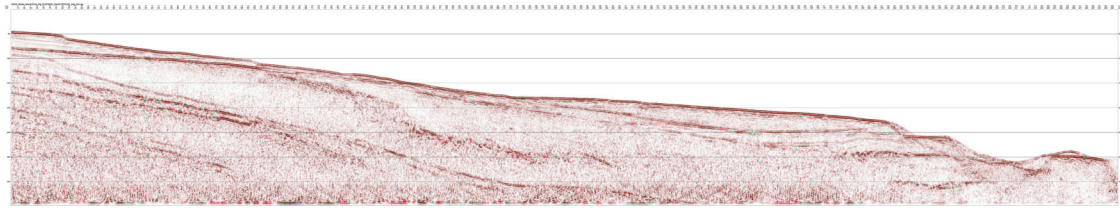


Figure 4.7 Seismic Line SS 10 2006/01

- Unit 1: 0-160 ms has parallel, continuous, regularly spaced reflectors of low amplitude;
- Unit 2: 160-320 ms has weak reflectors and is more transparent than the unit above;
- Unit 3: 320-370 ms has high amplitude continuous reflectors overlying acoustic basement.

Down slope from the start of the line the first reflector disturbances and offsets (faults) occur in Unit 1 at Common Depth Point (CDP) 170, upslope from the seafloor failure scarp at CDP 205 (WD 400 m at top of scarp). From the seafloor scarp down to CDP 580 about half of Unit 1 (80 ms) has been removed and both the remaining Unit 1 reflectors and all of Unit 2 reflectors show evidence of down slope disturbance. Below CDP 580 (WD 770 m) there is another scarp formed by a slide removing all of Unit 1 and half of Unit 2. This second scarp lies directly above an increase in slope of the acoustic basement. The failure surface for this slide is at or very near the sea floor and extends down to CDP 1110 (WD 1330 m). Unit 3 can be traced beneath this surface but with much lower amplitude. The sediments overlying Unit 3 thin from 80 ms below the scarp at CDP 580 to 50 ms at CDP 1110.

Below CDP 1110 down to CDP 1880, a relatively thick lens of sediment debris lies directly on Unit 3. The lens has its maximum thickness of 400 ms at a water depth of 1500 m. Its eastern extent is truncated by erosion, part having slid further into deeper water. Beneath the debris deposit at CDP 1810, Unit 3 has also moved down slope and is thrust over itself.

Underlying Unit 3 from CDP 580 to CDP 2000 is a mid-slope sediment basin up to 1200 ms thick (CDP 1160, WD 1340 m). These sediments can be divided into two units:

- Unit 4: weak continuous reflectors with higher amplitude reflectors at base.
- Unit 5: diffuse reflectors.

Unit 4 has its maximum thickness of 200 ms at CDP 1640 where the reflectors are near horizontal. Between CDP 1240 and 1400 the unit lacks internal reflectors and could be slumped. Up dip, particularly above CDP 1200, the unit thins rapidly and onlaps the underlying Unit 5. Landward, Unit 4 pinches out at CDP 870. Its eastern extent is truncated at the sea floor by erosion.

Unit 5 reflectors are generally seaward dipping with offlap at the top below the overlying Unit 4, and they onlap the underlying basement. They also become more horizontal seaward of CDP 1640.

Acoustic basement cannot be continuously traced beneath the sediments on this line. Nevertheless it can be divided into three types based on the characteristics of the reflectors. The nature of the contact between each basement type is not clear on this line.

- Basement 1: Parallel (horizontal or dipping) and folded reflectors. Start of line to CDP 310.
- Basement 2: Faulted blocks defined by high amplitude reflectors. CDP 1150-1310.
- Basement 3: Discontinuous high amplitude reflectors that are horizontal, seaward or landward dipping. CDP 310-1150.

Below a water depth of 2000 m (CDP 2020) it is difficult to analyse this line due to the rough topography and side echoes, but high amplitude reflectors are present.

4.3.1.2. Interpretation of Line 1

Basement Type 1 is probably relatively flat lying Triassic or Permian sediments of the Sydney Basin. It underlies the upper slope on this line. The boundary between it and Basement Type 3 is near the start of this line but cannot be clearly identified.

The fault blocks associated with Basement Type 2 were probably formed during rifting of the continental crust c.100-80 mybp. At this location the strata involved are most likely Palaeozoic.

Basement Type 3 is interpreted as volcanic because the discontinuous, disruptive internal reflections are characteristic of lava flows. On their upslope portion they are subhorizontal to landward dipping, but beyond the break in basement slope they dip seaward. Similar sequences

have been drilled on the continental margins of the north Atlantic (Rockall Plateau: Roberts et al., 1984, Norway: Eldholm et al., 1987, Greenland: Larsen et al., 1994) where they are known as 'seaward dipping reflectors' and are mostly subaerial flows interbedded with minor sediment. Volcanics with similar seismic characteristics occur on the Western Australia margin (Symonds et al., 1998), the Kerguelen Plateau (Borissova et al., 2002) and the Norfolk Ridge (DiCaprio et al., in press). The more prominent reflectors in the basement seaward of CDP 890 could be sills in Unit 5 sediments and/or more seaward dipping flows interbedded with the sediments.

These volcanics are younger than the rifting because they overlie, or intrude, sediments that overlie the rift fault blocks to their east. The volcanics are also older than some strata in Unit 5 because these strata onlap the volcanics indicating the volcanics were already a topographic high when those sediments were deposited. Evidence from this seismic line alone discounts an alternative possibility that Basement Type 3 is a faulted up block of Permian Gerringong Volcanics. The Gerringong Volcanics are part of the Sydney Basin that outcrops as interbedded lavas and sediments along the coast 60 km west of this location (Retallack 1999).

East of CDP 2020 in deeper water near the end of the line the basement appears to be at or near the surface and is possibly also volcanic.

The sedimentary Units 4 and 5 accumulated in a subsiding post-rift basin and are interpreted as Upper Cretaceous mudstones with more sand-rich layers in Unit 4 causing the stronger reflectors. Rocks of this age and lithology have been dredged previously from this margin (Heggie 1993).

Unit 3 is a widespread, flat, relatively thin unit that unconformably overlies Basement Types 1 and 3 as well as the Cretaceous sediments. Its high amplitude suggests it is well lithified and based on its geometry and earlier dredge hauls from this margin it is interpreted as a glauconitic limestone (Heggie et al., 1993, Quilty et al., 1997). The dredge samples were well cemented calcarenite consisting of shallow marine fauna that dated it as Paleocene. It appears that Unit 3 represents an extensive, flat continental shelf of Paleocene-Eocene age with low input of siliciclastics allowing for the formation of a relatively thin but laterally continuous glauconite and carbonate horizon. It is important to note that this shelf has been tilted to its present dip since the Eocene and may have been down-faulted in deeper water as some dredge samples were from water depths of over 3000 m.

Sedimentary Units 1 and 2 represent post-Eocene sedimentation on this margin. They reach their maximum combined thickness at the shelf break (not on this line) and thin down slope. Where the Quaternary-Pliocene sediments have been sampled on the slope they have variable carbonate content (15 to 60%) and a mud content ranging from 25% to 95%. The composition and texture cycles recognised down core reflect the glacial-interglacial sea level cycles. Internal reflectors in Units 1 and 2 suggest that the lithology has similar variations back in time caused by the relative balance between terrestrial input, particularly nearness to deltas, and ocean productivity. Progradation in Units 1 and 2 is the result of hemipelagic sedimentation on the upper continental slope which could be enhanced during lowstands when carbonate sediments are swept off the shelf and deposited as wedges on the upper slope.

The sediment wedge on this line has failed on two internal surfaces that cannot be specifically identified. A contributing factor causing a thicker section to fail further down slope may be the break in slope of the underlying basement at that point. This has allowed differential compaction to steepen the sediments and weaken them at this point by faulting. Upslope, the lower sediment section has remained but has moved enough to display disrupted bedding and low angle faulting. Despite there being two horizons that failed, it appears to be just one event. Evidence for this is the relatively large lens of debris down slope with no indication that it is made up of two parts.

Regarding the timing of the Shovel Slide, it can only be said that it is the youngest event identifiable on this seismic line. There is no evidence on this line for sedimentation since the slide event occurred. However, the lower frequency seismic sources used in this survey would require several meters of sediment to have accumulated before they would be recognisable as a 'drape' or 'pond' on the surface topography.

4.3.1.3. Analysis of Line 2

Line 2 is a 10 km tie line in deep water (~2,500 m) between Lines 1 and 3 and it crosses the major slide in the region known as the Bulli Slide ([Figure 4.8](#)). The line shows high amplitude, subhorizontal reflectors at and just below the sea floor. At the start of the line there is an acoustically transparent wedge of sediment.

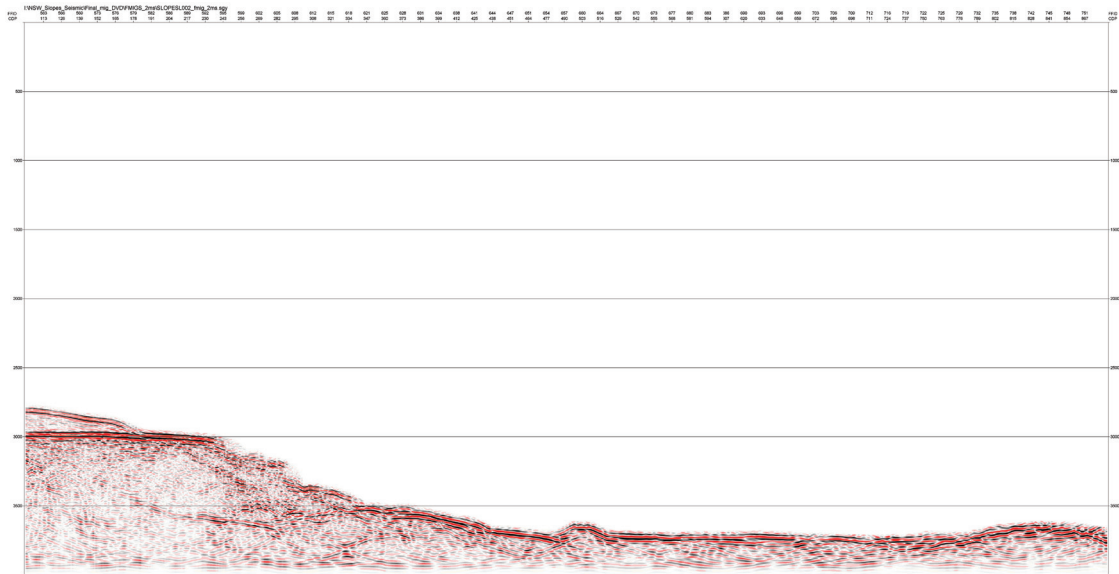


Figure 4.8 Seismic Line 2

4.3.1.4. *Interpretation of Line 2*

The sediment at the start of the line is the edge of the debris slump deposit described for Line 1. Between CDP 250 and 350 there is more debris slump deposit. There is no evidence for any other significant sediment thickness on the sea floor. The basement reflectors are interpreted as volcanic rock of Basement Type 3. They form the slip surface for the distal part of the Bulli Slide.

4.3.1.5. *Analysis of Line 3*

This line starts in 2760 m of water and goes upslope following the axis of the Bulli Slide and ends in 250 m of water. It is 32 km long and approximately 10 km north east along the continental slope from Line 1 (Figure 4.9). The aim of this line was to determine the nature of the sea floor ridge on the upper slope and its relation to the major slide on its seaward side.

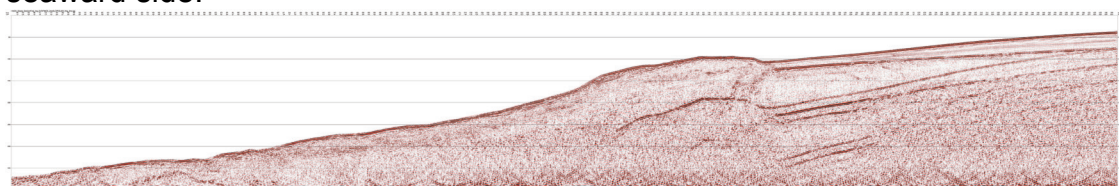


Figure 4.9 Seismic Line 3

The landward end of the line has a sediment wedge similar to Line 1, but here Units 1 and 2 (370 ms) are slightly thicker for the corresponding water depth of 330 m. Unit 1 has some distinct internal progradation (CDP 2390 to 2610) and Unit 2 has distinct downlap onto Unit 3 between CDP 2000 and the end of the line. Unit 3 is again high amplitude, flat and 30 to 50 ms thick.

The sediment wedge thins down slope and ends abruptly where it abuts a topographic basement high on the seafloor. Unit 1 onlaps the high forming a topographic basin at 800 m water depth. Unit 2 has more discontinuous reflectors with variable dips between CDP 2000 and the high. Unit 3 has a distinct thickening (CDP1840-1880) as it nears the high.

The only other sedimentary reflectors on this line are a lens (100 ms thick) of high amplitude discontinuous reflectors on the seaward slope of the high between CDP 1430 and 1600. This may be equivalent to Unit 4 on Line 1.

The three types of basement defined for Line 1 are again present.

- Basement Type 1: Subhorizontal parallel reflectors between CDP 1870 and 2060 are 60 ms thick and overlie folded reflectors which continue from CDP 2060 beneath Unit 3 until the end of the line.
- Basement Type 2: A single faulted block defined by high amplitude dipping reflectors at CDP 510 and 200 ms sub-sea floor (WD 2500 m).
- Basement Type 3: Discontinuous high amplitude reflectors with irregular dips but mostly dipping seaward from 2500 m water depth (CDP 440) to the top of the high at a water depth of 700 m (CDP 1670).

The reflectors are parallel to the sea floor over most of this distance and at least 1000 ms thick. Except for the Unit 4 lens of sediment, the basement appears to outcrop over this interval until it goes subsurface beneath the sediment wedge at CDP 1820. There is an indistinct but near vertical boundary with Basement Type 1 near CDP 1870.

4.3.1.6. Interpretation of Line 3

The basement fault blocks in deep water are similar to those in Line 1 which is about 10 km to the south and they are at a similar depth below sea level. They are also interpreted as Palaeozoic basement, faulted during rifting.

On this seismic line Basement Type 3 dominates all lithologies. It clearly outcrops as a topographic high on the upper slope at 700 m water depth. The high and the predominantly seaward-dipping reflectors are interpreted as lava flows perhaps with some interbedded sediment. They form the 'slip surface' for the Bulli Slide. Nearly all the overlying Units 4 and 5 present in Line 1 are missing here. This volcanic Basement Type 3 rock again overlies the faulted basement and is older than the sedimentary remnant of Unit 4 on its seaward slope. It is also older than Units 1, 2 and 3 as they onlap it on its western margin. Its western boundary is indistinct below Unit 3, but must be steep as Basement Type 1 occurs within 4 km. On this line, the volcanic high is part of an outcropping ridge along the margin and the subsurface volcanic high identified in Line 1 is its southern continuation. Its extent, uniformity of dip down slope on its seaward side, sub horizontal flows on its crest and its thickness of at least 1000 m are against it being interpreted as a faulted block of Palaeozoic Gerringong Volcanics. Basement Type 1 consists of a thin sequence of flat lying Permo/Triassic unconformably overlying readily identifiable folded Palaeozoic rocks.

The only sediments overlying the volcanics on the seaward side are a remnant lens upslope of the slide surface. This lens cannot be a Tertiary accumulation as the volcanic ridge was a barrier throughout this time. It most likely correlates with Unit 4 of Line 1 and consists of marine sandstones and mudstones of Late Cretaceous age.

On the landward side of the volcanic ridge, sedimentary Unit 3 is again a flat deposit of uniform thickness on an unconformity surface. The volcanic ridge on this line would have been a volcanic island in the Paleocene/Eocene sea, as there is a distinct current scoured channel and fill structure in Unit 3 where it abuts the volcanic ridge. Unit 3 is again interpreted as a coarse-grained glauconitic shelf limestone.

Units 1 and 2 show evidence of progradation but no slumps or incipient faults presumably because of the buttressing affect of the volcanic ridge. The loss of coherence of the reflectors in Unit 2 as it approaches the volcanics may be a lateral facies change as more sand is deposited and mud winnowed by the increased currents around the volcanic high. Both Units 1 and 2 onlap the volcanic high. The Bulli Slide is the youngest event recognised on this seismic line as no sediments can be identified as post slide.

4.3.1.7. *Analysis of Line 4*

Line 4 is a 15 km long line that ties the upslope ends of Lines 3 and Line 5. It starts in a water depth of 300 m and follows a very flat sea floor to the north to end in 370 m water depth (Figure 4.10). An along-strike section of the sediment wedge is recorded in this seismic line. Unit 1 consists of continuous and parallel reflectors and maintains a thickness of 220 ms over the length of the line. Unit 2 is also characterised by parallel reflectors but they are of lower amplitude. The lower reflectors in this unit are discontinuous because they fill the topographic lows in the underlying Unit 3. The thickness of the unit varies from 60 (CDP 915) to 140 ms (CDP 260). Unit 3 is again a high amplitude reflector 40 ms thick and draped over the underlying topography.

Basement underlying Unit 3 consists of slightly wavy, near horizontal reflectors (Basement Type 1). They have a thickness of 100 ms, below which the multiples of the overlying strata make analysis impossible.

4.3.1.8. *Interpretation of Line 4*

The basement rocks for this line are flat lying sedimentary strata, probably belonging to the Permo/Triassic of the Sydney Basin. The relief on this unconformity surface is gentle and less than 50 ms. It is significant that there are no valleys cut into it. This reflects the lack of any drainage basin landward of this part of the shelf.

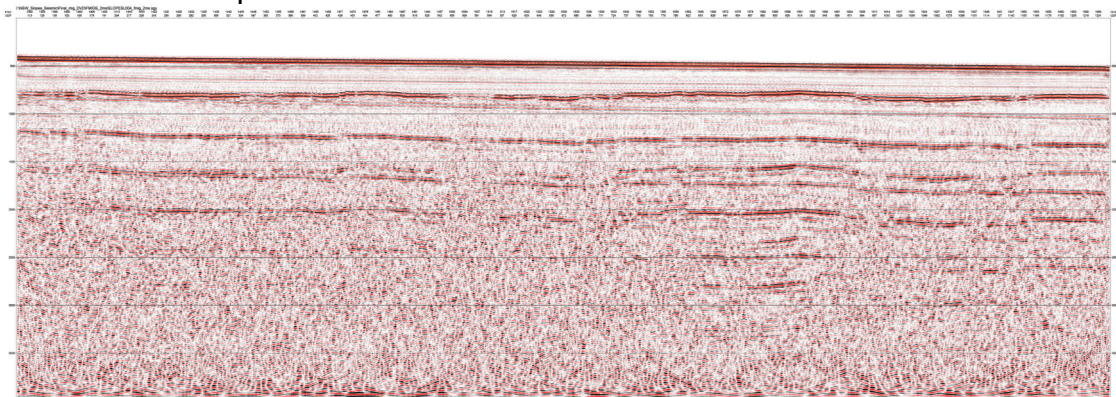


Figure 4.10 Seismic Line 4

Unit 3 again has all the characteristics described for previous lines and is a typical calcarenite shelf deposit. It was able to be deposited as a drape over the topography because the topographic relief is so gentle.

Unit 2 filled the slight depressions on the top of Unit 3 first, as the toe of a prograding wedge built out as the shelf subsided. Sediment in Unit 2 is probably mud-rich because of the continuity of low amplitude reflectors. The lack of channels or slump features suggests it formed by a relatively slow accumulation of marine muds off the shelf break, rather than a prograding delta.

Unit 1 is also remarkably uniform in the thickness of reflectors, their continuity and the fact that they all remain parallel to the present day sea floor. No channels or slumps are present.

4.3.1.9. *Analysis of Line 5*

Line 5 runs down slope for 18 km from water depths of 340 to 1500 m. It crosses a surface slide obliquely. Its aim was to trace the subsurface northern extension of the basement ridge crossed on Line 3 and identified in the subsurface of Line 1. It is parallel to and 15 km along slope from Line 3 (Figure 4.11).

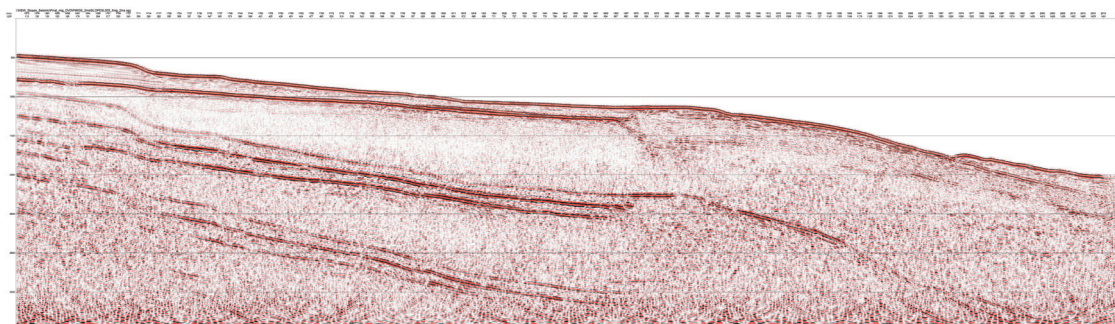


Figure 4.11 Seismic Line 5

The sediment wedge extends from the start of the line to CDP 900 where it terminates by onlapping a relatively steep landward side of a basement high. The wedge consists of three seismic units. Going down slope the Units 1 and 2 can be divided into an undisturbed and a disturbed length.

Unit 1 is 220 ms thick and shows progradation down to CDP 252 where there is a scarp on the sea floor with low angle faults displacing the underlying sediment down slope. Unit 2 conformably underlies Unit 1, and is 70-80 ms thick. The faults extend into Unit 2. The top third of Unit 1 is missing and the remaining lower section of Unit 1 and Unit 2 are both disturbed by sediment slumping. From CDP 610 to 780 there is a lens of high amplitude reflectors 30 ms thick at the base of Unit 2.

Unit 3 is 40-50 ms thick and consists of high amplitude, continuous reflectors that are relatively flat and overlie basement. This unit forms a surface that is inclined seaward at a slightly lesser slope than the sea floor.

Between CDP 900-1080 and between CDP 1200-1290 there is probably a thin drape of Unit 1 sediment over basement but it is difficult to resolve. Between CDP 1080 and 1200 there is a sediment lens (Unit 4?) that can be resolved and is 70 ms thick and thins both up and down slope. Down slope from CDP 1290 there is a slump deposit (Unit 4?) that thickens to 250 ms at the end of the line.

This slump deposit is underlain by seaward dipping reflectors of Basement Type 3. These seaward dipping reflectors are at least 1000 ms thick and extend upslope with no convergence to the basement high where they are more flat lying. The western margin of the basement high has reflectors that dip seaward and shallower reflectors that dip landward. Landward of this high and underlying Unit 3 are relatively flat reflectors (Basement Type 1).

4.3.1.10. Interpretation of Line 5

The most recent features on this line are the two slides/debris flows (Slides 1 and 2 on Figure 4.6). One is in the down slope part of the sediment wedge and the second is on the face of the seaward dipping basement reflectors. The flow path of the upper slide and debris flow was diverted to the north of this line and into a canyon head because of the shallow subsurface volcanic ridge. The volcanic ridge is a continuation of the ridge identified on Lines 1 and 3 and may continue to deepen along slope to the north east and be exposed at greater depth in the canyon floor where further slumping can be recognised on the multibeam bathymetry. The material that is missing is late Cainozoic and has failed along a surface about a third from the top of Unit 1. Disturbed bedding in the sediment remaining suggests it has moved on the Paleocene/Eocene limestone surface of the underlying Unit 3. The lower slide has moved only about 4 km down slope as a relatively coherent block. It is probably Cretaceous sediment (equivalent to Unit 4 on Line 1).

Basement Type 3 is again interpreted as volcanic, probably formed by subaerial lava flows interbedded with sediment. The uniform nature of the reflectors and the variable (but generally seaward dip) is typical of flows. At this location the measured seismic penetration of 1000 ms means

they are at least 1000 m thick (assuming a velocity of at least 2000 ms⁻¹). The western margin of Basement Type 3 is again an abrupt, steep contact with flat-lying Permo /Triassic beds of the Sydney Basin.

4.3.1.11. *Analysis of Line 6*

Line 6 is a 31 km long strike line tying Lines 1, 3 and 5 (Figure 4.12). It starts in the north east and crosses Line 5 in 1250 m of water and runs roughly along slope crossing Line 3 at 1150 m water depth and Line 1 at 1260 m water depth and ending on the sediment wedge at 1140 m. It crosses both the Bulli and Shovel Slides.

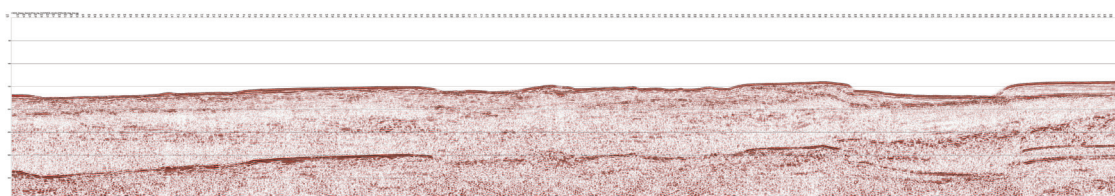


Figure 4.12 Seismic Line 6

From the start of the line to CDP 170 there is 80 ms of slumped sediments (Unit 4) overlying Basement Type 3 correlating well with where it crosses line 5. The high amplitude but discontinuous reflectors in the basement are near horizontal and penetration is generally around 1000 ms. Between CDP 170 and 420 the basement is at, or very near, the surface. From CDP 420 to 1030 there is an identifiable lens of sediment of variable thickness (<80 ms) overlying a relatively rough Basement Type 3 surface. Between CDP 1030 and 1660 the line passes over the upper failure surface of the Bulli Slide. Basement Type 3 is at or very near the surface except for a small ridge of sediment left behind after the slide.

On the southern margin of the Bulli Slide the basement rises 50 ms and two seismic sequences overlie the basement. They thicken along line to the edge of the Shovel Slide at CDP 1940 where they are 400 ms thick. The lower sequence progrades out from the basement high whereas the upper sequence onlaps and drapes the high. At this location, immediately north of the Shovel Slide, the upper sequence can be identified as Units 1, 2 and 3 down to 200 ms and the lower sequence as Unit 4 from 200 to 450 ms depth. Unit 4 has high amplitude reflectors at its base and has a maximum thickness of 250 ms beneath the slide (CDP 2010) then thins

(eroded?) southward to zero at CDP 2440. It is the same as Unit 4 on Line 1, as it can be correlated where the two lines cross.

Where the line passes over the Shovel Slide (CDP 1940 to 2250), Units 1 and 2 are missing. The failure seems to have occurred on the high amplitude top reflection surface of Unit 3. Some sediment (disturbed?) remains on the northern third of the floor of the slide. South of the slide Units 1 and 2 are 300 ms thick and they thin gradually to 260 ms at the end of the line.

Below Unit 4, and with an apparent dip to the north-east, there is 700 ms of sediments that can be correlated to Unit 5 on Line 1 where the two lines intersect. The northern contact of these sediments with the Basement Type 3 is difficult to determine. This may be due to the line being oblique to the strike of the strata and basement ridge. Basement beneath Unit 5 has discontinuous high amplitude reflectors that also rise to the south and may be the continuation of Basement Type 3 at depth. There are diffuse but high amplitude reflectors beneath Basement Type 3 that may be Basement Type 2.

4.3.1.12. *Interpretation of Line 6*

From the start of this line to the southern edge of the Bulli Slide there are volcanic flows at or near the sea floor and down to a sub-sea floor depth of at least 1000 m. They are near horizontal because this is a strike line. They are again interpreted as subaerial flows that may be interbedded with sediments, particularly below about 500 m, and they can be correlated with similar volcanic seismic facies on the dip Lines 1, 3 and 5. They are overlain in part by a thin layer of Cretaceous sediment (Unit 4) that slumped, and some that is *in situ*. The southern margin of the Bulli Slide corresponds to a rise in the volcanic basement. South of the Bulli Slide, the volcanics are buried by a prograding wedge of sediment (Unit 4), overlain and onlapped by Units 1 to 3. The exact relationship to the volcanics and their boundary with it is not clear. There is onlapping and draping of Units 1, 2 and 3, but it is also possible that the prograding sequence is a lava delta rather than Unit 4 sediments. The 800 m thick Unit 5 has apparent dips north-east on this line and south-east on Line 1, so its true dip is more to the east which is the direction of the main excavation by the Bulli Slide. Its relationship to the volcanic high is unclear, but may consist of intruded sills and be interbedded with flows. The Cretaceous section (Units 4 and 5)

thins to 500 ms at the end of this line.

Below Unit 5, and possibly interbedded with it, are reflectors similar to those in Line 1. These are again interpreted as sills. A block faulted basement may underlie them and both become shallower towards the end of the line.

The Shovel Slide appears to have failed on Unit 3 on this line. The high amplitude reflectors of Unit 3 are very close to the sea floor at the southern margin of the slide scar. It is not possible to determine how much sediment overlies this failure surface in the slide area.

4.3.2. Analysis of High Resolution TOPAS Data

The subsurface profiling in the Sydney/Illawarra region was useful in characterising the Shovel and Bulli slides and the presence or absence of hemi-pelagic sediment drape ([Figure 4.13](#) and [4.14](#)). The seafloor morphology in this region is characterised by a large number of incipient failures and creep features on the surface. Hemi-pelagic drape, where imaged, appears to be restricted to a relatively thin layer, suggesting that the failures occurred comparatively recently in this region. There is some localised evidence of previous failure events in the subsurface.

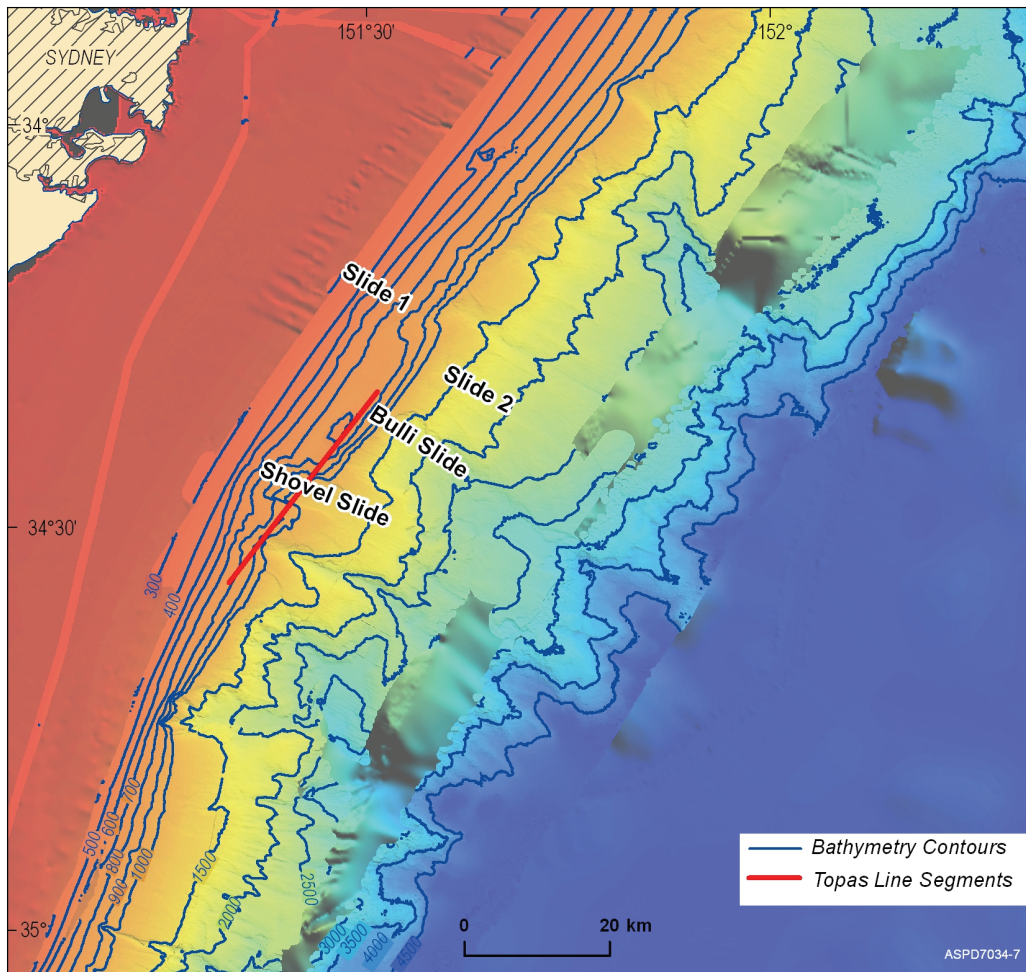


Figure 4.13 Location of TOPAS transect across the Bulli and Shovel slides

The seabed and sub-bottom reflectors on the upper slope in this region are mainly flat, with several basement outcrops evident. Sub-bottom reflections are highly conformable, and it is not possible to clearly distinguish individual depositional packages. This series of parallel sub-bottom reflectors are underlain by a strong, laterally extensive reflector with smoothly undulating morphology. This reflector forms the acoustic basement across much of the shelf in this region at around 10–60 ms (~7–45 m). Localised areas on the upper slope display strong shallow basement reflections, and show thinning hemi-pelagic drape towards basement outcrop and canyons. Seabed reflections within canyons are prolonged and indistinct or hyperbolic, with little sub-bottom penetration, suggesting rocky substrates with little or no sediment cover.

In the southern part of the Sydney/Illawarra region, to the south of the Shovel Slide, the seabed morphology on the upper slope becomes more undulose and sub-bottom penetration is variable, generally poorer

than areas further north. The laterally extensive pelagic drape visible across the greater part of the survey area, is not apparent in the data in this area. At the very southern edge of the Sydney/Illawarra region, a series of shallow erosional features, similar to those evident within the Shovel Slide, can be seen in the seabed morphology. These are manifested as a series of sinuous crests with indistinct, prolonged seabed reflections and faint, intermittent sub-bottom reflections. As these features extend downslope, their morphology becomes more extreme, the steepening walls giving rise to a series of overlapping hyperbolic reflectors at varying elevation.

4.3.2.1. Shovel Slide

Nine sub-bottom profiler lines intersect the Shovel Slide. Data quality is reasonable in the upper slope region, with penetration averaging 13 ms (~10 m). Within the slide, sea floor penetration is minimal, although the morphology of the slide scar is clearly imaged. The data reveal a hummocky morphology on the floor of the slide, with rills and gullies ranging in height to approximately 50 ms (~38 m). The head scarp is distinctly visible and some deposition on the lower slope is apparent.

Evidence of pelagic sedimentation within the Shovel slide is minimal in comparison to the slides in the Myall region to the north (see later section on the Myall region). This suggests that the failures in the Sydney/Illawarra region are relatively recent, or that active down slope sediment transport is occurring within the slide scars.

Upslope from the Shovel Slide, well bedded sediments are visible to a depth of 25 ms (~19 m), and there is evidence of a small buried slide just above the head scarp.

Subsurface penetration to the south of the Shovel Slide is around 13 ms (~10 m) and the data reveal well bedded sediments which show recent evidence of creep in a series of small faults which reach the surface. To the north of the slide, the seafloor reflector becomes irregular and prolonged with no sub-bottom penetration, signifying an exposed bedrock outcrop (the Bulli Basement Block).

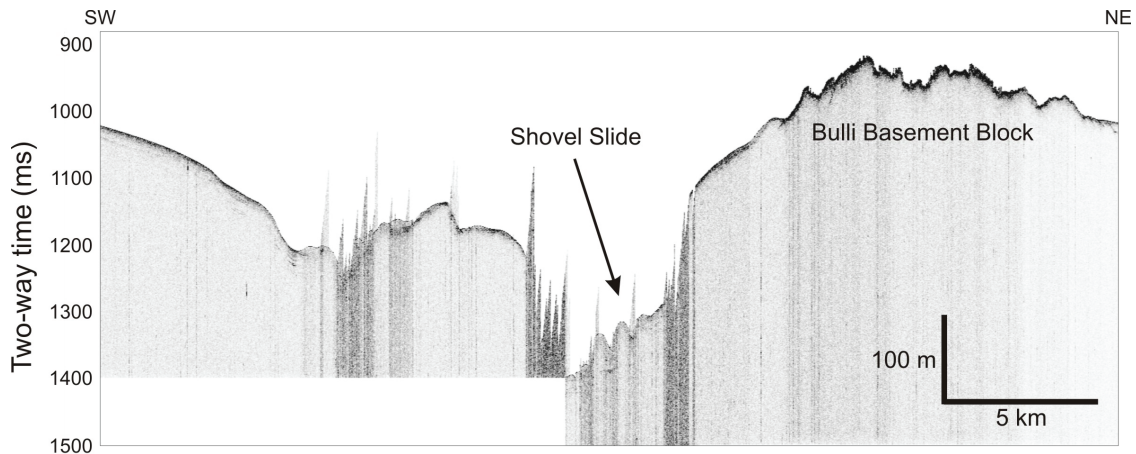


Figure 4.14 TOPAS profile across the shovel slide and adjacent Bulli basement block

4.3.2.2. *Bulli Slide*

Seven sub-bottom profiles intersect the Bulli Slide and surrounding region. The combination of steep seabed morphology and deep water resulted in lower than average data quality in much of the sub-bottom profiler data acquired across the Bulli Slide.

The seabed within the slide was poorly imaged, with no coherent seabed reflection, although the overall shape of the excavation and the side walls are evident. Data across the north-eastern wall of the slide reveal an irregular seabed with minimal sub-bottom reflections, indicating little sediment cover and a rugged morphology on the lower shelf.

The Bulli Basement Block is manifested in the data as a prolonged, irregular seabed reflection with no sub-bottom reflectors. At the north-western edge of the bedrock complex, the seafloor reflection and sub-bottom characteristics abruptly change, with sub-surface penetration reaching a depth of 10 ms (~8 m). Further to the north of this complex, a series of acoustically transparent features indicates a possible previous failure that has been covered by an irregular drape (~ 3 ms or 2 m). A faint second reflector at 40 ms (~30 m) beneath the sea floor is also evident.

Upslope of the Bulli Basement Block intrusive or volcanic complex, seafloor penetration is good, revealing finely bedded sediments to a depth of around 13 ms (~10 m). Small faults can be seen in the profiles, and a series of movements are visible on the sea floor. Some sections display evidence of historic failure in the subsurface, characterised by erosional and depositional features.

4.3.3. Geomorphology

4.3.3.1. Results of geomorphic interpretation

Multibeam bathymetry was collected in the Sydney / Illawarra region over water depths of 300 to 3500 m (Figure 4.15 and 4.16). These data allow characterisation of the geomorphic features on the continental slope in an area extending along the margin for 135 km and across the margin for 35 km.

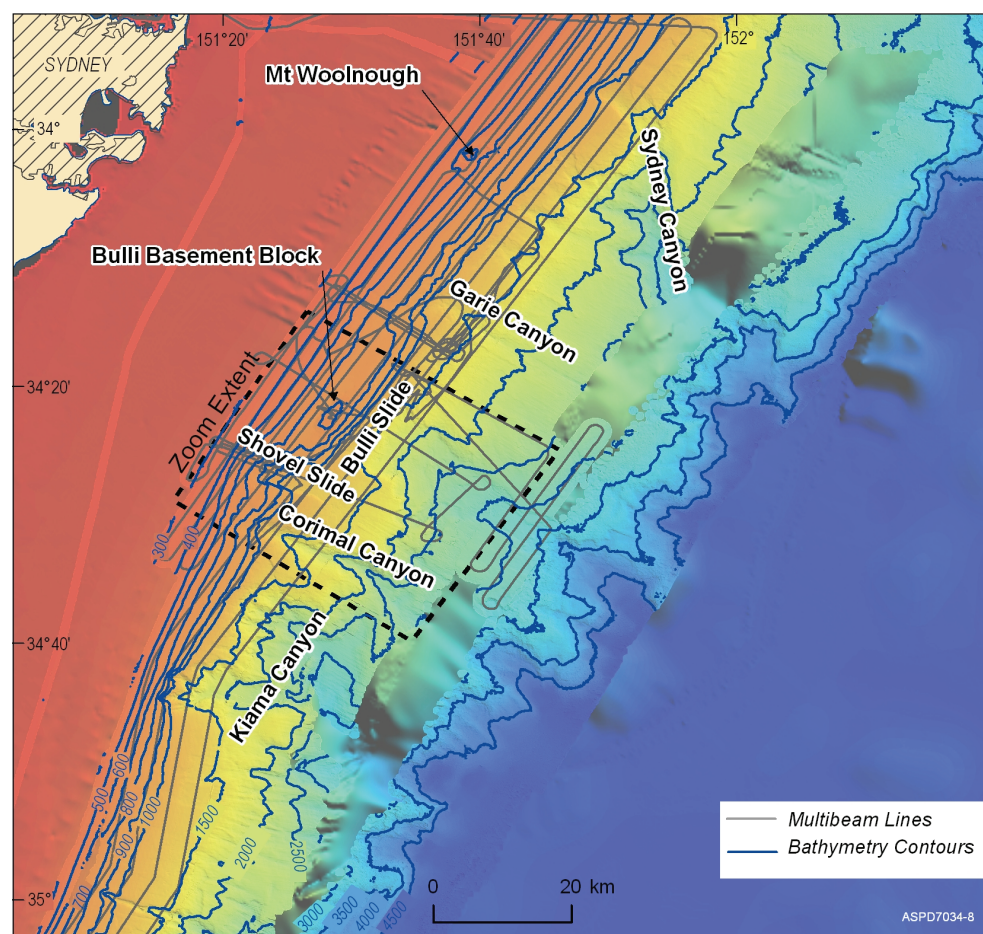


Figure 4.15 Overview location of the Shovel slide and Bulli slide

The southern 25 km of margin in the Sydney/Illawarra region has a different orientation to that further north. The structural contact with the abyssal plain continues the Jervis Bay region strike of 020° whereas the isobaths on the upper slope are more northerly at 015°. The continental slope is 40 km wide and the gradients are: A uniform 4.7° from 400 to 2000 m, then a 1.2° terrace 2000 to 2200 m followed by an increase in gradient for the mid-

slope (9° but largely un-surveyed) and a very steep (30° from 4000 to 4500 m) and deeply dissected lower slope below 3800 m.

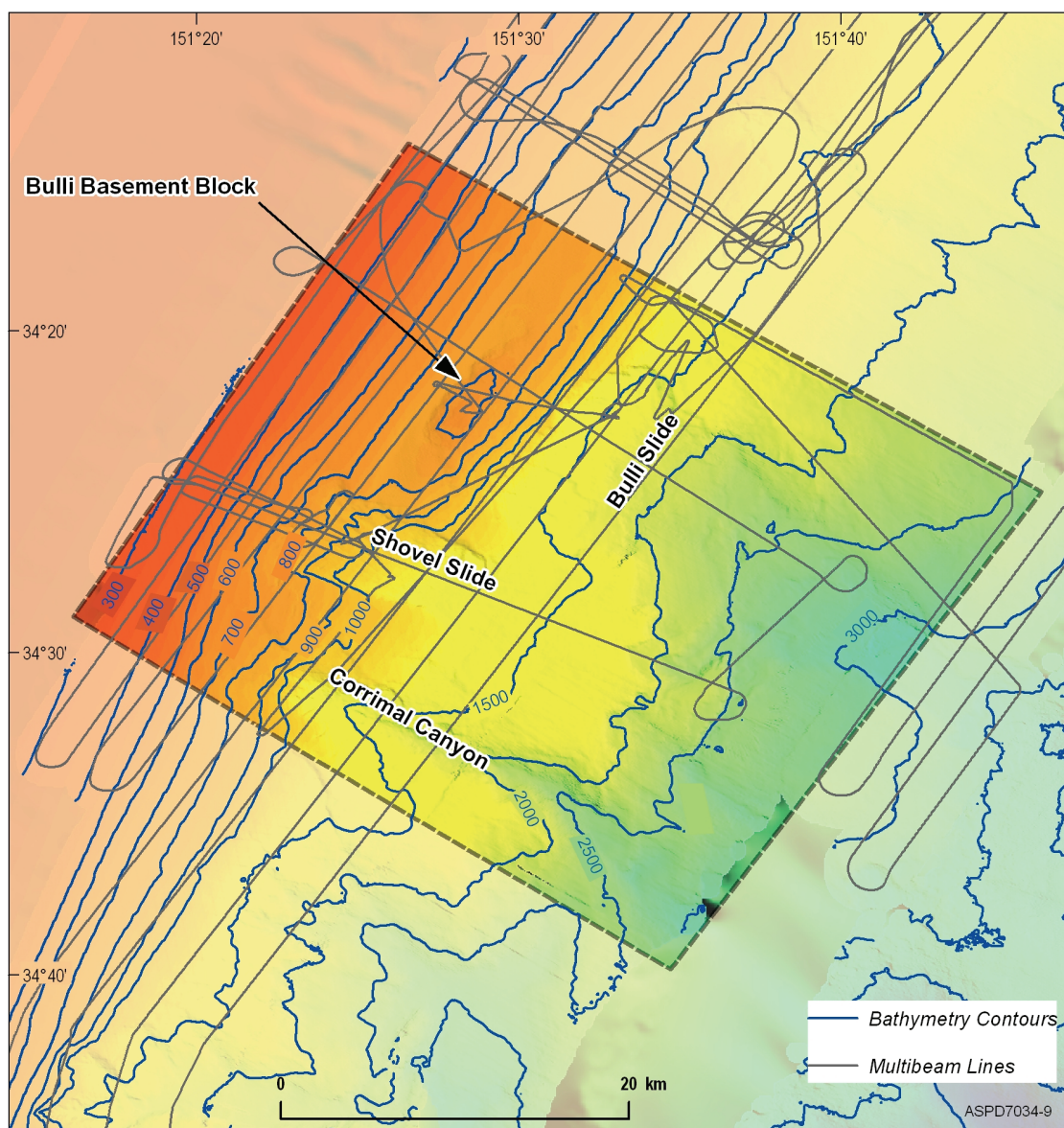


Figure 4.16 Location of the Bulli Basement Block, and the Shovel and Bulli slides

The upper slope above 1800 m is devoid of canyons and in general lacks the increase of slope in the 1500 to 2500 m interval characteristic of the Jervis Bay region. It is relatively smooth with some low relief mass movement features. A debris flow deposit (34.8201°S ; 151.1966°E) occurs at 560 m on slopes of 5.3° . The head of this slump extends into water shallower than the 400 m edge of the survey. Three linear ridges and scours centred on 34.9256°S ; 151.1872°E at a water depth of 836 m are sub-parallel to isobaths. There are small incipient slump scars all down the

slope which become bigger and more common below 1100 m. For example there is a 3.5 km scar at 34.9412S; 151.2087E and water depth of 942 m.

At the southern part of this area there has been significant mass movement on a 10 degree scarp between 1600 and 1900 m. Over a distance of 8 km, chevron slides perhaps 100 m thick have moved 1-2 km down slope. There are 30 m depressions above the slide blocks (34.9804S; 151.3082E)

The next 25 km of this region is characterised by a complex retrogressive canyon system (Kiama Canyons [Figure 4.15](#)) that is located at a change in strike direction. North of this location the strike of the lower slope is 035° (was 020°) and the strike of the upper slope 030° (was 015°).

The southern part of the Kiama Canyon complex consists of three parallel, closely spaced linear canyons that trend east with three linear tributaries joining them from the north-west. They are all incised into the upper slope and have eroded back to the 750 m isobath (34.7390S; 151.2441E). These tributaries join where the floor descends to 1900 m and where it opens out to be 4 km wide with steep relief of 500 m (1500 to 2000 m) on the northern side and with a small dome and prominent ridge part way up the southern side of the canyon (34.7471S; 151.3265E, WD 1634). The floor then narrows down slope to 1.5 km and is deflected north by a resistant dome. This steep sided dome is 7 km wide at its base and rises 500 m above the surrounding sea floor at its summit (34.7676S; 151.3993E, WD 1634 m). In contrast the northern tributaries of the Kiama Canyon complex form a broad amphitheatre eroded by retrogressive sediment failures in the mid and upper slope. The most recent crown scarps can be clearly seen at 900 m (e.g. 34.6078S; 151.3313E and 34.5572S; 151.3612E). They join with the southern tributary at 3100 m.

Corrimal Canyon (centred around 34.2289S; 151.6324E [Figure 4.15](#)) is a distinct linear erosional feature. It extends down slope for over 20km from 940 m to over 2800 m water depth with a gradient of 4.9 degrees. The upper part of the canyon is 400 m deep and 4.5 km wide. It displays a multi-phase erosional cross-section, evidenced by a wide canyon with a narrower incision in its floor. The inner valley starts in the floor at 1640 m water depth, is 1 km wide and 100 m deep. The valley sides show individual slumps from 900-3000 m in width. The upper canyon is characterised by smaller retrogressive slides that extend back 1.5 km from the canyon wall with 40 m high headwall scarps. A relict erosional feature (possibly a retrogressive slump) also occurs above the canyon

head, extending upslope to a depth of 560 m.

The Shovel Slide is a straight-sided slide centred at 34.4519S; 151.4358E (Figure 4.15) that extends down slope for 14 km between depths of 400 m and 1315 m. The slide consists of an erosional upper slide 7.5 km long and a depositional lower slide mass 6.5 km long. The upper slide is up to 7 km wide, narrowing to 5.5 km near the base. The base of the slide is asymmetrically deeper to the south, with the southern lateral scarp up to 200 m high and the northern scarp stepped, and up to 120 m high. The floor of the slide exhibits many linear features ranging from 2-40 m deep, 50-500 m wide, and up to 5.5 km long. The main slide has a bifurcated head, and includes several small slumps along the side walls. The total estimated volume of the Shovel Slide is 7.97 km³.

A large outcropping basement block occurs on the upper slope above the Bulli Slide centred at 34.3712S; 151.4828E (Figure 4.15) and extending for 11.4 km along slope. It has a relief of at least 111 m, extending from 787-676 m on the upslope or western margin and from 662-990 m (328 m) on the eastern side. The basement feature has a broad elongated mound shape, with an erosional moat along the western margin, presumably due to the south flowing East Australian Current. A depositional lee ridge has accumulated sediment in the southern or downdrift area behind the basement block. There are several minor seabed features that have significant relief and rugosity lying 5 km and 12 km north of the main Bulli block (Figure 4.15). This suggests that basement is close to the surface throughout this region north of the basement block at least as far as Garie Canyon.

The Bulli Slide is the largest gravity failure feature in the Sydney / Illawarra Region and is centred at 34.3955S; 151.5376E. It has an arcuate plan shape with a maximum width in the upper erosional slide area of 11.35 km, where a relief of 380 m occurs from 1330 to 1710 m at the maximum width cross section. The slide feature descends from 950 m to over 3300 m water depth over a distance of 22.3 km. This represents a seabed slope of 5.9°. The lower part of the slide widens to 14.5 km and has a relief of 660 m from 1800-2460 m. The Bulli Slide is a complex feature and may have a composite, multiphase history. It is located immediately down slope from the large Bulli Basement Block and this feature may have strongly influenced gravity failure processes (e.g., by differential compaction). Internally the upper part of the Bulli Slide consists of at least three distinct sections. The middle section is around 2 km wide and up to 50 m higher

than adjacent sections. The southern section is lower in elevation and has 1-2 large grooves in its surface. The northern section is the lowest, but has a slope of 1.5° (a fall of 70 m over 2.5 km) to the south where it abuts the middle section. The margins of the slide are up to 200 m high and show frequent examples of collapse and down slope movement, creating blocks on the slide floor up to 50 m thick and 1000 m wide. While the upper part of the slide is complex and contains several sections and displaced blocks, it appears to be largely erosional down slope for at least 5 km. Over the next 9 km the slide has debris accumulated on the floor, and then returns to an erosional character for the remaining 10 km of our imagery. The slide continues beyond this to the junction with the Tasman abyssal plain in over 4500 m depth.

The chevron slides lie between the Bulli Slide and Garie Canyon (Figure 4.15). They are centred at 34.2962S; 151.5897E and consist of two main V or chevron-shaped slides adjacent to each other. The slides are up to 6.6 km wide and up to 40 m deep. The crown scarp appears to be 1.2-2 km upslope from the displaced mass. Compared to the adjacent Bulli and Shovel Slides, the chevron slides are smaller and do not appear to have suffered as much displacement. Seismic data indicate some ponded sediment in a basin at the top of the displaced mass, suggesting a possible older age for this feature. Erosional chutes lead down slope from each of the chevron slides, the northern chute is up to 52 m deep and around 2 km wide and the southern chute is up to 40 m deep and 1 km wide.

The two slides, upslope and south of Garie Canyon, have their head scarps located at around 400-500 m water depth. The slides are centred at 34.2570S; 151.5108E, extend around 10 km along slope and around 7 km down slope. The northern slide appears to be retrogressive with respect to the head of Garie Canyon and connects to it down slope and to the north. The southern slide debris has been translated 2.5 km down slope and redeposited. This southern slide is one of the few slides that exhibit both a slide scar and a complete adjacent slide mass deposit. This may be because the Bulli Basement Block provides a down slope buffer to retain the translated slide mass. This southern slide mass is around 3.5 km long and contains abundant blocks and hummocky surface with around 5 m of relief and an overall volume of more than 0.2 km^3 . The adjacent northern slide is of similar dimensions and volume, but the lower translated mass has retrogressively failed into Garie Canyon. Overall the relief across both slides is a maximum of 35 m. Both the northern and southern slides have a

relatively gentle head scarp with around 10 m of relief. The northern slide has a large slide block retained near the head scarp, indicating down slope creep of the slide mass.

Garie Canyon is similar to the other canyons in that it is a linear erosional feature that extends down slope from around 950 m to 2500 m water depth, a distance of 22 km over an average slope of 4°. This canyon is centred at 34.2295S; 151.6355E and has a characteristic abrupt head scarp with 120 m of relief. The widest section of the canyon is 4.1 km where it has a relief of over 200 m. It narrows down slope to a width of 2.5 km and a relief of 170 m. Further down slope it opens to 5 km wide and 130 m of relief. This canyon is less well defined than other canyons in the Sydney / Illawarra Region, and like the others has a scarp more pronounced on the northern side. Retrogressive slides at the head of the canyon are up to 8 km wide, with side scarps of up to 30 m relief.

Between Garie Canyon and the southernmost tributary of Sydney Canyon there ([Figure 4.15](#)) is a large block 5 km by 14 km with upslope failure scarps from 800 m down to a major surface failure scar at 1100 m. There is also shedding by gravity slides on its down-slope margin below the 1500 m isobath. Its surface slope averages 4.6° over 14 km from 800 m to 1800 m. A volcanic (?) pinnacle 100 m high is located (34.2092S; 151.7386E) on the 1700 m isobath on the down-slope margin of the block.

The head of Sydney Canyon consists of slump scarps in 880 m of water (centred around 33.9471S; 151.8072E) that open down slope into a broad amphitheatre 4 km wide with 140 m relief at 1000 m. The relief on the slumps is subdued and slope-parallel, perhaps because they are draped by younger sediment or have been modified by the EAC. From here the canyon runs down slope to the south-east for 11 km to 1800 m. The southern side is linear and steeper than the northern side. On its northern side there are three parallel narrow ridges running approximately N-S with 20-30 m of relief. Subdued slump scarps are common on the continental slope on either side of the canyon from around its head to 1800 m where it turns to the south and is linear and oblique to the continental slope for a further 12 km to 2800 m. It then turns SE for 20 km to 3850 m before turning south again for a further 12 km to the abyssal sea floor. The total length of the canyon is 55 km.

Four parallel tributary canyons join the Sydney Canyon from the west. They start as slumps at water depths of 750 to 950 m ([Figure 4.15](#)) and have eroded relatively straight paths directly down slope to the Sydney

Canyon. They join the main canyon as it runs south and where the floor descends from 2300 to 3100 m over a series of steps with 'plunge pools'. The four tributary canyons are relatively shallow (100 to 200 m deep and ~2 km wide at the 1250 m isobath), run down slope, and appear to have been initiated by back-stepping gravity slides. Many small gravity slides are evident in the heads and sides of these canyons down to 1900 m. Above this depth the adjacent continental slope on the north side is 4.3° , and below it becomes a more gentle slope of 2.5° .

Relief in the main canyon is greatest (750 to 600 m) where the canyon floor is between 1800 and 2500 m, the steepest side is initially the western side but below a floor depth of 2100 m the steepest side is on the east (seaward) as the floor continues to descend to the south. A linear ridge forms its eastern side, like a rampart along this length.

At 3850 m the floor of the canyon steps down 300 m into a 'plunge pool' that is over 100 m deep (water depth 4210 m) in the 3.5 km wide floor (34.2730S; 151.9915E). At this point the canyon sides have relief of 600 m up to the adjacent continental slope depths of 3600 m. The canyon exits on the abyssal plain at 4896 m as a broad channel, 6 km wide and 400 m deep.

Between the four tributaries there are three sediment blocks forming three down slope ridges. Many gravity slides are evident on their upslope margin and sides to a depth of 1900 m where there is a break in slope. Between the Sydney Canyon and its first tributary there is a fourth block of sediment. This block is 7 km by 7 km and 100 to 300 m thick. It lies at water depths between 1100 and 1700 m. Evidence for incipient gravity slides cover its surface, which has a slope of 6.2° . The equivalent slope interval immediately north of Sydney Canyon is only 4.2° . Its down-slope side has been cut away by the Sydney Canyon.

The upper slope above the Sydney Canyon and the 750 m isobath is a featureless depositional area except for one seamount and outcrops around its base. Mt Woolnough (referred to by fisherman as 'Browns Mountain' ([Figure 4.15](#))) rises 130 m from the surrounding sea floor (~550 m) to three peaks, the shallowest being 383 m (34.0333S; 151.6579E). It is a rugged feature (1 km wide at base) and is the eroded remains of a basalt cone. Associated smaller outcrops extend 4 km to the NE with up to 50 m of relief. Another 4 km to the SE in 780 m of water are five *en echelon* ridges of rock (high backscatter) 1.3 km long with up to 25 m of relief. They are 300 m apart and strike SW slightly upslope.

4.3.3.2. *Discussion of geomorphic interpretations*

The change in strike of the base of slope in the Sydney / Illawarra region is probably related to a change in direction of initial rifting and spreading. It implies a structural feature running down slope possible a transform fault. Evidence for this structural boundary is the linear nature of the southern tributary canyons that follows this boundary. On the southern side of this canyon at the mid slope are two resistant domes and a resistant ridge. They are interpreted as a synrift plutonic intrusion similar to Mt Dromedary and to those found on the slope further south described by Hubble et al., (1992) and dated at 100 mybp.

Linear ridges and scours along the slope above 850 m are probable evidence for the EAC modifying the upper slope sediment and older sediment slumps by generally smoothing them. The effect of the EAC encountering the Mt Woolnough seamount and nearby rock obstacles can be clearly seen in the sediment bedforms. The current eddies in the lee (south side) have eroded a 40 m deep moat at the base of the seamount with a broad (800 m wide) 10 m high depositional levee forming a 2 km tail downstream. There is a similar sediment ridge extending 2 km on the north side (winnowed shell lag?). The smaller outcrops are probably dykes and have also caused erosion scours between them and parallel to current with adjacent parallel (N-S) depositional ridges together with moats eroded in the lee sediments. The seamount has been dredged and is basalt (J Keene pers. comm. 2007,). It is the remnants of a basalt cone/plug with associated dykes outcropping on the nearby seafloor.

The Bulli Basement Block extends for 11 km along slope. The basement block represents a relatively uncompactable buttress at the seabed. Cainozoic sediments deposited down slope of the basement block contain high water contents and would compact at relatively faster rates than the basement block. As a result the gradients in this area would increase and thus increase the risk of sediment failure. It is then significant that the largest slide in the Sydney / Illawarra Region, the Bulli Slide is located immediately down slope of the basement block and extends along slope for approximately the same distance.

On the western side of the Bulli Basement Block, the south-flowing EAC has scoured a deep moat. On the downdrift southern side, a sediment drift has accumulated in the lee of the igneous intrusion. This sediment drift has formed a ridge and accumulated around 40 m of sediment above the regional slope trend. Immediately south of the lee drift is the lateral scarp of

the Shovel Slide. This scarp is steep and in several locations has a moat or shallow channel adjacent to the scarp. This moat and a number of bowl-shaped depressions on the scarp have not been infilled by sediment transported southward and prograding the lee sediment drift. This indicates either that the Shovel Slide acts as a conduit for down slope sediment transport or not enough time has elapsed since the slide, for sediment to infill these features. This would indicate a more recent age on the failure and impact of any tsunami generated.

The linear features on the Shovel Slide scar range from 2-5 m deep and 50-200 m wide to 40 m deep and 500 m wide. They are interpreted as erosional gullies and have a V-shaped profile and show some bifurcation down slope. It is possible they were formed initially by basal erosion during the mass failure and have been modified since by the processes of erosion and deposition but it is more likely that the features relate to erosional processes which have occurred since the slide events. The slide scars now provide conduits for down slope sediment transport, resulting in little accumulation of sediment in the scars. The bifurcated nature of the gullies argues against an alternative hypothesis that the gullies were formed as basal slide grooves during scraping of the displaced slide mass across a soft seabed. The later development of these features is also supported by the fact that the sediment cores did not penetrate into the unfailed sediment (see later discussion). The strongest evidence that they were caused at the time of the mass failure, is that they don't always follow the steepest gradient and some are discontinuous.

The deflection of the Sydney Canyon to the south by a ridge oblique to the slope in the mid-slope is the result of a structural feature of the underlying geology. This ridge (which forms the eastern side of the canyon in the mid slope), along with the three ridges near the head of the canyon, may be igneous dykes. Steps and plunge pools in the floor of the canyon below 2300 m are caused by outcrop of resistant strata.

Two relatively large blocks of sediment occur on slopes greater than 6 degrees between 800 and 1700 m water depth and may be a potential slide risk. They are between canyons and show evidence of slippage on their upslope surface. One is between Garie Canyon and the southernmost Sydney Canyon tributary and the other block is between the Sydney Canyon and its first tributary.

4.3.4. Sediment Cores

4.3.4.1. Gravity Core SS10 2006 01GC01

Fourteen cores were collected during this survey ([Figure 4.4](#)) This first core was 4.5 m long and was acquired from latitude -34.317 longitude 151.578, in 1214 m water depth. The core logs are in [Appendix C](#). The core top was dominated by slightly sandy clayey mud with forams. Gradually darkens to olive grey at 20 cm. From 20-120 cm the sediments were a grey bioturbated and mottled mud with whole and shell fragments throughout. With occasional dark grey organic blotches From 120-220 cm the sediments are a bioturbated mottled dark grey slightly sandy mud with occasional 1cm coarse foram sand patches with dark grey organic material scattered throughout, and occasional shell fragments. At 352 and 361 cm the fabric was a dark grey with mottled darker grey and olive green segments, scattered with coarser shelly pockets. At 220 – 333 cm the sediments were very dark grey organic mottles throughout with increasing clay content with depth. Moderately bioturbated occasionally laminated with dark grey slightly sandy mud. This is followed down core by a homogenous dark grey sandy mud with minor bioturbation. Sandy shell layer was observed at 397-399 cm with shell fragments, small gastropod and bivalve (333 – 420 cm). This core was selected for a Geotechnical sample at 420-450 cm to assess the strength of the overall fabric and shear strength.

4.3.4.2. Gravity Core 03GC02

This 3 m core was located at latitude -34.461 longitude 151.435, in 1194 m water depth. The top 0 – 52 cm of this core is an olive grey fine sandy mud with occasional shell fragments scattered throughout. From 52 – 151 cm sediments are olive grey muddy fine sand with sand fraction dominated by terrigenous grains and shells and shell fragments of forams, gastropods and pteropods. Sand sized shell fragments are scattered throughout. Further down the core the sediment is very fine dark grey sandy mud with pockets of sand at 207 and 225 cm composed of shell and terrigenous grains. This core was selected for a geotechnical sample at 242 – 273 cm to assess the strength of the overall fabric and shear strength. Further down the core 273 – 303 cm, the fine dark grey sandy mud contains terrigenous grains and shell fragments and forams.

4.3.4.3. *Gravity Core 04GC03*

This 4.4 m core was located at latitude -34.428 longitude 151.422, in 947 m water depth. The top 25 cm of this core is olive grey very fine sandy silt with shell and shell fragments. At 25 cm and again at 27 – 30 cm there are lenses of medium sand and the top 30 cm have scattered shell fragments throughout section. The sand content increases lower in the core and forms a dark grey silty fine sand from 40cm. A sandy lamination at found at 70 cm. The section from 70 – 314 cm is homogenous with scattered shell fragments in medium sand to gravel throughout. From 314 cm to the bottom of the core there is an increase in silt content resulting in a fine sandy silt.

4.3.4.4. *Gravity Core 05GC04*

This 5.15 m core was located at latitude -34.378 longitude 151.546, in 1518 m water depth. The surface layer is lighter in colour compared to the rest of the core, slightly lighter olive grey muddy sand. There are multiple discontinuous layers – which appear to be bioturbation, with mottles at 20 cm and a burrow at 23 cm. A sandy biogenic layer is observed at 30 cm, and at 67cm a gastropod was found in a shelly hash. Deeper down the core at 174 cm, bioturbation layers are observed and at 195 cm there is mottling. At 220-222 cm coarse grained shelly hash layer and at 240-340 cm the sediments are bioturbated throughout, small burrows infilled with darker carbonaceous sediment. At a core depth of 400 cm and 413 cm, there is high density of bioturbated layers. Further down the core it is lightly bioturbated with burrows infilled with darker sediment with mottling at 482 cm.

4.4. HUNTER REGION

The Hunter region extends approximately 100 km along slope offshore from McMasters Beach to Birubi Point, and has a relatively wide continental shelf (up to 50 km) compared to the rest of the survey area ([Figure 4.17](#) to [Figure 4.19](#)). In this region three seismic lines were acquired (from south to north Lines 11, 10 and 9), in addition to multiple TOPAS profiles over depths of 180 to 1200 m, and three sediment cores on the mid to upper slope ([Figure 4.20](#)).

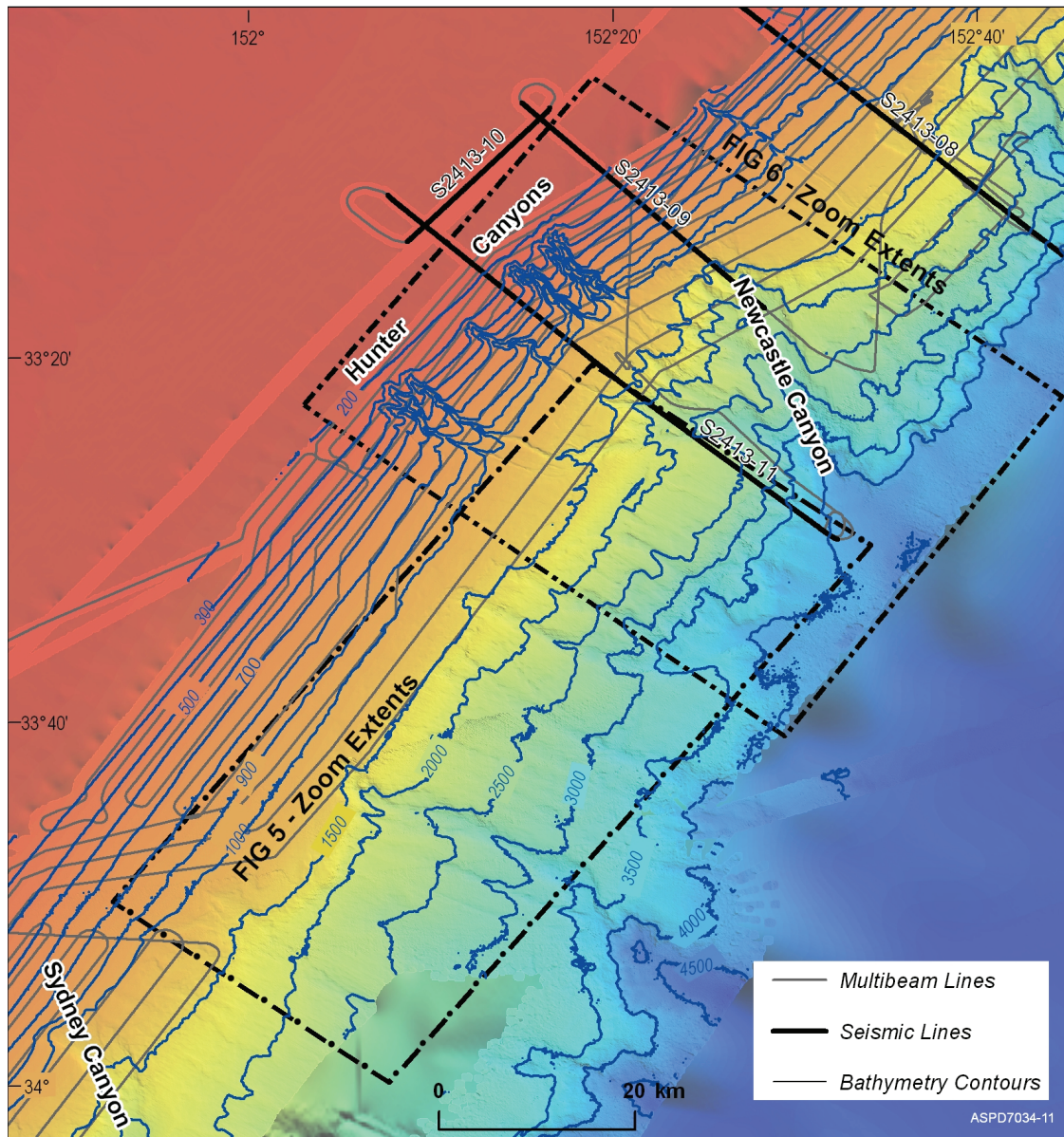


Figure 4.17 The Hunter region extends approximately 100 km along slope offshore

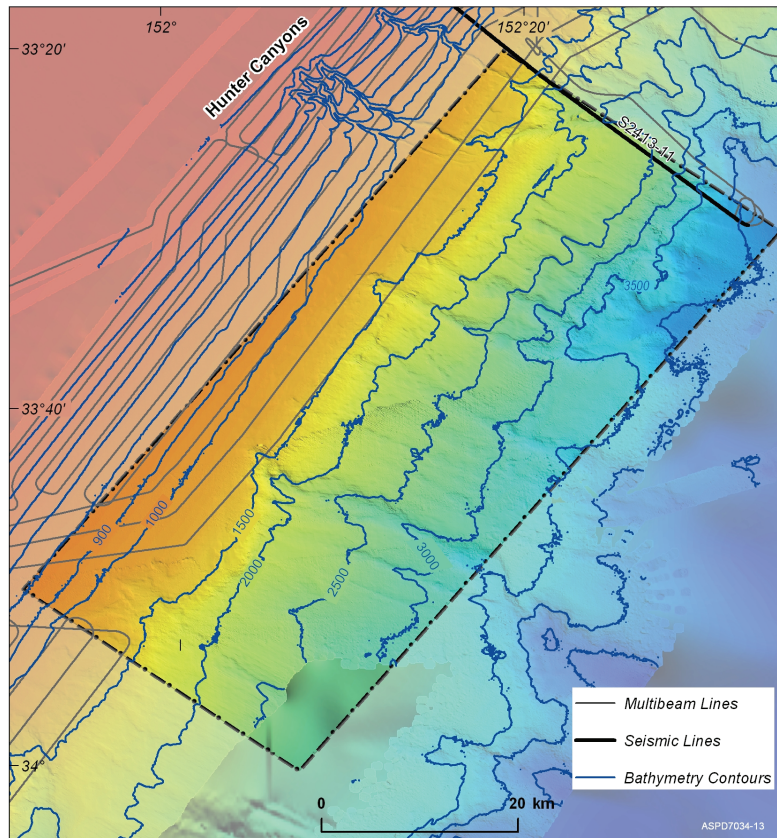


Figure 4.18 Zoom extent of 'Figure 5' within Figure 4.17

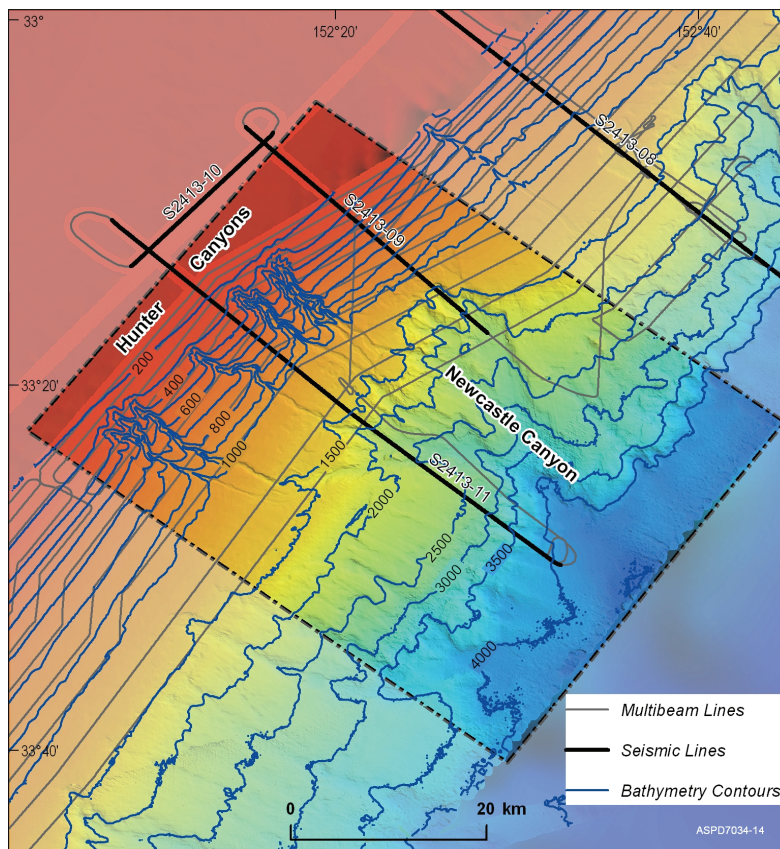


Figure 4.19 Zoom extent of 'Figure 6' within Figure 4.17

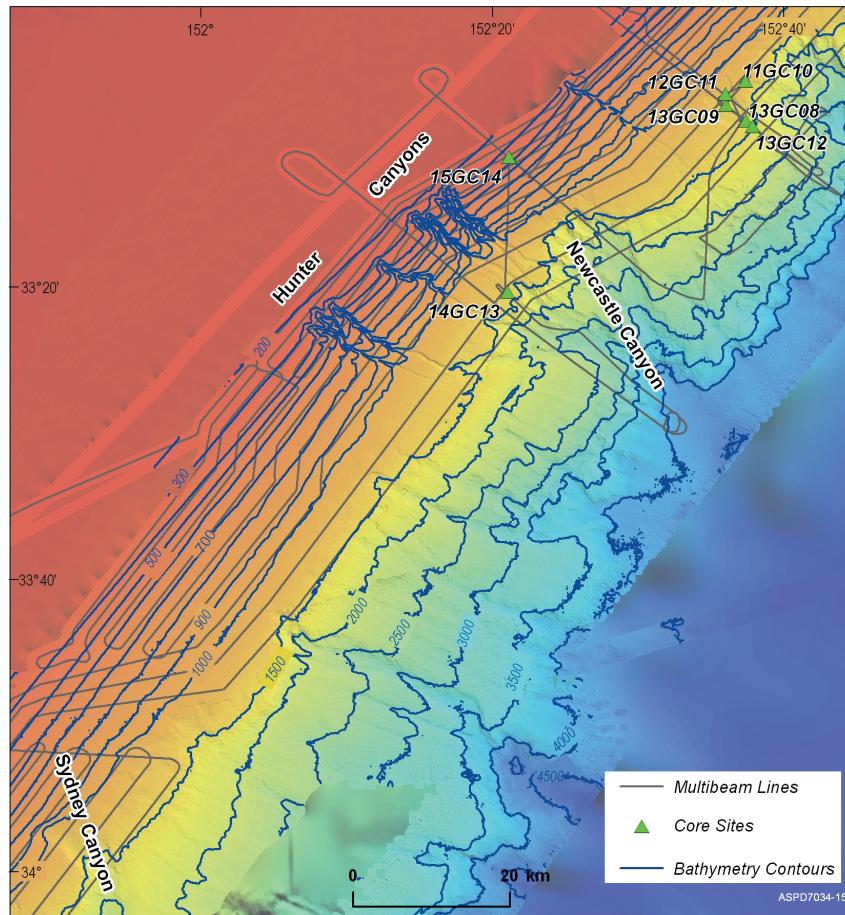


Figure 4.20 Core sites within the Hunter Region

4.4.1. Seismic Analysis

4.4.1.1. Analysis of Line 11

This line starts on the outer shelf in 140 m of water and goes down slope for 52 km between two of the small Hunter tributary canyons (Figure 4.21). The line then descends into the main Newcastle Canyon and up its southern side before continuing down slope to 4000 m. The line was located to determine the failure surfaces for the slides on the upper slope between the tributary canyons, and to assess whether the underlying geology was related to unusual small depressions in the slide surfaces.

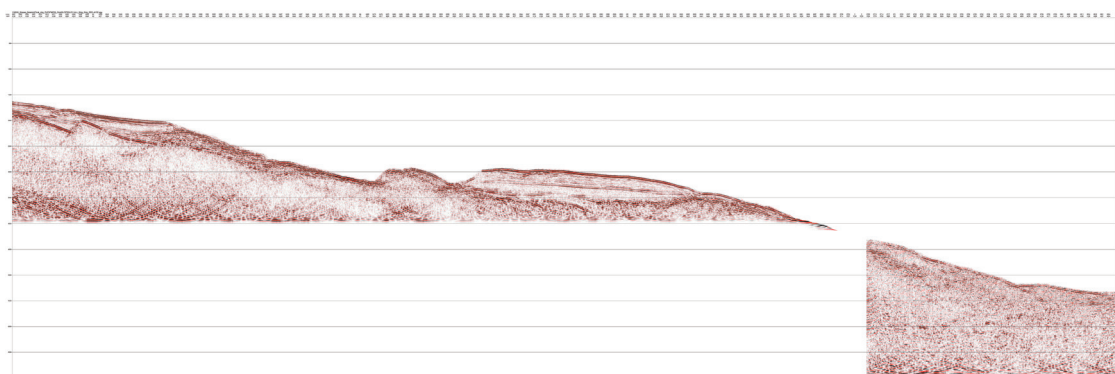


Figure 4.21 Seismic Line 11

At the start of the line, Units 1 and 2 are 570 ms thick and there is some relief on the underlying Unit 3. Reflectors in Unit 3 are relatively low amplitude on this part of the shelf. At CDP 775 (WD 150 m) Units 1 and 2 remain 570 ms thick but Unit 3 reflectors now have their high amplitude character. Units 1 and 2 reach a maximum thickness of 600 ms at the shelf break (CDP 1010, 180 m WD). Unit 3 is a uniform 50 ms thick.

The boundary between Unit 1 and 2 is not distinct in this line. There is a gradational transition from Unit 2 into the overlying more prominent reflectors in Unit 1. Both units are progradational and thin seaward into deeper water. At a water depth of 300 m (CDP 1225) small faults and disruption to the reflectors occur in the upper part of the section and these become more common down slope. A break in sea floor slope at CDP 1370 (420 m WD) may be related to two significant faults in the subsurface of the two units.

At CDP 1800 there is a slight increase in the slope of the basement surface. This coincides with a change in basement type from sub parallel and folded reflectors of Basement Type 1, to more diffuse and discontinuous but higher amplitude reflectors seaward (Basement Type 3). Unit 3 continues at the same slope and overlies a wedge of Unit 4 which onlaps the basement.

CDP 1800 also coincides with a major failure scarp at the surface. Above the scarp (900 m WD) Units 1 and 2 are 180 ms thick, while they are only 60 ms thick below the scarp. The failure surface appears to be near the boundary between the units. What is left of Unit 2 is also disturbed. Unit 3 continues as a dipping, planar surface until it is terminated by a failure scarp at CDP 2400 (1520 m). Down slope from 1420 m water depth (CDP 2270) Unit 3 is at or near the sea floor.

The basement steepens again at CDP 2070 where seaward-dipping reflectors are present in Basement Type 3 and it progrades onto underlying and distinctly block faulted Basement Type 2. Distinct seaward-dipping sedimentary reflectors (Unit 5) have filled between the blocks and onlap both basement types. High amplitude reflectors occur up dip in Unit 5. Unit 5 is overlain by Unit 4, but on this line the boundary to more continuous higher amplitude reflectors is less distinct.

The thickest section of Units 4 and 5 (400 ms) occurs above the major basement fault at CDP 2190 (WD 1325 m). The upper reflectors are disturbed and the sea floor has small depressions at this location.

Seaward of CDP 2310 high amplitude, discontinuous reflectors again overlie the fault blocks. These distinct reflectors dip landward and the unit thickens seaward with Unit 4 onlapping. Unit 4 outcrops on the scarp in 1600 m of water. Down slope from this point the reflectors dip seaward and parallel the sea floor into the floor of the Newcastle Canyon. This canyon floor has the reflector characteristics of Basement Type 3.

From CDP 2970 to 3425 the line crosses a block on the south side of the canyon. Truncated reflectors are present on the canyon side of the block and the reflectors wedge out on the down slope side (2500 m WD). This block consists of Unit 4 (300 ms) and Unit 5 (300 ms) and overlies block-faulted basement (Type 2). There is a thrust fault in the upper part of Unit 4.

Down slope from the edge of this block (CDP 3425) Basement Type 3 again occurs at the surface but poor data quality make analysis difficult for the remainder of the line.

4.4.1.2. Interpretation of Line 11

The relatively strong reflectors throughout the shelf and upper slope sediment wedge may be the result of more input of terrigenous sands at this location offshore from the Hunter River. Moving down slope, slumps first appear in the upper part of the wedge. Some of these disturbed reflectors could also be former sea floor channels. Distinct faults below 400 m water depth indicate the unstable nature of this sediment wedge. Below 900 m water depth, slides have removed most of Units 1 and 2 and nearly all of these units have been removed below 1400 m water depth.

The top of Unit 3 is again characterised by high amplitude reflections, indicating a high acoustic impedance contrast perhaps due to lithification of Unit 3. The unit has a relatively flat surface and a constant

slope seaward down to 1500 m water depth, beyond which it too has been removed by slumping.

The slump scar of the upper units again coincides with a change in slope and type of basement. Basement slope steepens and changes from folded and relatively flat lying strata of possible Permian age to diffuse higher amplitude reflectors interpreted as volcanics. A wedge of Cretaceous sediment (Units 4 and 5) onlaps this basement and has high amplitude reflectors (sills?) in its lower strata.

Seaward of the volcanics, the Cretaceous sediments fill the half grabens of the block faulted basement (Permian?). It is significant that the sediment directly above the largest fault is disturbed and distinctive circular depressions occur in the sea floor. These depressions are likely to be caused by methane gas and fluid from the Permian coal measures escaping along the fault plane.

Near the break in slope of the sea floor at 1520 m there are distinctive reflectors in the subsurface interpreted as volcanics. They include landward dipping flows and seaward dipping flows. Additional evidence for them being volcanic is a resistant hill on the top of this scarp a few kilometres to the north. The relative age of these volcanics can be determined because they overlie rifted basement and are onlapped by the Cretaceous sediment. The volcanics outcrop on the sea floor down into the canyon.

The block on the south side of the canyon is clearly sedimentary and interpreted as Cretaceous. It can be divided into two Units 4 and 5 with the upper unit having more high amplitude and continuous reflectors. The lower unit has discontinuous high amplitude reflectors in its lower part. These may be sills. This block has moved down slope as some strata in the upper unit show thrust faulting. The multibeam derived bathymetry confirms this interpretation.

4.4.1.3. Analysis of Line 10

This line is an 18 km long tie line joining Lines 9 and 11 on the outer shelf (Figure 4.22). The flat sea floor remains at a water depth of 150 m along the line. It is difficult to divide the seismic section into Units 1 and 2 because of the interference of the multiple. Above the multiple there are parallel and continuous, low amplitude reflectors of Unit 1. Unit 2 may thin to the north and downlap onto Unit 3. Below the multiple, Unit 3 can be

defined as a relatively high amplitude reflector that has up to 70 ms of gentle relief on its surface. Units 1 and 2 have a combined thickness of 500 ms at the northern start of the line, and 450 ms at the southern end of the line.

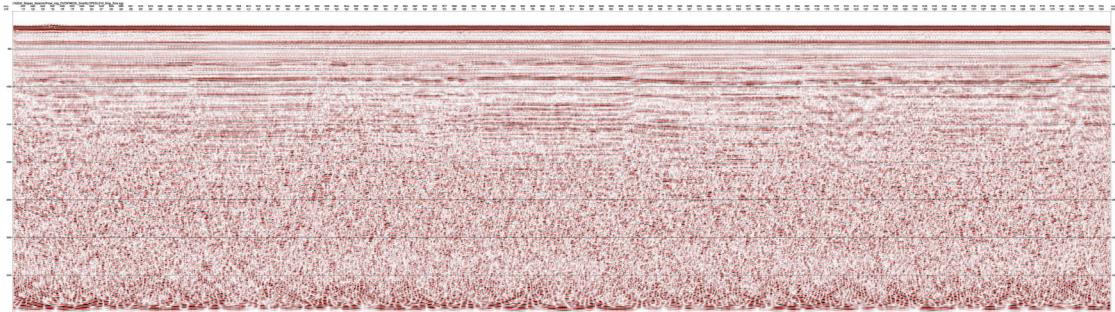


Figure 4.22 Seismic Line 10

4.4.1.4. *Interpretation of Line 10*

The main interpretation from this section is the uniform nature of sedimentation in Unit 1 of the sediment wedge and the possible thinning of Unit 2 south to north at this location on the shelf. This might indicate that Unit 2 in this area is siliclastic rather than hemipelagic drape as a result of a local sediment source from rivers. Reflectors (strata) do fade laterally and others appear but there are no channels, mounds or any indications of slumping. Unit 3 is draped over a relatively flat basement.

4.4.1.5. *Analysis of Line 9*

Line 9 extends for 30 km, starting in 2350 m of water. It goes up the axis of the Newcastle Canyon and upslope onto the outer shelf, before ending in 150 m of water (Figure 4.23). This canyon system has eroded further into the slope than others and the aim of this line was to determine if the underlying geology provided an explanation.

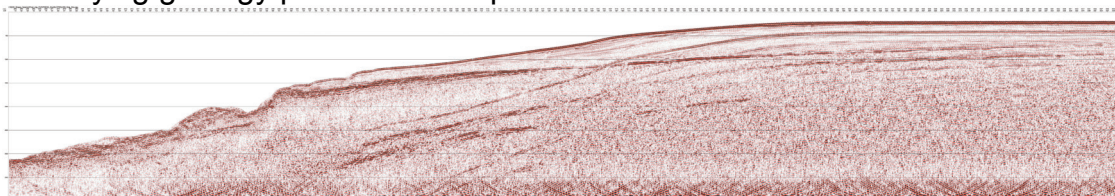


Figure 4.23 Seismic Line 9

The sediment wedge is well defined by the character of the reflectors. At the shelf break (CDP 1735, WD 180 m) Units 1 and 2 are at their maximum thickness of 650 ms and Unit 3 is well defined as a high amplitude reflector 50 ms thick. At CDP1392 there is another break in sea floor slope. Here Unit 1 is 300 ms thick and Unit 2 is 270 ms. The reflectors in Unit 1 prograde and thin down slope more than those in Unit 2. Down slope from CDP 1250 (WD 550 m) there are faults and slumps recognisable in Unit 1. They may also be in Unit 2 but that unit lacks distinct reflectors. At CDP 1200 there is a change in underlying basement from folded strata (Basement Type 1) to high amplitude reflectors (Basement Type 3). The nature of the contact between these two basement types is not clear in this section. At CDP 1060 there is a break in slope of the basement surface.

Below CDP 880 (WD 900 m) there are four steps in the sea floor leading down to a scarp at CDP 660 (WD 1200 m). The first two steps have removed Unit 1, and Unit 2 is removed by the next two steps. Unit 3 continues to the top of the scarp where it outcrops and is truncated. The scarp itself and the sea floor below the scarp are characterised by wavy, high amplitude reflectors that are discontinuous and have irregular dips (Basement Type 3). There is a possible slump deposit in 2000 m of water at CDP 290

4.4.1.6. Interpretation of Line 9

This line clearly shows the sediment wedge and how it has failed in stages where it thins seaward over the underlying volcanic basement. The volcanics are less well defined on this line and there is no outer high. They generally dip seaward and are themselves truncated by slope failure where the sea floor descends into the head of the Newcastle Canyon. Volcanic basement appears to be at or near the sea floor down canyon. There is no Cretaceous sediment basin preserved on the slope along this line.

A change in slope of the basement at CDP 1060 is directly beneath a small slump in the near surface sediments. Additional faults and slumps occur upslope in the prograding beds of Unit 1.

4.4.2. Analysis of High Resolution TOPAS Data

The main feature imaged in the sub-bottom profiles collected within the Hunter region is a series of channels ([Figure 4.24](#)). A large number of

incipient failures and creep features are also evident from the seafloor morphology in this region and a layer of hemi-pelagic drape is visible up to 20 ms (~ 14 m) below the seabed reflection.

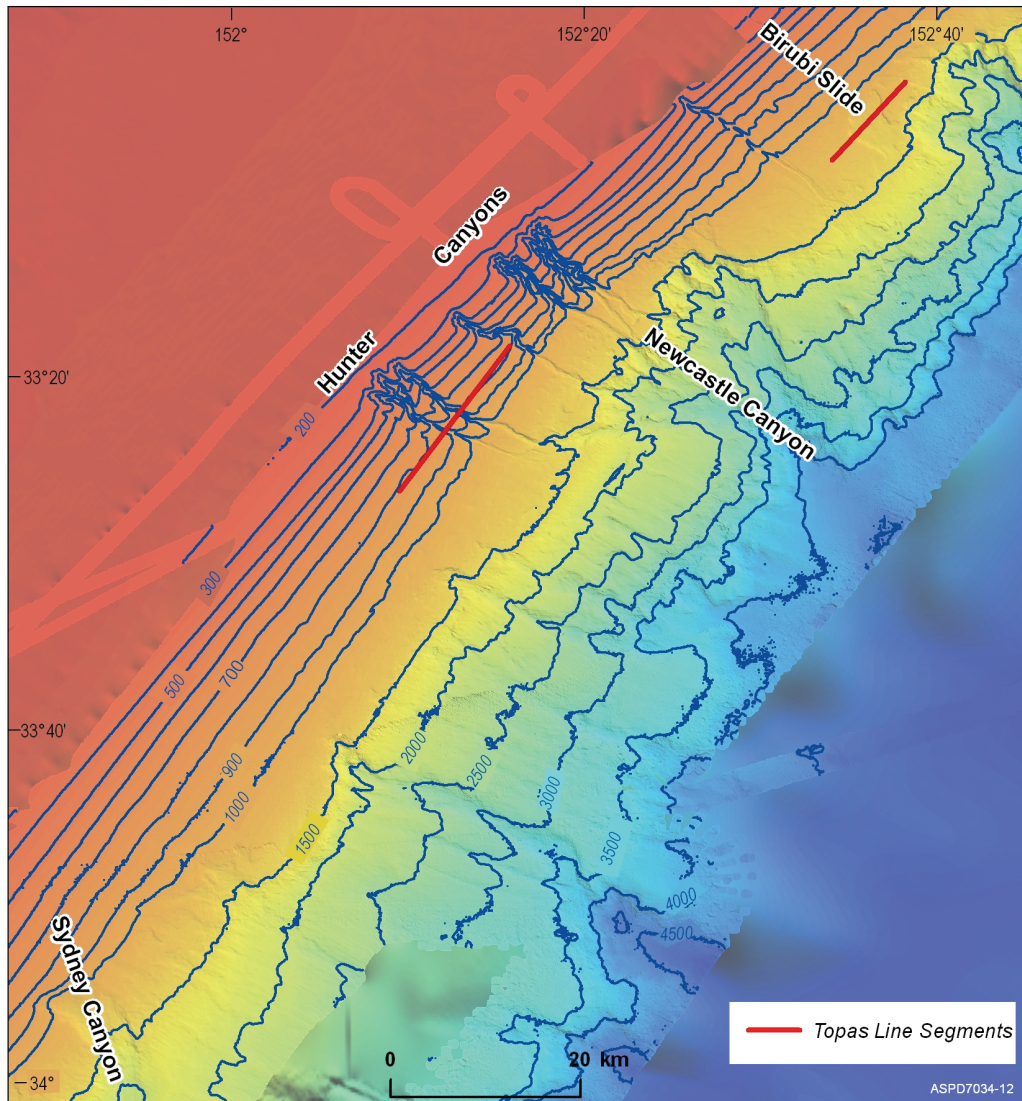


Figure 4.24 Location of TOPAS transect in the Hunter Region

Seabed and sub-bottom morphology on the outer shelf and upper slope in the Hunter region is generally flatter than in the Myall region to the north. Sub-bottom penetration is good, with some reflectors evident as deep as 150 ms (~115 m). A series of laterally extensive, sub-parallel reflections are evident in this region. The data reveal a thinning sediment drape down slope. An intermittently strong sub-bottom reflector with variable morphology can be seen in the data on the outer shelf at around 75–100 ms (~50–75 m sub-bottom). This reflector is relatively flat in some

areas, while in other regions becomes quite rugose, generally conforming to the seabed morphology. It forms the seabed reflector within the floors of the active channels which dissect the upper slope, south of the Yacaaba slide.

Data across the channels are generally good, with sub-bottom penetration averaging 100 ms (~75 m).

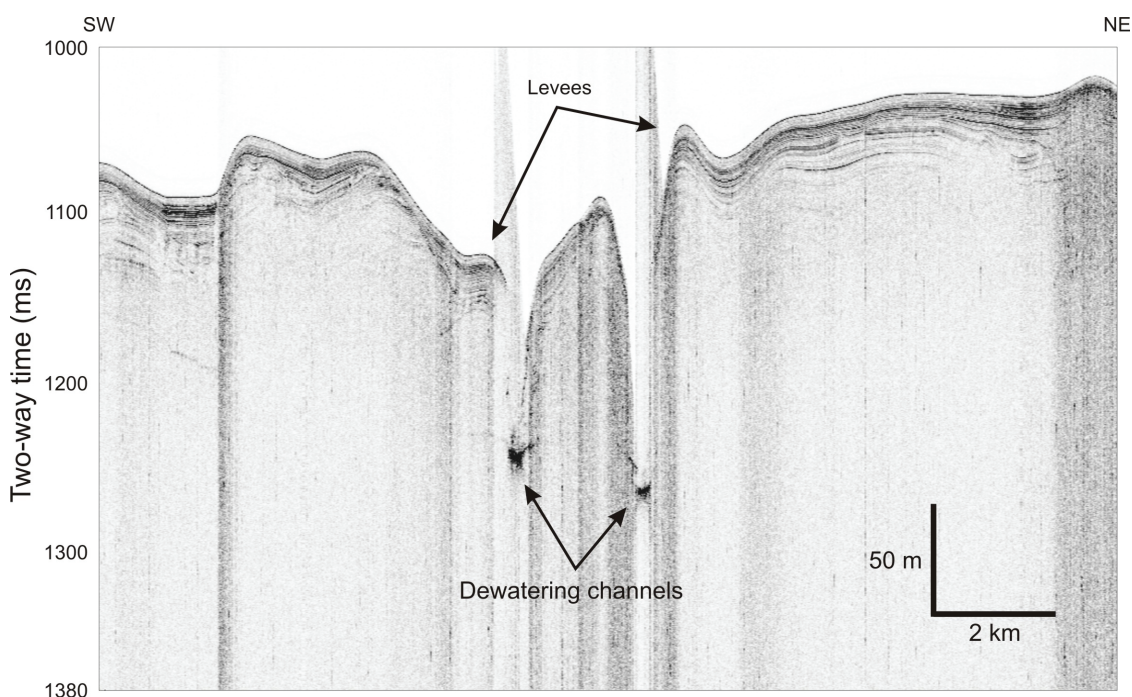


Figure 4.25 Profile across two of the dewatering channels

4.4.3. Geomorphology

4.4.3.1. *Geomorphic interpretation results*

The continental shelf in the Hunter region is relatively wide (over 50 km) and the coastline has a broad embayment between Norah Head and Port Stephens. This embayment corresponds broadly to the Hunter Valley onshore, and marks a major change of coastal orientation as well as a change of the general trend of the margin from 040° to 022°. A number of distinctive geomorphological features are found in the Hunter Region continental margin.

North of the Sydney Canyon the slope maintains a strike of 035° and is approximately 60 km wide. For 60 km the upper slope above 900 m is relatively smooth and free of slumps and canyons. Below this depth there is

a continuous zone of multiple slumps between the 900 and 1500 m isobaths.

Average gradients along a profile of the sea floor north of the Sydney Canyon are: 2.7° from 300 to 1100 m (a distance of 20 km), 4.2° from 1100 to 2000 m (10 km), 3.3° from 2000 to 3400 m (25 km) and 18° from 3400 to 4500 m (5 km). Overall the continental slope can be divided into an upper slope down to 2000 m that becomes steeper below 1100 m, a gentle mid-slope from 2000 m to 3400 m that is not completely surveyed, and a very steep and incised lower slope below 3400 m with an abrupt contact with the near-horizontal abyssal plain at 4700 m.

Immediately north of Sydney Canyon and extending into the southern end of this region there is evidence of many slips between the 1000 and 1700 m isobaths. For most of these failures the slide scarps are 1 to 4 km long and the material has slid 1 to 2 km down slope. Ten kilometres from the southern boundary these slides become a complex of retrogressive slides starting at 900 m that feed into a broad canyon (centred on 33.8456S; 151.9844E, WD 1400 m) in the lower part of the upper slope before becoming a more distinct straight canyon in the mid-slope and lower slope.

The northern flank of this canyon has four parallel ridges (33.7921S; 152.0078E to 33.7963S; 152.0692E; WD 1100 to 1600 metres) trending along slope at 025°. The outer one is longest (6 km) and forms a slope-parallel scarp of 400 m (1600-2000 m av. 7.5°). These ridges could be dykes or the seafloor expression of buried basement rocks. It is also possible that the lower two are rotated slump blocks as they have distinct depressions on their upslope sides. The two shallower ridges may be formed by the EAC flowing past hard outcrop. Poor data quality makes them difficult to interpret. Above the ridges the slope has a gradient of 2.4° (600 to 1100 m). Below the scarp formed by the lower ridge the slope is 4° from 2000 to 3400 m. Starting at the 2500 m isobath below the scarp two small (1 km wide, 200 m deep) linear canyons have eroded the slope. A series of steps in the floors of these canyons indicate older strata. They join a larger canyon at 3800 m. The head of this larger canyon to the north (centred around 33°43.608'S; 152°5.836'E; WD 1880 m) has eroded into the upper slope sediment wedge by retrogressive slides extending back to 900 m water depth. At 3800 m the floor of this canyon descends 500 m over a series of steps into a basin 2 km wide and 200 m deep (floor at 4550 m with a down canyon lip at 4350 m). These major steps in the

canyon's thalweg indicate resistant strata probably caused by underlying (?) Paleozoic rock. The lower continental slope is again steep at 11° (3400 to 4500 m). The canyon floor can be traced with the limited available data to 4886 m where it is still 500 m deep and 6 km wide.

North of this canyon for the next 25 km there are no significant canyons on the mid or upper slope but many overlapping slips do occur between 1000 and 1500 m water depth. However, immediately north of the canyon is an unusually straight ridge trending 020° for 5 km along the slope (33.6741S; 152.0957E; WD 1108 m). It has a 100 m scarp on its seaward side and could represent a basement block with an incipient sediment slide on its seaward face. A similar but more subdued ridge occurs further north at 33.5821S; 152.1676E in 1225 m of water.

Down slope of these ridges in 1350 m water depth is a steep scarp (centred on 33.6756S; 152.1215E but extending along slope). It is formed by sediment sliding a few kilometres down slope. These slides feed into a small linear canyon on the mid-slope and lower slope.

Continuing north, the next canyon head in the upper slope is at 33.5533S; 152.2003E; WD 1560 m and is also formed by numerous retrogressive slides that have eroded into the upper slope sediment wedge. Crown scarps are clearly visible back-stepping to water depths of 1100 m. They appear to be relatively young.

On the northern flank of this canyon the surface has failed in a rectilinear shape. The straight crown scarp is 100 m high (WD 1250-1350 m) and 4 km long (centred on 33.5301S; 152.2137E) and ends abruptly where bedrock pinnacles (volcanic?) are exposed (33.5195S; 152.2280E). The slide mass has moved 2 km down slope and come to rest at 1500 m. There is a canyon on the mid and lower slope below this slide. Similar slides occur until the Hunter Canyon is reached in water depths of around 1600-2000 m. These slides are continuous along slope for over 30 km. One of these slides (centred at 33.4661S; 152.3238E) exhibits an intact block that has moved approximately 5 km down slope, but unlike most other slide masses, it has come to rest a short distance down slope, retained its overall geometry and has not continued to the base of the continental slope and been destroyed.

Beyond the shelf in the northern part of the Hunter region, the most obvious features on the continental slope are a series of seven canyons termed the Hunter Canyons, seaward of the Hunter River mouth and centred around 33.3051S; 152.2038E. The location of their shallow

termination appears to correspond to similar canyons seaward of the Shoalhaven and Manning River mouths to the south and north. These canyons begin in around 200 m water depth and maintain their form into at least 1500-2000 m depth, some 15-20 km seaward.

Between 200-800 m depth, the upper canyon walls show a complex rill erosion pattern with incision of around 350 m and canyon widths of 1-2 km. This rill pattern is developed in the uppermost sediment wedge and is situated directly offshore from the Hunter River and is in water depths that would suggest its age is at least Pleistocene and predating the most recent sea level lowstand around 15 ka.

Six of the seven channels feed into a large bifurcated lower slope failure. The seventh, most southerly channel and shortest at 6 km long, drains a slope of around 4.3° . Starting at the upper slope at a water depth of 365 m, it terminates on the mid slope at 800 m WD, failing to reach the lower slope. Its channel is 250 m wide and side walls have slopes of $15-20^\circ$. The other six canyons are of similar size and length (16-18.5 km to the nick point) and all terminate in the larger lower slope failure centred around 33.3599S; 152.3879E. These six channels initiate at the break in slope at water depths averaging 231 m. At the relatively shallower depths they are V shaped, sinuous, 500-1000 m wide with $20-25^\circ$ walls. In deeper waters such as between 1200-1300 m they become linear, flat bottomed and terraced. A canyon at the northern extent of this region occurs 18 km north of the others and does not terminate in the large slope failure. It ends around 1300-1400 WD and links down slope to several small failures 1-2 km wide and around 100 m deep. This canyon maintains a V shaped profile along its entire length.

A large box canyon failure centred around 33.3599S; 152.3879E occurs in around 1200 m WD and extends along slope and down slope for 22 km, before ending in around 4000 m WD. This box canyon, informally known as the Newcastle Canyon, is interpreted to have mainly developed in bedrock with around 400 m of relief at its head, possibly resulting from down slope failure along bedrock faults. Within the canyon are a number of irregular topographic features on the order of 400 m high and 2 km wide that are most likely eroded volcanic intrusions (e.g., at 33.3005S; 152.4509E) or basement blocks. The box canyon contains a number of individual failures that coalesce down slope, finally forming a single narrow canyon 7 km wide with over 800 m of relief, terminating on the abyssal plain.

Topas data show that the continental margin sediment wedge thins near the upslope margin of the Newcastle Canyon, but retrogressive failure here is sufficient to undercut the base of the wedge and initiate extensive upslope creep, tension cracks and incipient failures. Some of these failures are in water depths of 1000-1500 m, are up to 150 m deep, 8 km long, at least 5 km wide and have crown scarp angles of 15-20° (e.g., at 33.2249S; 152.4092E). On the floor of one slide are numerous collapse depressions, elongate to circular features up to 1000 m wide and 70 m deep (e.g., at 33.3373S; 152.3491E; and 33.3166S; 152.3250E).

The upper continental slope of the Hunter Region is unusual in that it has a distinct depositional feature in the shape of a braided stream / submarine delta. This sediment accumulation was clearly imaged on TOPAS seismic data and contained a series of prograding clinoforms with distinct changes in slope associated with the deposition of individual delta sediment packages. It is these sediment packages that are incised by the upper reaches of the seven canyons off the Hunter River. The upper sediment packages also have incipient failure features present on them including slides and tension cracks.

The lower continental slope off the Hunter Region is composed mostly of outcropping bedrock with steep fault scarps over 1000 m high on slopes exceeding 10°. The lower slope occurs as a relatively linear escarpment with a consistent trend of 031°. This lower slope contains several pinnacles that are 200-400 m high and 1 km wide. These features seem to occur along linear trends and are interpreted as volcanic intrusions, possibly basaltic in composition.

4.4.3.2. Discussion of geomorphic interpretations

The Hunter Region is a seaward continuation of the Hunter Valley on land. This valley occurs between the Triassic sandstone plateau to the south and the Carboniferous New England Fold Belt to the north (Schiebner and Basden, 1998). The Hunter River is a long-lived network that has a large drainage basin of around 22,000 km². Hodgins (1995) traced the thalweg of the Hunter Valley across the inner shelf. Projected seaward, this valley trend would intersect the shelf edge in the region of the Hunter Canyons. It seems reasonable that the main accumulation of recent sediment on the upper slope should exist seaward of the largest river in the region, and this also fits the pattern identified for the Shoalhaven and Manning Rivers.

However, it seems unlikely that the upper slope deltaic accumulation results from the latest Pleistocene lowering of sea level. This latest lowstand around 15-20 ka only extended to around 120 m below present sea level and established a shoreline in the Hunter Region on the midshelf. The shelf break in this area is greater than 150 m deep (Boyd et al. 2004) and deltaic accumulations there must result from earlier Pleistocene lowstands when the Hunter River reached the shelf edge.

On the mid slope between the Newcastle Canyons are a number of depressions on the seafloor. These are large features and for example, extend 750 m across slope, with side scarps showing slopes over 20° and floors 70 m below the rims. These features resemble those found on sidescan records from the Mississippi Delta known as “collapse depressions” and result from gas and fluid expulsion from subsurface Units (e.g., Prior and Coleman, 1980). There they are the precursors to seabed slides and often connect to them down slope. It is considered likely that the features found off Newcastle are also depressions formed from gas and/or fluid escape and hence are an indicator of seabed instability in this region.

4.4.4. Sediment Cores

4.4.4.1. Gravity Core 09GC08

This 4.83 m core was located at latitude -33.1400 longitude 152.6218, in 1424 m water depth. Light olive brown muddy sand dominated by forams with minor terrigenous silt sized grains (0 - 3 cm). Greyish brown sandy clay with sand fraction dominated by forams with minor silt sized terrigenous grains (3 - 40 cm). From 40 cm sediment gradually darkens to olive brown sandy clay. At 69 cm increasing organic streaks. 112 cm dark mottle. From 127 -175 cm very subtle bands (5-10 cm thick) with very slight colour changes. At 189-190 cm discontinuous sand layer dominated by forams and other shell fragments followed at 218 cm, a dark olive grey very slightly sandy clay. Small pockets of foram rich sand were observed at 227 cm, 239 cm, 275-278 cm, 312-316 cm. at 235-246 cm subtle slightly darker mottles and at 316cm, colour change to dark greyish brown with mottles of dark grey muddy sand. Large sand pockets at 389-398 cm. Organic streaks were observed throughout particularly in the lower section (418-483 cm) where the sandy clay had abundant organic streaks.

4.4.4.2. *Gravity Core 10GC09*

This 3.72 m core was located at latitude -33.122 longitude 152.599, in 1329 m water depth. Olive fine sandy mud with forams (0-2cm) with olive grey sandy clay with forams in sand fraction from 2-42 cm. Wood fragment 7-8cm (sub-sampled for future C-14 processing). At 42-54 cm the sediment was wetter and increasing sand content, still sandy mud. 56 cm an increasing number of organic streaks. At 80 cm the sediment darkens to dark olive grey and at 54-372 cm very low sand content, slightly silty mud. Pockets of gravel sized shells and shell fragments were found at 143 cm, 174 cm, 184 cm and occasional gravel sized shell fragments scattered throughout the core.

4.4.4.3. *Gravity Core 13GC12*

This 4.6 m core was located at latitude -33.1402 longitude 152.622, in 1420 m water depth. 0-5 cm of the core is an oxidised muddy ooze, at 5-8 cm, the sediment shows some dark mottles and again at 25-26cm. At core depth of 33cm the sediments are a sandy mud and from 36 – 100 cm the core revealed a homogeneous lightly bioturbated and mottled sand. At 325 cm there was a colour change, heavy mottling and the sediment was slightly muddier. Sandy lenses were noted at 328 cm and at 331-341 cm coarser lenses in finer mud matrix. At 341-351 cm it was a finer mud, fewer coarse lenses, bioturbated with darker grey lenses. Light and dark grey mottled lenses 351-361 cm and again the sediment was mottled to 391 cm. Sandy lens (1cm) at 390 cm and 425 cm.

4.4.4.4. *Gravity Core 16GC15*

This 1.17 m core was located at latitude -33.2013 longitude 152.3749, in 648 m water depth. The top of the core from 0-3 cm is a wet sandy mud, from 3-47cm it is homogeneous sand with occasional bivalves, gastropods, and carbonate tests. At 47-110 cm down core, the sediment is a bioturbated muddy sand, and at 110-117 cm the texture becomes firmer and drier.

4.5. MYALL REGION

The Myall region extends from offshore from Birubi Point (to the south of Port Stephens) to Seal Rocks in the north (Figure 4.26). It contains two seismic lines, eight gravity cores and a number of high quality TOPAS lines on the mid to upper slope (Figures 4.27 to 4.30).

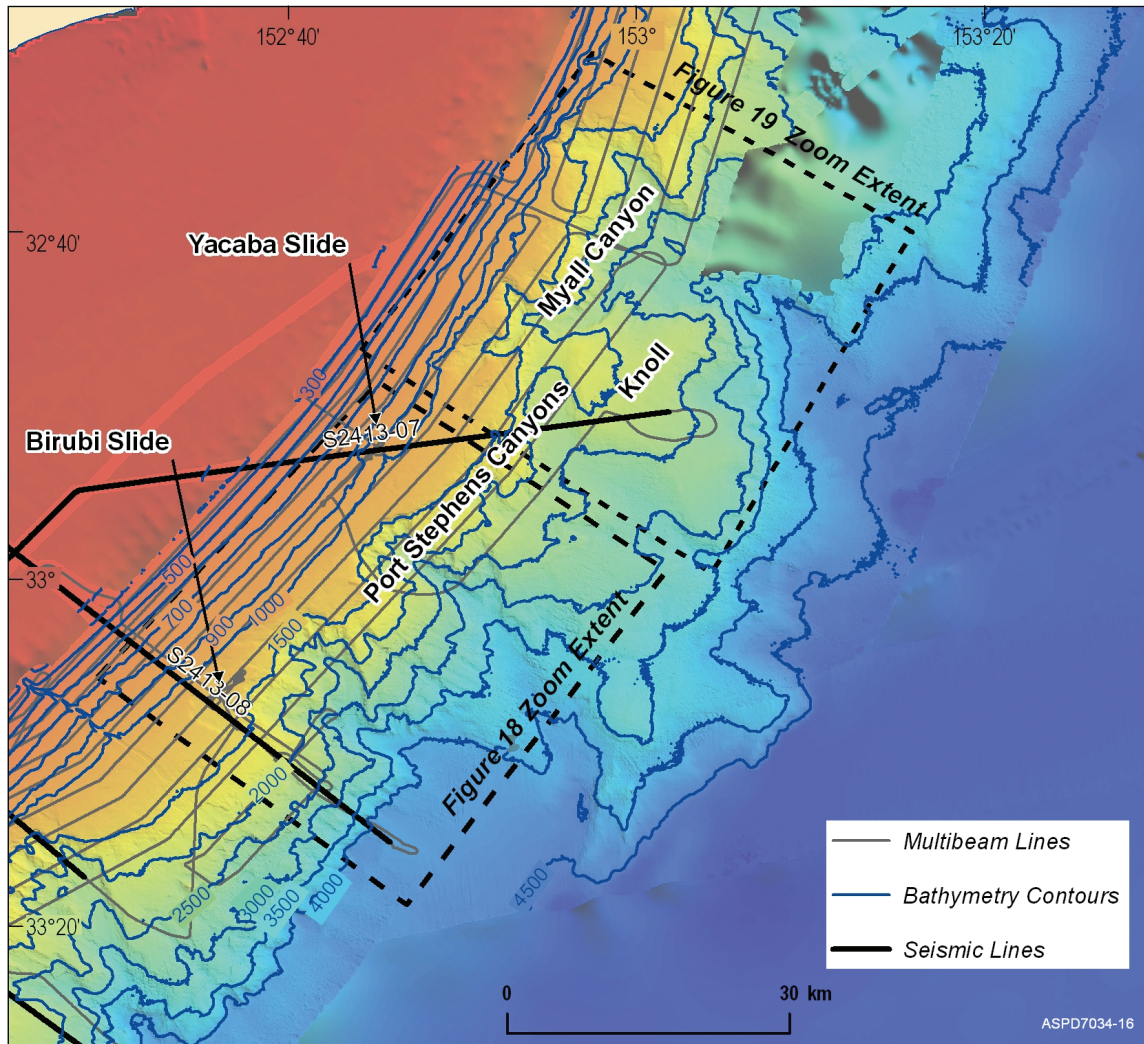


Figure 4.26 Myall Region

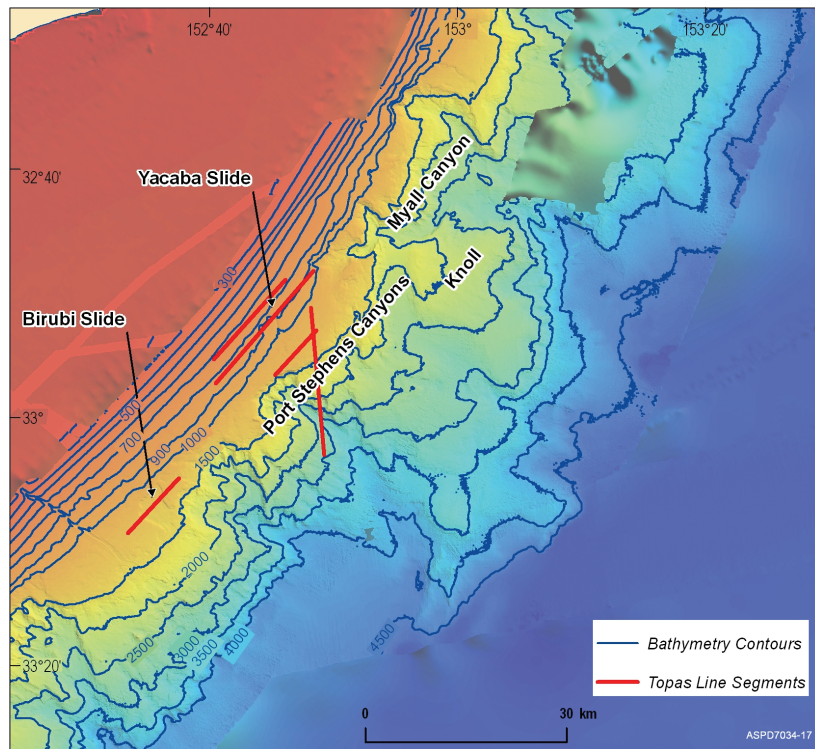


Figure 4.27 Location of TOPAS line transects

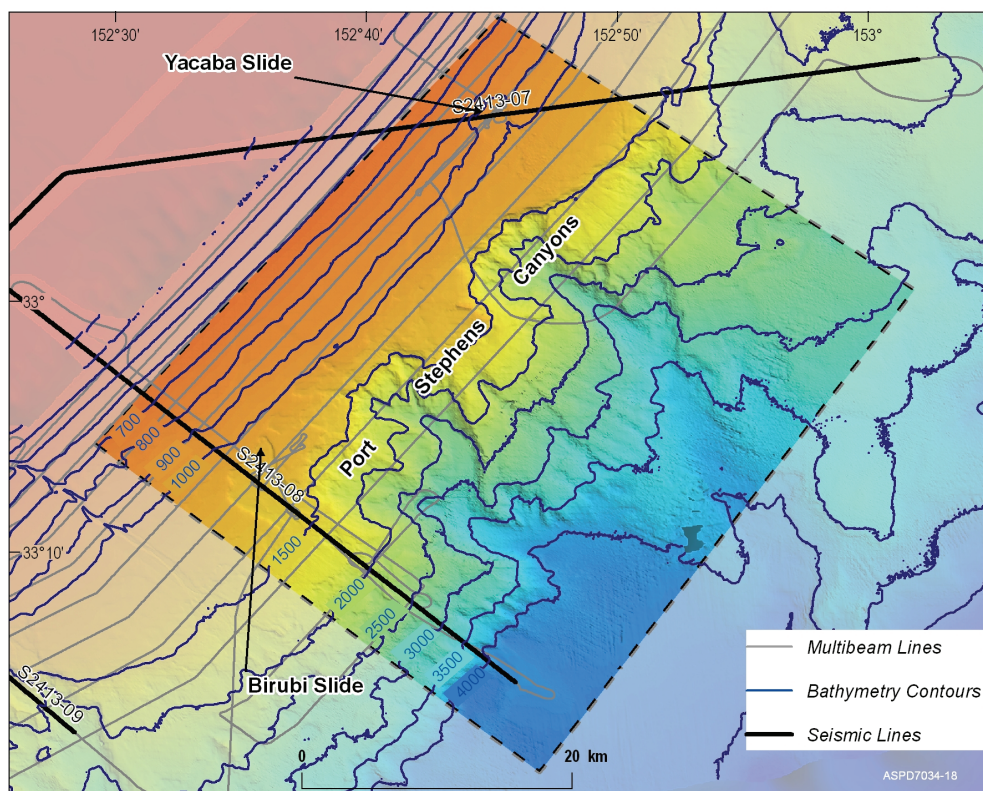


Figure 4.28 Location of seismic lines in the Myall Region

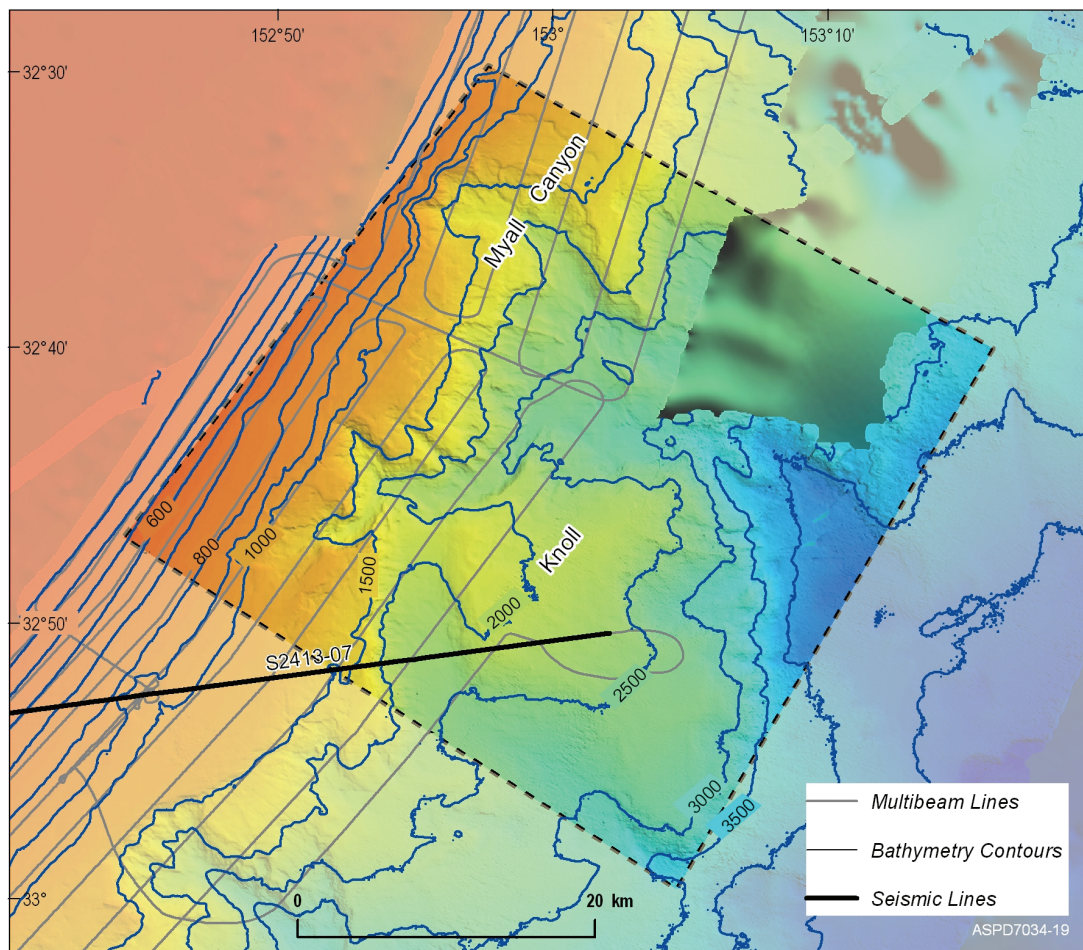


Figure 4.29 Bathymetry contours and seismic line in the Myall Region

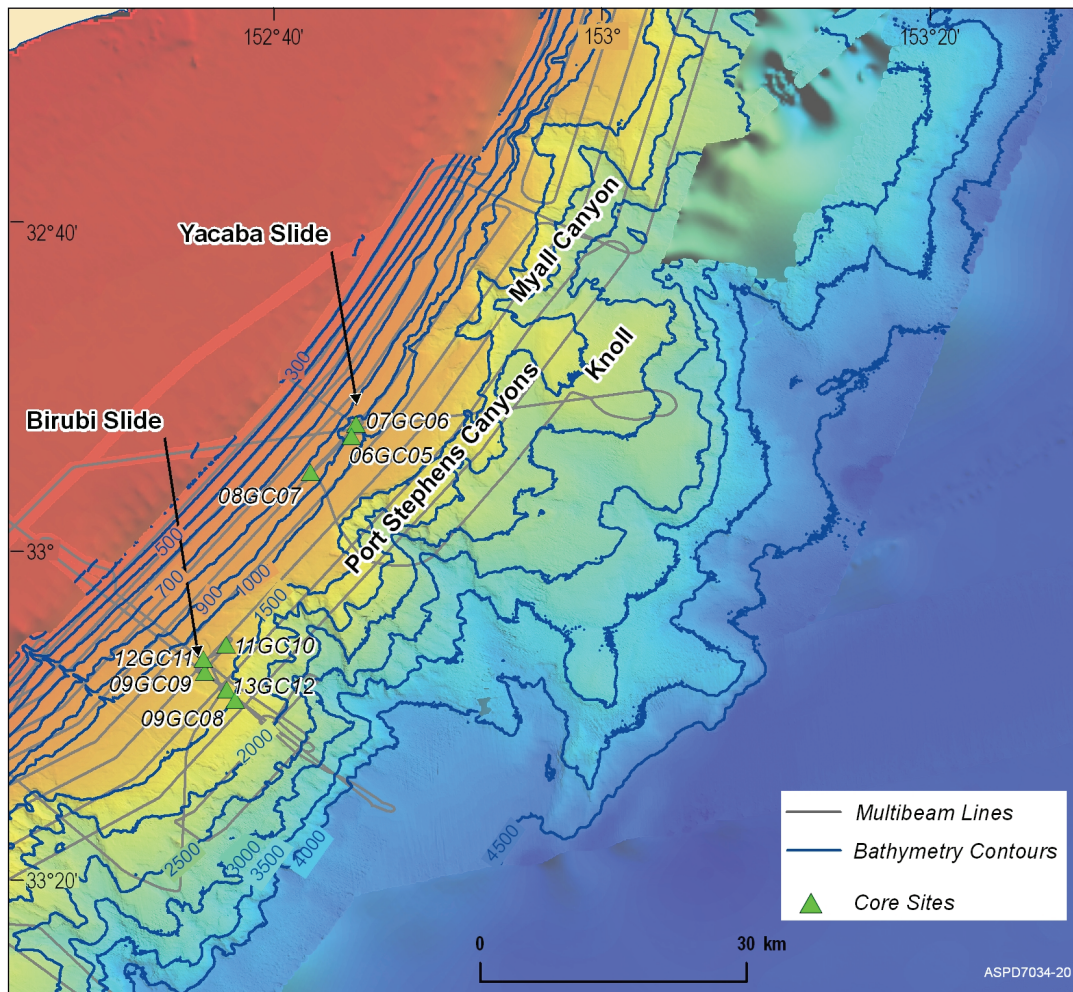


Figure 4.30 Location of core sites in the Myall Region

4.5.1. Seismic reflection profiles

4.5.1.1. *Analysis of Line 8*

Line 8 starts on the outer shelf in 150 m water depth where it crosses Line 7 and then runs down slope and down the axis of the Birubi Slide to end in 3000 m water depth (Figure 4.31). The total line length is 48 km. The aim of this line was to determine what part of the sequence failed, what formed the failure surface, and the nature of the underlying geology.



Figure 4.31 Seismic Line 8

At the start of the line, Units 1 and 2 cannot be distinguished because of multiples and Unit 3 is a less distinct reflector than it is elsewhere. Their total thickness is 550 ms. Unit 3 becomes a more distinct high amplitude reflector at CDP 590. At the shelf break (WD 160 m) the sediment wedge is at its maximum thickness of 620 ms (Units 1 and 2) and 50 ms (Unit 3) overlying folded basement (Type 1). At CDP 1050 the boundary between Units 1 and 2 is no longer obscured by the multiple. The water depth here is 300 m and Unit 1 is 320 ms thick and Unit 2 is 230 ms thick. At CDP 1170 (WD 450 m) the first sub-surface faults are recognisable in Unit 1. Seaward of this the disturbance in the reflectors increases. At CDP 1680 there is a distinct mound or slump fold in the lower part of Unit 2. Slump faults extend to the surface at CDP 1715 and 1850 (WD ~1000 m). Over this interval there is also a change in basement type. At CDP 1770 the folded Basement Type 1 has contact with diffuse but high amplitude reflectors typical of Basement Type 3. A channel fill in Unit 3 abuts the western edge of this Basement Type 3.

A basement high occurs at CDP 1980 and is draped by Unit 3 which in turn is overlapped by Unit 2. The sediment wedge thins over this high (the combined thickness of Units 1 and 2 is 80 ms) and on its seaward side the wedge has failed. The slump scarp is directly above this increase in slope of the basement on the seaward side of the high.

The failure surface for the Birubi Slide appears to be at the base of Unit 2. Most of Units 1 and 2 have been removed except for a remnant at CDP 2430 because the slide has diverted to the Port Stephens Canyon north of this line. Unit 3 maintains a consistent slope and continues beneath the slump and overlying sediment and ends where it is truncated by the sea floor (CDP 2600) in water depth of 1600 m.

From CDP 2090 to 2600 a sediment – filled basin up to 700 ms thick underlies Unit 3. Reflections in this basin dip seaward and can be divided into Units 4 and 5. Their upper terminations show an offlap relationship beneath Unit 3. The lower reflectors in Unit 5 are interbedded with very high amplitude discontinuous reflectors. They in turn overlie weakly defined block faulted basement (Type 2).

Seaward of CDP 2600 the sea floor is rough. There are slump units on the surface and reflectors in Units 4 and 5 are truncated by the sloping sea floor. Strong, discontinuous reflectors are again present in Unit 5 and overlie block faulted basement.

4.5.1.2. *Interpretation of Line 8*

The distinguishing feature on this line is a volcanic basement ridge. It is less well defined than on Line 7 but has similar characteristics. On its seaward side there is a significant section (~800 m) of Cretaceous sediments similar to those described previously (Units 4 and 5). The lower part of Unit 5 is intruded by sills and overlies block--faulted basement.

It is significant that the failure scarp of the Birubi Slide, which occurs in Units 1 and 2, is located directly above the volcanic high and at the landward pinch out of the underlying Cretaceous section. It is likely that differential compaction could have oversteepened the sediments that failed. They appear to have failed along a surface at the base of Unit 2.

The Cretaceous sediments become more horizontal down slope and they outcrop on the sea floor (1800-2500 m WD). More volcanics appear to be interbedded with them here and block faulting can be recognised beneath them.

4.5.1.3. *Analysis of Line 7*

Line 7 starts in 2300 m of water and runs obliquely across and up the slope to end on the outer shelf in 150 m of water (Figure 4.32). The line is 62 km long. The aim of the line was to determine the relationship of an isolated block to the adjacent continental slope. This 400 m high block is separated from a scarp in the slope by a broad valley. The line also passed over a slump scar (Yacaaba Slide) on the upper slope.



Figure 4.32 Seismic Line 7

Units 1 and 2 can again be distinguished by the density of reflectors. Continuous reflectors occur throughout Unit 1 whereas in Unit 2 the reflectors are faint except near the base where they infill topography on Unit 3. On the shelf the units are difficult to separate because of multiples but total thickness is 550 ms at the end of the line (WD 150 m). All reflectors are parallel to the sea floor and near horizontal. There is a broad basement high (Type 1?) at CDP 4660 and Units 1 and 2 thin to 300 ms by

onlapping of the reflectors at the base of Unit 2 onto Unit 3 which in turn drapes the high.

At CDP 4180 Unit 3 first appears as a high amplitude reflector (30 ms) on basement. It is 450 ms below sea floor (WD 150 m). Seaward of this point gentle progradation occurs in the reflectors of both Unit 1 and Unit 2.

The sediment wedge (Units 1 and 2) gradually thickens as Unit 3 becomes deeper. At the shelf break (170 m w. d.) the shelf sediment wedge is at its maximum thickness of 550 ms. Seaward of the shelf break, the wedge gradually thins. Unit 3 remains at 30 ms thick and is slightly uneven as it follows basement topography. At CDP 3250 (WD 300 m) the seismic record is clear of interference from multiples, Units 1 and 2 are clearly defined and are each 260 ms thick, while Unit 3 overlies folded strata (Basement Type 1).

There is no evidence of buried channels or slumps until water depth 450 m (CDP 3020) where the first fault occurs in the lower part of Unit 1 and folded reflectors indicate slumping down slope from the fault. Seaward of this point, the parallel reflectors at the base of Unit 2 become more distinct and clearly infill the topography on Unit 3.

The basement from CDP 3020 to 2320 is relatively flat and continues to slope seaward but at a lower angle than the sea floor. It consists of landward dipping reflectors and folded strata. This is Basement Type 1. At CDP 2320 the top of the basement steepens seaward and is block faulted (Basement Type 2). This break in slope of the basement coincides with a slump scar on the sea floor and is also the start of a sediment basin overlying basement. This block faulted Basement Type 2 continues to CDP 1720. Beneath Unit 3 from CDP 2320 to 1848 are seaward dipping reflectors with the characteristics of Unit 5 described earlier. Between CDP 2400 and 2190 (WD 800 to 950 m) all of Units 1 and 2 have slumped on the surface of Unit 3. Up to 70 ms of slumped sediment remains on Unit 3. From CDP 2190 to 1848, Units 1 and 2 continue to thin and Unit 3 continues as a flat surface with the same slope. At CDP 1848 all three units end where they onlap a high.

From CDP 1848 to 1650 (1100 to 1175 m WD) there is a flat-topped high that is at or near the sea floor. The high consists of high amplitude reflectors of Unit 4 that are conformable with the underlying reflectors of Unit 5. Units 4 and 5 reach their maximum thickness of 600 ms below this high. They are underlain from CDP 1720 to 1430 by high amplitude

discontinuous reflectors similar to Basement Type 3 that become more regular and landward dipping (between CDP 1430 and 1360). Units 4 and 5 pinch out at CDP 1430 and onlap the Basement Type 3.

From CDP 1650 to 1430 there is a wedge (150-200 ms) of Units 1 and 2 underlain by Unit 3. The lower part of the wedge is slumped while the upper has prograded seaward from the Unit 4 high. The wedge ends at water depth 1500 m where the Basement Type 2 comes to the sea floor (CDP 1360). The basement forms a 50 m high topographic ridge at this point and its subsurface reflectors are sub-horizontal.

Seaward of this basement ridge from 1520 to 1600 m water depth is another thin (80 ms) wedge of sediment, probably Units 1 and 2. The 600 m high scarp seaward of this consists of outcropping Basement Type 3 with internal seaward dipping reflectors. From the base of the scarp at CDP 1130 to CDP 800 there is a flat-floored valley filled by three seismic units. The upper unit onlaps the volcanic basement on the landward side consists of high amplitude reflectors and is defined as Unit 1a. On the seaward side this unit appears to drape over the block forming that side of the valley. Beneath this unit in the valley is 250 ms of low amplitude, irregular reflectors that lens out upslope against the basement ridge. Beneath this is 250 ms of high amplitude discontinuous reflectors.

The block forming the seaward side of the valley consists of 900 ms of sediment. The upper 500 ms of parallel reflectors are gently dipping seaward and similar to Unit 4. They are truncated on the valley side and draped by Unit 1a. Beneath Unit 4 is 400 ms of poorly defined reflectors. This is Unit 5 and it continues under the valley and pinches out against the Basement Type 3 at the base of the scarp. Basement Type 3 underlies Unit 5 with high amplitude seaward dipping reflectors which become near-horizontal beneath the valley and can be traced beneath the block. There is some evidence that broken, tilted reflectors (Basement Type 2) occur beneath this basement Type 3.

4.5.1.4. Interpretation of Line 7

This seismic section is dominated by the presence of a major volcanic ridge that outcrops between water depths of 1500 to 2200 m. It has seaward-dipping reflectors on its seaward side and landward-dipping reflectors on its landward side. It is interpreted as a volcanic ridge consisting of subaerial

lava flows which may have sediments interbedded. Beneath the sea floor on both its seaward and landward margin there are discontinuous high amplitude reflectors interpreted as sills intruding sediments of Unit 5. Because the volcanic ridge is onlapped on its landward side by Unit 4, and sills are only present in the lower part of Unit 5, the volcanics must be contemporaneous with Unit 5.

The large block seaward of the volcanic ridge consists of over 1000 m of sediments, interpreted as being Cretaceous in age. This sediment block, consisting of Units 4 and 5, has been displaced down slope and was originally attached to the seaward face of the volcanics. Part of Unit 5 can be traced beneath the valley and remains attached to the volcanic ridge. The reflectors in this unit have been disturbed by the slumping event.

The age of the slumping event predates the draping by Unit 1a. Unit 1a has high amplitude reflectors because it consists of redeposited sediments at the base of the scarp and laterally the reflectors become low amplitude as the sediment becomes a hemipelagic drape over the block. The 80 ms or more of draped sediments present at this depth would represent tens of millions of years. It is equivalent in time to Unit 1 of the sediment wedge on the outer shelf and upper slope.

On the landward side of the volcanic ridge there is at least 600 m of Cretaceous sediment (Units 4 and 5) overlying basement. There is evidence for sills intruding the lower part of Unit 5 and these sills overlie block faulted basement. The upper reflectors of Unit 5 appear to prograde into a channel against the volcanic ridge. Most of Unit 4 has been removed on this side of the volcanic ridge, presumably by erosion. This erosion, possibly by slumping, must have occurred before the deposition of the interpreted Eocene/Paleocene-aged Unit 3 because Unit 3 onlaps the *in situ* strata of Unit 4.

The relationship of Units 1, 2 and 3 with the volcanic ridge is less well defined but they also appear to fill a palaeo-channel as they onlap the volcanic high.

A slump failure in the Cainozoic sediment wedge is the youngest event identified on this line. The slump where it is crossed by this line appears to have failed at the base of Unit 2. A variable amount of slump material remains in the slump scar but any post-slump sedimentation that may have occurred cannot be identified with the resolution of this seismic.

4.5.2. Analysis of High Resolution TOPAS Data

The seafloor in the Myall region is characterised by a smooth undulating morphology, with generally good sub-bottom penetration of up to 100 ms (~75 m). Sub-bottom penetration on the slope in the northern Myall region, however, is generally poor, with penetration typically less than 20 ms (~15 m). Sub-bottom reflectors are intermittent and discontinuous. The data reveal several areas of shallow localised fill (less than 20 ms or ~ 15 m deep and 1 km wide). Proximal to the shelf edge, sub-bottom penetration dramatically increases to between 20 and 50 ms (~15–38 m), and in some areas reaches beyond 70 ms (~50 m). This regional variation in sub-bottom penetration is probably due to changes in seabed sediment composition, with areas of soft hemi-pelagic mud providing better penetration than areas with coarser sedimentation.

Sub-bottom reflections on the slope in the Myall region reveal a series of distinct depositional episodes, each consisting of largely coherent, undulating sub-parallel reflections of varying thickness. Each depositional unit is non-conformable with earlier units, suggesting alternating periods of sediment starvation and/or erosion, and deposition. The top-most unit appears as a largely undisturbed and regionally extensive hemi-pelagic drape. Features such as channel cut and fill, slump and fill, and shallow normal fault displacement, are evident in the underlying units. The data also display areas of strong, shallow acoustic basement reflections and show thinning pelagic drape towards basement outcrop and canyons. Seabed reflections within canyons are prolonged and indistinct or hyperbolic, with little sub-bottom penetration, suggesting rocky substrates with minimal sediment cover.

The main features profiled in the Myall region were the Yacaaba and Birubi Slides. Sub-bottom profiler data indicates that this area has experienced multiple failure events in the past, however much of this activity has been covered by a layer of hemi-pelagic drape ([Figure 4.33](#)). The regions that portray multiple failure events in the subsurface seem to correlate to the more recent failures of the Yacaaba and Birubi Slides, as well as the subdued slides north east of the Yacaaba slide which form part of the southern Myall Canyon. The region between the Birubi and Yacaaba Slides consist of stratified sediments. These patterns suggest that regions which have failed in the past, and have been overlain by pelagic drape, are more susceptible to failure than those areas which resisted failure in earlier times.

4.5.2.1. *Yacaaba Slide*

Six sub-bottom profiles intersect the Yacaaba Slide and surrounding area. Data quality across the slide is generally good, especially in the upper slope with an average penetration of up to 100 ms (~75 m).

Data acquired 3km upslope of the Yacaaba headscarp display undisturbed, bedded sediments, indicating that this upslope area has remained stable in the past. Sub-bottom reflections define a 16 ms (~12 m) thick package of semi-parallel reflectors that overlie several stronger, although less laterally coherent, reflectors. To the southwest these stronger reflections define a narrow incised channel. Whilst there are no coherent reflections within this channel, similar stronger reflections to the northeast define a possible channel, or older slump, that has been filled by bedded sediments.

In the region immediately upslope of the Yacaaba Slide, the data reveal a complex range of opaque, transparent and stratified acoustic responses. The chaotic character of these reflections indicates a complex history of erosion and deposition that can be attributed to multiple movement and failure events. Transported rotated blocks are apparent within this sequence, and these appear to have ponded sediments which have infilled the gaps between the blocks. Deposition of the sediment ponds may have occurred concurrently or during a later slide event. Faulting and the scouring and filling of channels can also be seen in the data. These features are overlain by a 10 ms (~7 m) thick laterally extensive drape of bedded sediment with a distinct basal reflector.

The coherency of the drape indicates that the instability occurred prior to this more recent deposition, with the area subsequently remaining stable and inactive. Similar slump and fill features are evident to the southwest and northeast, although data in some areas appear unaffected by movement processes, characterised by packages of well bedded sediment extending to depths of at least 50 ms (~40 m). This indicates that instability has been localised, with some sections of the slope withstanding failure.

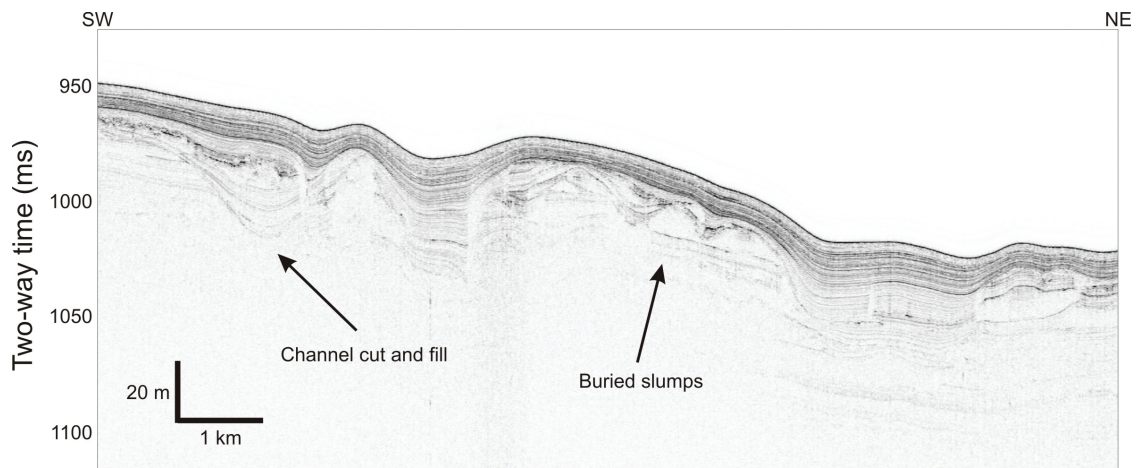


Figure 4.33 Buried slump features upslope from the Yacaaba Slide

Within the Yacaaba Slide, the data shows a series of coherent parallel sub-bottom reflectors, conformable with the seabed reflection. Beneath this package of reflectors, a strong, relatively flat reflector forms the acoustic basement, and may represent the slide surface or basement structure. Figure 4.34 shows sediments within the slide appear coherent and are overlain by a thick pelagic drape.

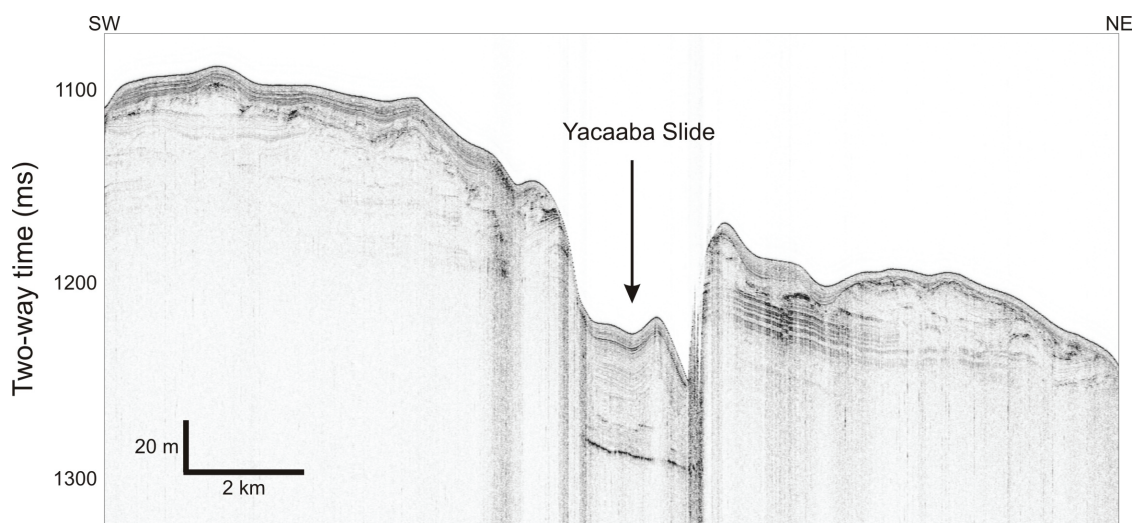


Figure 4.34 Profile across the Yacaaba Slide.

Several profiles intersect the depositional lobe downslope of the Yacaaba Slide scar. A coherent, prolonged and irregularly shaped basal reflector is visible that may indicate an erosional surface or basement geology and is probably an extension of the surface imaged beneath the slide scar (Figure 4.35 and 4.36). This reflector is non-conformable with the seabed reflector, in some areas almost outcropping, while in others covered by up to 20 ms (~15 m).

The region west of the depositional lobe is characterised by incipient failures, and displays variable seabed morphology. To the east, reflections define highly stratified, undisturbed sediments, with an erosional boundary separating the two sediment sequences.

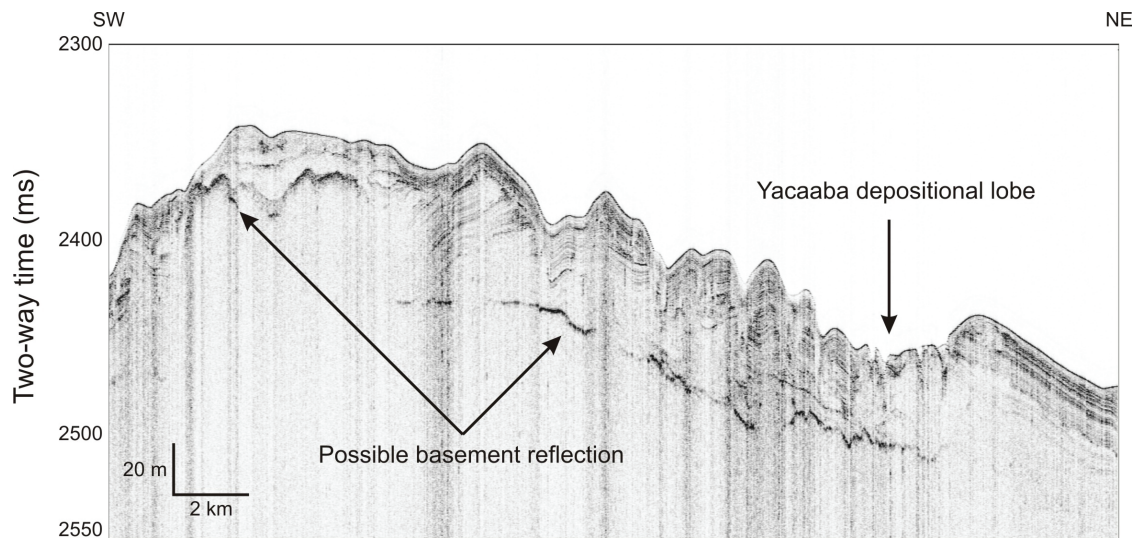


Figure 4.35 A strong basement reflection extends beneath the Yacaaba Slide

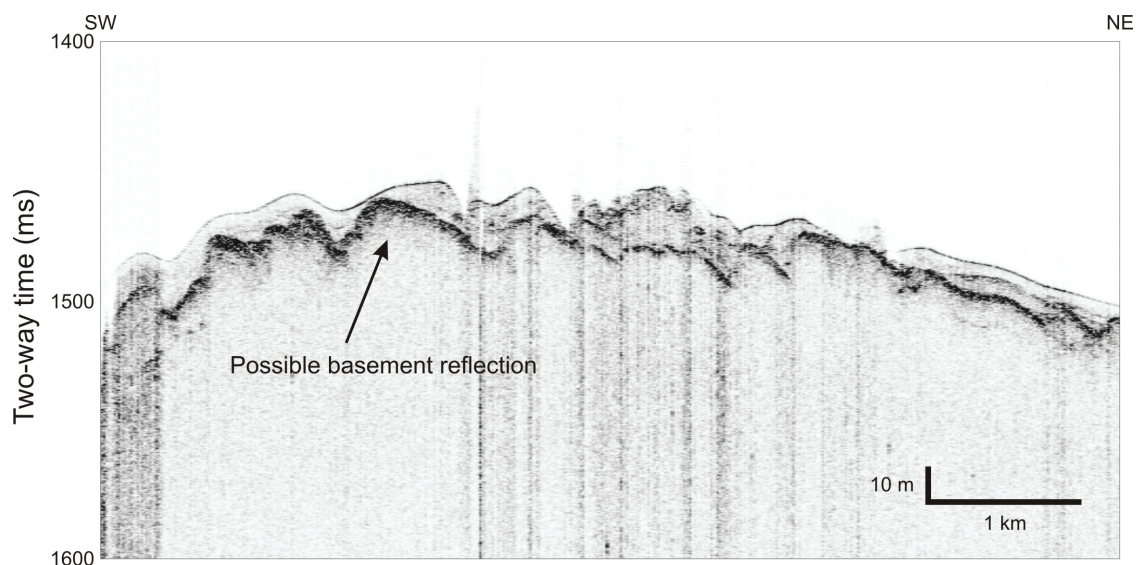


Figure 4.36 Basement reflection downslope of the Yacaaba Slide

4.5.2.2. *Birubi Slide*

Eight sub-bottom profiler lines intersect the Birubi Slide and surrounding area. Data quality across the slide is generally good, especially in the upper slope with penetration on average, up to 100 ms (~75 m).

Data on the upper slope reveal a 16 ms (~12 m) thick package of semi-parallel reflections which overlie several stronger, although less laterally coherent, reflections at depth. These undisturbed reflections suggest that this area has remained stable in the recent past.

In the region upslope of the Birubi Slide, the sub-bottom profiles show a complex range of opaque, transparent and stratified acoustic responses. The chaotic character of these responses indicates a history of erosion and deposition that can be attributed to multiple movement and failure events. These features are overlain by a 10 ms (~7 m) thick laterally extensive drape of well bedded sediment with a particularly strong basal reflector. The bedded nature of the drape indicates recent sediment stability in the region. Some areas appear unaffected by movement processes, characterised by well bedded packages of sediment extending to depths of at least 50 ms (~40 m). This indicates that instability has been localised, and that some sections of the slope have withstood failure or retained coherency during failure.

The extensive pelagic drape imaged across much of the region, is evident within the Birubi Slide, suggesting the slide scar is relatively old (Figure 4.37).

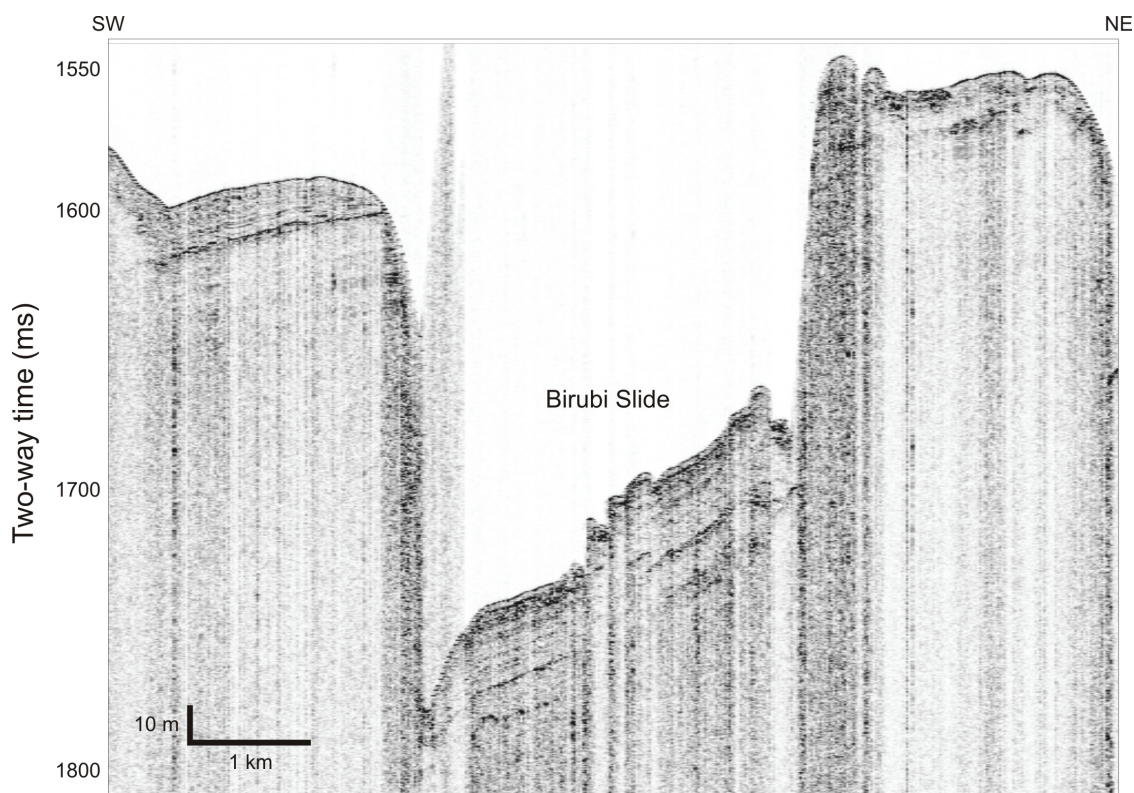


Figure 4.37 Profile across Birubi Slide

4.5.3. Geomorphology

4.5.3.1. *Results from geomorphic interpretation*

In the Myall Region the continental shelf is 29-35 km wide, much narrower that further south in the Hunter Region, and the shelf break is shallower, around 120-140 m WD. (Boyd et al., 2004). The outer shelf consists of carbonate sediments that occur as hardgrounds and exposed cemented mounds (e.g., at 32.6857S; 152.7589E) seen when the ship track crossed the shelf edge off Port Stephens and also described regionally by Boyd et al. (2004). There are two prominent coastal headlands at Port Stephens and Sugarloaf Point. The onshore bedrock geology changes from Permian/Triassic sediments of the Sydney Basin in the Hunter Region to Carboniferous New England Fold Belt volcanics and sediments in the Myall Region (Scheibner and Basden, 1998). Apart from some prominent sand bodies off Port Stephens and Sugarloaf Point, the continental shelf is relatively flat. However, the continental slope is over 25 km wider in the Myall Region and the lower slope has an abrupt seaward shift off Port Stephens. Multichannel seismic data (see seismic section of this report) indicates that the additional material is made up of Mesozoic rift basins and the offset at Port Stephens is likely a transform fault. The continental slope in the Myall Region has two large, complex box canyon features; the Port Stephens Canyons and the Myall Canyon. These features are wide (32 and 37 km respectively) and deep (over 1000 m of relief).

The southern, Port Stephens Canyon consists of two roughly similar-sized tributary box canyons (centred at 32.9957S; 152.6956E and 32.9994S; 152.8116E) that coalesce on the abyssal plain in over 4000 m WD. On the ridge between the two tributaries is a large mounded feature 200-300 m high and 2.5 km long interpreted as a volcanic intrusive.

The Myall Canyon is more complex with two main tributaries (centres at 32.7493S; 152.8970E and 32.6024S; 152.9907E) merging at around 2600 m WD and a “hanging valley” terminating against the main canyon around 1900 m WD. The overall orientation of the Myall Canyon appears to follow orthogonal joints or faults with major axes at 075° and 353°. Like the Newcastle Canyon further south, the Port Stephens and Myall Canyons are developed in bedrock on the lower continental slope. The southern tributary canyon has three channels feeding into it which appear to have formed through retrogressive failure. The northern tributary has widths and lengths of ~3.5 km, 80 m scarps on the northern side and

20 m on the southern slide and a head scarp of 60 m. The middle feature has 65 m high scarps on the southern side, 60 m on the northern and a head scarp of 70 m. Both its width and length is 2.5 km. The third most-southern tributary is less well developed and lower relief (20 m) when compared to the others.

Large blocks of the lower continental slope seem to have been displaced further down slope. An example of this (centred at 32.8119S; 153.0027E) is an isolated knoll, 17 km wide and 26 km long that is incised by the Myall Canyon on the northern side. On the western landward margin this knoll is separated from the continental slope by a 300 m deep U-shaped valley up to 5 km wide. The Port Stephens Canyon has undercut the Tertiary sediment wedge on the upper and mid slope and initiated a series of creep, tension crack and slide features between 600-1500 m WD. The two largest slide features seen in this region are the Birubi and Yacaaba Slides.

The Birubi Slide (centred around 33.1220S; 152.5955E) ranges from 3-5 km wide, is a minimum of 6 km long and has edges up to 140 m high over slopes of 20°. The slide mass has continued on down the Port Stephens Canyon and is no longer identifiable. The floor of the slide has a slope of around 3° and the slide has a failure volume of ~2.31 km³. The Birubi Slide is surrounded by many smaller-scale bathymetrically-discrete failures from lower to upper mid slope.

The Yacaaba Slide begins in a relatively shallow 800 m WD and its erosional form extends to 970 m WD, is up to 3.6 km wide and 3 km long (centred around 32.8770S; 152.7467E). This slide is unusual in that it has formed a debris flow that has been preserved further down slope with more than 80 individual blocks up to 40 m high strewn across a debris apron 5 km long and 4 km wide. The maximum total failure is around 0.24 km³.

The area between the Birubi and Yacaaba Slides is a continuous expanse of slides, tension cracks and faults developed in the Tertiary sediment wedge on regional slopes of 3-4°. These slides continue on to the upslope continuation of the Myall Canyon southern tributary and the northern wall of the northern Myall tributary. In both these Myall Canyon localities the slides are in the order of 2-6 km wide and 3 km long with scarps up to 100 m at the margins. Immediately north of Myall Canyon on the lower slope is another displaced bedrock block 8 km wide and extending down from 2000 m WD to below the limit of data resolution. This block appears to have moved from 400-2000 m down slope.

4.5.3.2. *Discussion of geomorphic interpretations*

The shelf edge off Port Stephens has an interpreted carbonate hardground and a series of buried temperate carbonate reefs and cemented carbonate dunes. These may have been a conduit for sediment transported off the shelf during sea level lowstand, as the lowstand shoreline merged with the shelf edge in this region after being well inshore further to the south. In addition, the shelf break region from Sugarloaf Point to Port Stephens is a preferred site for separation of the EAC from the shelf, offshore migration and eddy formation (Godfrey et al. 1980)

Like elsewhere, the canyons on the lower slope in the Myall Region are box canyons developed in volcanics and sedimentary basement. In contrast, the slides of the upper slope are developed in the sediment wedge. The large offset of the margin at Port Stephens may coincide with the onshore extension of a rift origin transform fault and this ties with the seismic interpretation of Cretaceous Basins developed north of this margin offset but none to the south.

4.5.4. **Sediment Cores**

4.5.4.1. *Gravity Core 06GC05*

This 4.65 m core was located at -32.871S 152.753E, in 922 m water depth. The sediments are largely homogenous throughout the core interspersed with several sandy shelly lenses. There is apparent bioturbation more pronounced in upper 50 cm than below. With a cohesive sandy mud/muddy sand from 5-105 cm. In the next metre from 105 – 205cm, there is the same fabric yet it has an increased water content. And over the next metre (205 – 305 cm) there are sections with slightly coarser sediment. Deeper in the core (305-405 cm) there are coarse sections which contain gastropods and darker sediment lenses. A geotechnical sample was taken at 405 – 435 cm, to test the fabric strength. Medium sand-sized gastropods scattered throughout lower section with coarser sediment in finer mud matrix (435 - 465 cm).

4.5.4.2. *Gravity Core 07GC06*

This 4.31 m core was located at -32.876S 152.751E, in 934 m water depth. The core top is characterised by a sandy mud with shelly debris. Increasing moisture content 0-7cm and an increasing bioturbation to 60 cm.

Bioturbated with sandy fractions throughout (70 – 170 cm) with medium sand-sized gastropods down core at 170 – 270 cm. Further down the core there is decreasing bioturbation but some shelly pockets with infilled burrows and a distinct sand lens at 400 -402 cm.

4.5.4.3. *Gravity Core 08GC07*

This 5.05 m core was located at -32.92S 152.707E, in 828 m water depth. Shelly sandy material (0 – 2 cm) and noticeable high water content (5-6 cm) followed by a 12 cm lens of sandy material, lighter in colour. Gastropod at 23 cm and light mottling at 33 cm.

Bioturbated throughout with occasional medium sand sized gastropods. Discrete lenses of fine-grained material (43 – 295 cm) with decreasing bioturbation and denser material (lower water content) from 295 cm. Increasing shell content from 295 – 443 cm with a dark shelly mud clast at 470 cm. Sandy mud / muddy sand with dark carbon-rich bioturbation (?) with multiple lenses was observed at 474 – 505 cm.

4.5.4.4. *Gravity Core 11GC10*

This 5.32 m core was located at -33.095S 152.621E, in 1183 m water depth. The sediment at the top of the core (0-3 cm) is olive darkening slightly at 3-8 cm. At 10-14 cm it is lightly mottled, sand is infilling burrows and biogenic clasts are found throughout the core. For example at 34-37 cm large infilled burrow, at 52-54 cm echinoderm with large spine is in life position, yet at 56 cm the sediment becomes more compacted, less bioturbated.

The core sediments at 72-172 cm bioturbated homogeneous muddy sand, and again at 172-372 cm. At core depth 316-338 cm, a three 2cm thick sand lenses with subtle mottling was encountered. At 372-382 cm subtle mottling with darker lenses, bioturbated sandy mud. At 382-472 cm homogeneous sandy mud with bioturbation and mottling, and at 515-520 cm, a lens of coarse grained biogenic hash was noted.

4.5.4.5. *Gravity Core 12GC11*

This 4.27 m core was located at -33.1095S 152.599E, in 1257 m water depth. There is slight oxidation on core top along with bioturbation from several organisms. At 33 cm an echinoderm spine, a calcareous tube worm was located at 40 cm, a bivalve trail through core where as at 66-166 cm along with several distinct lenses of shelly hash throughout. Further down

the core at 166-427 cm, the sediments are a homogeneous sandy mud, and bioturbated throughout.

4.6. MANNING REGION

The Manning region was the most northern area surveyed. It extends approximately 80 km along slope north from Seal Rocks ([Figure 4.38](#)). No seismic lines or cores were acquired in this region, and TOPAS lines were not processed due to poor return quality. New multibeam data was collected between depths of 280 and 2800 m.

4.6.1. Geomorphology

4.6.1.1. Results from geomorphic interpretation

The continental shelf in the Manning region widens to 40 km off Forster and is relatively flat with carbonate hard grounds and mounds near the shelf break Boyd *et al.* 1999, 2004. The structure and geometry of the features on the continental slope in the Manning Region shows some differences to the features in the southern part of the survey area.

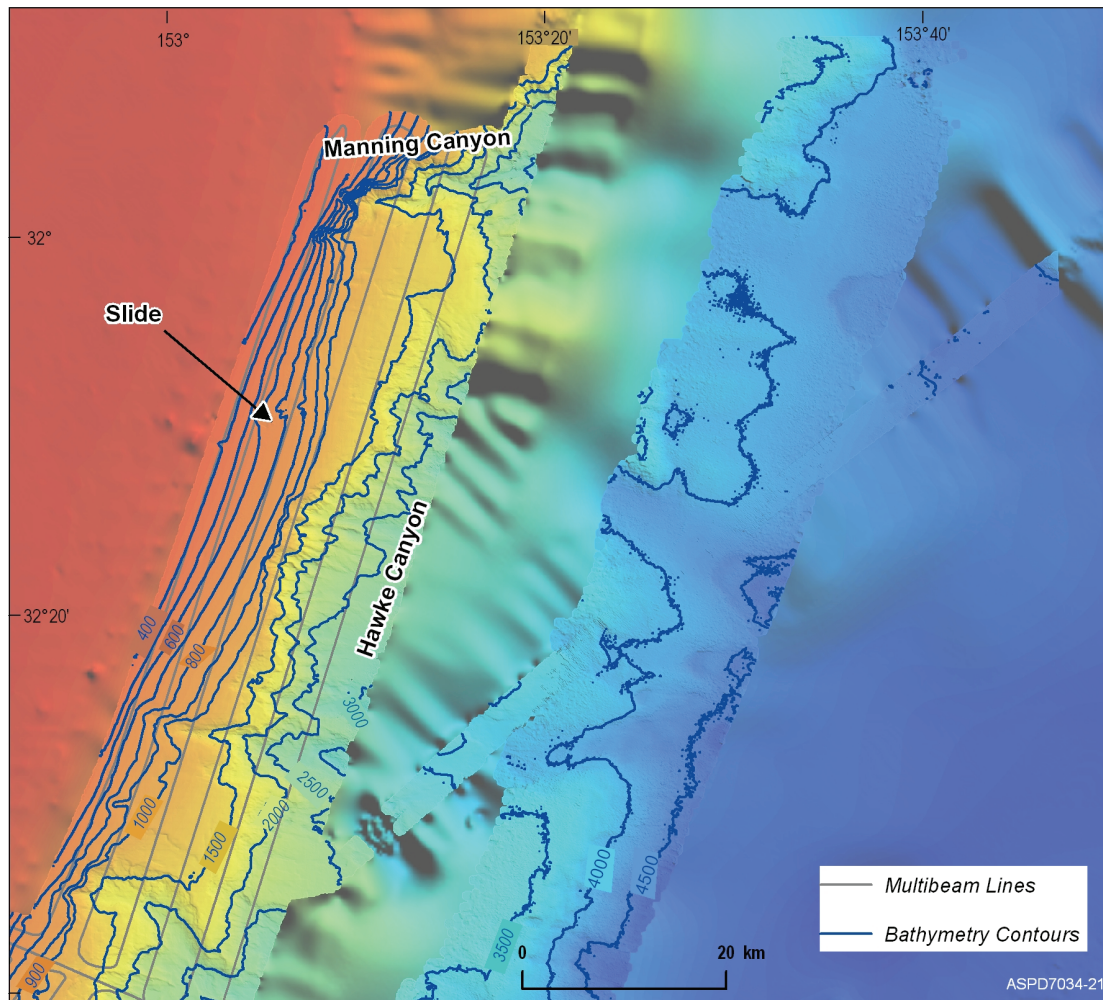


Figure 4.38 Manning Region

At the southern edge of the region a linear canyon extends landward and is flanked further landward by a broad sediment failure around 11 km wide and 9 km long with cracks and incisions over 100 m high around the perimeter. This appears to be a slide with subdued relief possibly indicating greater age than other nearby features or alternatively a slide mass that has faulted along the margins but not translated far down slope.

Immediately to the north, the Hawke Canyon, is a large, continuous feature eroded into bedrock centred around 32.3061S; 152.9582E that occurs over a 48 km long arcuate failure surface with a landward scarp beginning around 850 m WD, extending down slope over 1400 m and displaying a slope of 17°. Current imaging coverage does not permit accurate visualisation of the lower features in Hawke Canyon but there are several mounds similar to those interpreted as volcanic intrusions further south. The southern margin extends landward in a more linear canyon form

and is flanked further landward by a broad sediment failure around 11 km wide and 9 km long with cracks and incisions over 100 m high around the perimeter. This appears to be a slide with subdued relief possibly indicating greater age than other nearby features or alternatively a slide mass that has faulted along the margins but not translated far down slope. The contrasting geometry of Hawke Canyon indicates a different structural and/or bedrock control compared to the Sydney Basin rocks further south.

Further north is Manning Canyon, situated off the mouth of the Manning River at 31.9705S; 153.1854E. The canyon in its central portion is around 5 km wide and 1000 m deep. There are minor tension cracks on the landward margin but the Manning Canyon does not seem to have initiated retrogressive failures upslope of its headwall. The canyon axis has a series of S-shaped bends indicating control by orthogonal structural features.

Sixteen kilometers south of the Manning Canyon head, on the upper slope beginning in around 470 m WD, is another small slide 3 km wide and 2 km long centred at 32.1549S; 153.0907E. It terminates down slope in a debris flow, similar in geometry to the Yacaaba Slide.

5. Discussion

5.1. REGIONAL SYNTHESIS

5.1.1. Seismic Data from the Central NSW Slope

Non-volcanic basement occurs as relatively flat lying strata, folded and dipping strata or block-faulted strata. Flat lying basement strata on the upper slope in Lines 1 and 3 are interpreted as Triassic or Permian sandstones and shales. They overlie folded earlier Palaeozoic rocks. These form the block faults in deeper water. The northernmost Line 7 has basement strata (Permian/Carboniferous?) with a constant dip landward and block faulting starts at the relatively shallow water depth of 900 m. Lines 8, 9 and 11 all have folded basement on the upper slope presumably of Palaeozoic age. The southernmost of these (Line 11) has relatively flat lying basement overlying the folded strata. They could be Permian coal measures of the Sydney Basin and they are clearly block faulted further down the slope at 1300 m water depth.

A major feature of this slope revealed by the seismic survey is the presence of a considerable amount of post-rift volcanics, described in the sections above as Basement Type 2. They are clearly identified as forming a subsurface ridge on Lines 1, 3, 5 and 6 which also outcrops as a sea floor ridge. On the northern survey Lines there are two volcanic ridges on Lines 8 and 11, the outer one outcropping on the sea floor and forming a scarp below 1600 and 2000 m respectively. On Lines 7 and 9 there is a single volcanic ridge which outcrops at 1500 and 1300 m respectively and its seaward slope is a scarp. Internally, these volcanics have seaward dipping reflectors on their outer margin up to 1000 m thick (Lines 3, 5, 6 and 7), are generally flat lying at the ridge crest and some landward dipping reflectors are present on their upslope side. They are interpreted as subaerial flows with possibly some sediment interbedded.

The age of the volcanics is based on limited evidence, yet may be constrained to a narrow time interval. This is because they overlie the rifted basement and they appear interbedded with the lower part of the late Cretaceous sediments and are overlain by the younger Cretaceous sediments. Sills from the volcanics also appear to intrude these Cretaceous sediments. This evidence makes the age of the volcanics as late Cretaceous. They may be related to basalts of the initial spreading of the Tasman Sea.

This seismic survey has delineated for the first time significant mid-slope sediment packets or basins that can be divided into a lower transparent unit and an upper unit with more continuous reflectors. They are interpreted as late Cretaceous post-rift terrigenous mudstones and minor sandstones. Where they have been dredged on this margin the microfossils indicating lacustrine or marginal marine environments.

These Cretaceous sediments are present on all lower slope lines except Line 9. Lines 1 and 6 confirm a basin shape with maximum thickness on Line 1 of >1200 m (assuming a velocity of 2000 m/s) in a water depth of 1340 m. The strata in this basin onlap the seaward face of the volcanics and dip obliquely down the present day slope to the north-east. On Line 7 there is a Cretaceous basin with a thickness of > 600 m (WD 1100 m) on the landward side of a volcanic ridge, while on the seaward side of the ridge there is a slumped Cretaceous block of intact sediment at least 1000 m thick. A similar block consisting of 800 m of Cretaceous sediment occurs seaward of an outer volcanic ridge on Line 11. The slip surface revealed by multibeam bathymetry and the thrust faulting within the block confirm that this block has moved down slope. On Lines 8 and 11 there is at least 800 m and 400 m respectively of Cretaceous sediment between two volcanic highs.

On Lines 3 and 5 only remnants of Cretaceous sediment are left as most has been removed by slumping on the underlying seaward dipping volcanics. On Line 9 the Cretaceous sediments have probably been removed by headward slumping as the box canyons have eroded further upslope and into the volcanics on this line.

The lower sediment of this late Cretaceous sequence fills the half grabens formed by basement fault blocks and is interbedded and/or intruded by lavas or sills from the volcanic ridges. The upper sequence onlaps both the volcanics and older basement. The top of the Cretaceous strata show offlapping reflectors or are truncated by erosion prior to the deposition of Unit 3.

The high-amplitude reflector overlying the basement and Cretaceous strata and underlying the sediment wedge forms Unit 3 and extends over the entire region. This unit is generally <50 m thick and is flat with only gentle topography where it drapes the underlying unconformity on basement and Cretaceous rocks. It becomes less distinct beneath the present day shelf. It is interpreted as a glauconitic limestone of Paleocene/Eocene age similar to samples previously dredged from the

slope. This unit slopes seaward beneath the sediment wedge and continues down slope until it is truncated by slumping at steep canyon heads. On Lines 3 and 7 it is not continuous down slope as it onlaps basement highs. On Lines 8 and 11, where overlying sediment has been removed by slumping this unit forms a flat sea floor. The glauconitic limestone was deposited on a near horizontal shelf with at least two 'islands' breaking the otherwise relatively flat topography. Post deposition, this shelf has been tilted seaward to its present dip.

The sediment wedge consists of two prograding units and is present on every line on the shelf and upper slope. It is interpreted as post-Eocene in age and reaches its maximum thickness at the shelf break. Seismic Lines 7, 8, 9 and 11 are the only lines to cross the shelf break (at WD 170, 160, 180 and 180 m respectively) with corresponding thicknesses of 550, 620, 650 and 600 ms. The lithology is probably calcareous and terrigenous muds with a lesser amount of siliciclastic and carbonate sand. Near surface cores (<5 m in length) on the slope consist of glacial cycles of calcareous sandy muds and muddy sands. Beneath the sea floor on the upper slope, reflectors in Unit 1 downlap onto Unit 2 reflectors and Unit 2 reflectors downlap on Unit 3 or lower reflectors in Unit 2. Some reflectors at the base of Unit 2 are horizontal and fill the underlying topography on Unit 3. The top of Unit 3 is an unconformity surface. Strike Lines 4, 6 and 10 show continuity of beds in Units 1 and 2 along slope with no canyon fills or channel fills. This sediment wedge thins down slope and evidence for incipient failure appears as faults and slumps in dip Lines 1, 5, 7, 8, 9 and 11. The only dip line without incipient faults in the wedge is Line 3. On this line the wedge abuts an outcropping volcanic ridge. Similarly every line down slope except Line 3 has sections of the wedge missing due to slumping.

5.1.1.1. Relevance of Seismic Data to Submarine Slides

Based on the seismic data there are two distinct types of gravity slides on this margin. There are those related to the sediment bedding planes in the Cainozoic wedge and a second group that are related to the seaward face of volcanic highs.

The volcanic ridges often have seaward dipping reflectors that may facilitate instability of overlying sediments. Seaward dipping reflectors now parallel the sea floor under the slip surface of the Bulli Slide (Line 3) and

they also occur beneath the slump on Line 5 where the overlying Cretaceous sediments have moved several km down slope. This slump material is 200 m thick where the line ends down slope.

On Line 1, up to 1000 m of Cretaceous sediment are *in situ* and overlie dipping reflectors on the seaward side of a volcanic high. This is the only line that recorded significant amount of *in situ* sediment on the seaward side of a volcanic ridge and has the potential to move down slope. In the Hunter and Myall regions up to 1000 m of Cretaceous sediment has moved down slope as coherent blocks on the seaward face of volcanic ridges on Lines 7 and 11. The *in situ* Cretaceous sediment basins on Lines 7, 8 and 11 all have outer volcanic ridges that may act as a buttress and prevent their possible movement down slope. South of Line 8 resistant knolls and ridges can be identified on the multibeam imagery for 25 km along slope to the Newcastle Canyon. They are aligned with the outer volcanic ridge in the Line 8 seismic. They suggest the outer volcanic ridge extends south to the Newcastle Canyon. This is particularly important as the slope over this section has not failed. The mid-slope Cretaceous sediment basin identified in Line 8 probably continues south and is supported from failure by these volcanics.

The age of slumping on the outer face of the volcanic highs is difficult to determine. Draping by younger sediment suggests the slump on Line 7 is tens of millions of years old while lack of draping on the slumps in Lines 3 and 5 and the slump block in Line 11 suggest much more recent movement.

The sediment wedge above the planar Unit 3 is prone to failure as slabs and debris flows. All down slope lines except Line 3 show incipient faults and slumps up dip from earlier failures now exposed on the sea floor. The sediment wedge on Line 3 is buttressed by a sea floor volcanic high and this has prevented down slope movement. On Lines 7, 8 and 9 these incipient movements occur in the subsurface below the 450 m isobath. On Lines 1, 5 and 11 incipient movement is further upslope, as shallow as 370 m water depth.

Where failure has occurred in the sediment wedge it appears to be step-like, involving more of the sediment wedge with each step down slope. This implies failure planes within the sediment wedge as well as at the base on a much harder underlying Unit 3. The lower failure steps on Line 11 are characterised by small depressions. The seismic confirms that these depressions overlie major faults in the basement and thus are likely to be

formed by escaping gas or fluids. This may add to the slope instability.

The areas with the potential for slumping may be those where the thickness of the sediment wedge is greatest down slope of incipient faults. Five of the eight seismic lines have significant thicknesses of intact sediment (Units 1+2) occurring in water depths greater than 800 m and down slope from subsurface faults. On Line 6 there is 300 ms of sediment at 1040 m WD, Line 7 has 170 ms of sediment at 800 m WD, Line 8 has a 220 ms sediment thickness at 800 m WD, Line 9 has 250 ms of sediment at 800 m WD and Line 11 has 220 ms of sediment at 800 m WD. Of these lines the wedge on Lines 6 and 9 appears particularly vulnerable because the Line 9 wedge is underlain by a break in slope of basement and similarly for Line 6 assuming a continuation of the break in slope of basement on nearby Line 1. Line 9 also has the maximum thickness of wedge recorded in this survey of 650 ms at the shelf break.

Lack of draping or ponding of sediment on the failure planes and debris deposits indicates that the slides profiled in the sediment wedge are the youngest features resolved by the seismic.

5.1.2. Sedimentation and Stability on the Central NSW Slope

Several features of interest in the high resolution seismic, multichannel seismic and multibeam data help define the sedimentation and stability characteristics of the central NSW slope.

5.1.2.1. Incipient failures

The continental slope of central NSW contains a large number of incipient failures. These are mainly identified through tension cracks visible on the seabed. These features are often only meters to tens of meters high, but are associated with minor slippage of a few tens of meters and often show a buried fault beneath them. They occur across the entire depth range but are frequently distributed in the 700-1500 m depth range. They can often extend laterally along the slope for 5-10 km and link up with the head scarps of slides that have already occurred. Sites with extensive tension cracking extending a long distance along slope over large, well sedimented regions are indicative of a high risk of future failure.

5.1.2.2. *Canyons*

Canyons intersect the upper slope off the three major rivers imaged on this survey, the Shoalhaven, the Hunter and the Manning. In all three of these regions, at depths above the 500 m isobath, the seabed steepens across a sediment wedge and slopes reach 7-9°, compared to 3-4° on the rest of the upper-mid continental slope. It appears that there have been upper slope sediment depocentres off these three rivers in the Quaternary. Both multichannel and TOPAS seismic data from this voyage off the Hunter show prograding clinoforms with interpreted interbedded sandy and muddy units consistent perhaps with a shelf edge delta of probable Pleistocene age. The increased slope and more recent sedimentation promote a different form of slope erosion characterised by rills and gullies and small canyons rather than mass failures. Several of the canyons originating in these areas off major rivers have well developed levee systems on the middle slope. This indicates a depositional episode in their evolution. More recently this depositional phase seems to have ended and a secondary phase of erosion has occurred in the canyons, resulting in a terraced channel morphology.

5.1.2.3. *Types of sediment transport*

There are a range of sediment gravity transport types on the NSW slope. These range from small creep structures with or without tension cracks, to incipient slides that have not moved far from their source, slides with and without associated crown scarp faults, to large sediment slides, and large seabed failures that involve bedrock (volcanic basement or Sydney Basin/New England/Lachlan Fold Belt basement). The types of sediment gravity failures can be broken down into two types based on the process of transporting the displaced material. The first of these (Type 1) is where the displaced mass remains adjacent or near to the failure location. Type 2 is where the displaced mass has been transported away from the failure location. In the latter case, the displaced mass cannot usually be located down slope from the failure scarp. Even at the base of the continental slope, using the deeper multibeam data acquired by the French scientists on the Marion Defresne, there is no evidence for an accumulation of coherent slide debris at the base of the Bulli and Shovel Slides for instance. This suggests that the flow of sediment down slope has not remained coherent and has transformed into a density flow. In addition, down slope of many Type 2 failures are steep inclines related to bedrock failures that

exhibit a rapid change of slope and a scarp. It is unlikely that any mass flows could retain their coherence over such steep topography, again suggesting that the displaced slide masses are converted to density flows. These flows would accumulate at the base of the slope and this conforms to the presence of a thick sediment wedge in this location. It also explains the widespread absence of displaced slide masses on the continental slope like those documented in other areas such as the Santa Barbara Channel (Greene et al., 2006).

5.1.2.4. *Two zones and contrasting failure types*

The central NSW slope can be divided into 2 major zones, an upper zone between the shelf break at 150-170 m and 1100-1200 m, and a lower zone between 1100-1200 m and the Tasman Abyssal Plain. The upper zone corresponds to where the margin is covered by a mostly Tertiary sediment wedge (e.g., Davies 1979), while the lower zone corresponds to where rock outcrops on the slope. Over most of the central NSW slope, the rock is likely to be either volcanics of seismic Unit 2, or consolidated Paleozoic sediments, metamorphic and igneous rocks of the Sydney Basin and Lachlan Fold Belt. North of Port Stephens the basement rocks change character and are likely composed of New England Fold Belt rocks including volcanics and sediments of Carboniferous to Devonian age plus volcanics of seismic Unit 2. In addition, the lower slope contains a number of exposed volcanic intrusive and extrusive features that are interpreted to be more recent (probably Cretaceous to Cainozoic in age) and related to Tasman Sea break-up and hot spot migration.

The two major zones on the NSW slope exhibit two contrasting types of sediment failure. The upper zone shows examples of retrogressive sliding of unconsolidated Cainozoic sediments. Geomorphic evidence discussed above suggests that these unconsolidated sediment slides have experienced relatively recent motion. The lower zone shows down-slope movement and apparent rotation of large faulted blocks consisting of more lithified Cretaceous and possibly older rocks, probably related to rift processes during margin formation, followed by ongoing retrogressive failure.

5.1.2.5. *Style of erosion and deposition*

The style of erosion and deposition on the NSW slope appears to be

substantially different to that seen in many well documented examples from other passive margins of similar age such as that of the US Atlantic and Gulf Coasts. In essence the difference seems to be one of recent erosion on the NSW margin compared to deposition on most other margins. The fact that an extensive Tertiary wedge of sediments is developed on the NSW margin (Davies 1979, Boyd et al., 2004) is evidence that there was a previous period of deposition. However, this sediment wedge is only around 500 m in maximum thickness, and again the NSW margin is sediment deficient compared to other margins. Over its history, with ongoing subsidence caused by initial crustal thinning and later thermal cooling, the gradients on the margin have continued to increase, resulting in a style of retrogressive gravity failure over all of the lower slope and much of the upper slope. This has not been balanced by ongoing sedimentation, thus contributing to the present state of sediment instability where the overlying sediment wedge is continually undercut by slope failure over geological time, and this promotes modern episodes of failure.

One of the specific outcomes of the NSW margin style of sediment deficient retrogressive erosion is the morphology of submarine erosional and depositional features. Most continental margins are characterised by a network of submarine canyons and associated fans. These canyons are usually linear features, often connected upslope to river sources of sediment, and formed by erosional density currents. However the NSW margin canyons are “box canyons”. The only exceptions to this are the canyons connected to the upper slope off the major rivers of the Shoalhaven, Hunter and Manning. Box canyons are enclosed in an upslope direction and have not resulted from erosion by density flows. Instead these box canyon features appear to result from retrogressive gravity failure, possibly along the original normal faults associated with rifting. They are located in specific areas (e.g., the Sydney Canyon and the Newcastle Canyon) spaced around 15-50 km apart and are probably responding to underlying structural trends. Virtually all of these major box canyons have retrograded up to the base of the sediment wedge and are now initiating sediment slides above their headwalls. This provides one way of predicting future risk, as the most likely areas to experience problems are those with thick sediment wedges above a large box canyon that have not yet failed. Where these areas are combined with bedrock blocks or volcanic intrusions that have compacted differently to the surrounding sediments, the risk is increased further.

5.1.2.6. *Sediment correlation*

Detailed sediment correlation across the debris flow and associated slide scar off Port Stephens (the Yacaaba Slide) was possible using TOPAS sub-bottom profiler data. These data clearly demonstrated that the material below the base of the slide is not the same as the remaining material in the exposed walls of the slide. This observation, tallied with other similar observation in other slides such as the Shovel Slide, indicate that these depression features in unconsolidated sediment on the continental slope are definitely slides and not downfaulted blocks. However, it should be noted that the margins of the slides are also often the sites of associated faults. Hence faults and incipient cracks probably preceded the sliding process.

5.1.2.7. *Compaction*

There are numerous examples of interpreted sedimentary and volcanic bedrock features outcropping or thinly buried on the middle to upper continental slope. Where these features are surrounded by more recent post-break-up sediments, they are likely to compact at a much lower rate than the surrounding water-laden sediments and contribute to sediment instability down slope from the bedrock features.

5.2. HIGH RISK AREAS FOR FUTURE SUBMARINE LANDSLIDES

The entire central NSW continental slope appears to be prone to sediment mass movement, ranging from tension cracks to creep, faulting, debris flows and slides of all scales. Many of these appear to be related to underlying causes such as hard volcanic, metamorphic or lithified Paleozoic sediments close to the surface, or retrogressive failures upslope of box canyon heads. Taking these factors into consideration, and also the location of significant unfailed sediment accumulations, a prediction can be made about the location of high risk areas for future landslides.

Examples of these areas occur at:

1. A 10 km-long area off Newcastle between 300-1000 m water depth that has a large sediment accumulation developed on the upper

slope and is undercut by a large box canyon below a number of incipient failures. This feature is centred at 33.2343S; 152.3802E.

2. A 7 km-long area off the northern Illawarra region between 1150-1550 m. This region is adjacent to a failure and the crown scarp of this failure extends into the high risk region as a series of tension cracks. The adjacent failure has approximately 150 m of sediment missing and this is likely to be the thickness of the high risk region if it also fails. This feature is centred at 34.1961S; 151.6740E.
3. A 3.7 km long by 5.3 km wide area off Sugarloaf Point between 900-1300 m depth is undercut by a large box canyon. The entire sediment block is at least 50-100 m thick and surrounded by a tension crack and scarp up to 110 m high. Further upslope are several other tension cracks. This feature is centred at 32.5404S; 152.9794E.
4. A large 50 km-long, mostly unfailed area occurs offshore between the Hawkesbury River and Norah Head where a sediment accumulation between 400-1500 m water depth has wide-ranging tension cracks and small failures but no previous major canyons. On the mid slope there is a sediment slide that has moved down slope a distance of 5 km. This feature is 6 km long, up to 14 km wide and appears to be around 50 m thick. Geomorphologic interpretation suggests that this slide (unlike most others of this scale in this depth range) is one that has moved down slope and then stopped. Further future motion may still occur. This feature is centred at 33.4509S; 152.3647E.
5. A large depression has formed off Sugarloaf Point centred at 32.4532S; 152.9763E that has tension cracks around the southern margin and a subsided block at both the northern and western margin. The block is around 10 km long and 5 km wide with margins around 100 m high. Below the block on the northern side are two canyons 200-300 m deep that have undercut the block and appear to be generating retrogressive failures upslope.

6. Conclusions

As part of a wider program within Geoscience Australia this 15 day marine survey successfully developed a regional understanding to assess the implications of submarine landslides. The survey was tasked with identifying the nature of the substrate, recent and relict morphological features, deposition stratigraphy, and geologically recent slope failures along the NSW Continental Slope. The survey succeeded in locating numerous failed areas and areas prone to failure by identifying slope failure architecture and slip plane geometry across much of the continental slope.

Throughout the survey, multiple data sets were collected. These data sets include sea floor video, 9200 km² of swath data, sonar, 3414 line kms of sub-bottom profiling, 14 gravity cores, echo-sounder, radiometric dated sediments and 340 line kms of seismic. This data enhances our understanding of the nature of the NSW Continental Slope and is actively supporting the Geoscience Australia tsunami and inundation modelling program. This modelling will assist in the assessment of the high risk areas for potential tsunamigenic submarine slides that are adjacent to populations and critical infrastructure.

The study focused on 5 sections along the coast. These were the Jervis Bay, Sydney/Illawarra, Hunter, Myall and the Manning. The survey identified the Bulli Slide (~20 km³) a major slide along with others including: Shovel (7.97 km³); Birubi (2.31 km³); and Yacaaba (0.24 km³).

The data sets from this survey firmly indicate that significant areas of the central NSW Continental Slope have been prone to sediment mass wasting over time. The data also helped to identify the critical contributing factors for these features such as basement geometry, slope angle and overlying sediment thickness. Slope instability and failures were observed on the seafloor as: tension cracks; hummocky accumulations of sediment from the extremely slow downward movement of sediment (creep); small scale faulting; irregular redistributions of sediment (deposits from debris flows) and significant erosional slide scars on the sea floor. In addition, an enhanced understanding was developed on the general morphology of the NSW Continental Slope, including multiple incised valleys, mid shelf gullies, canyons and multiple styles of slope failure.

Analysis of the stratigraphy, detailed geometry, and structural qualities of the sediment fabric has improved the geotechnical

understanding of the strength and composition of the slope sediments. Determining the time of pre-existing slope failures was challenging, as none of the cores appeared to penetrate the un-failed surface, consequently no exact failure dates can be established. Radiometric dating of the slide sediments from limited data collected indicates that the most recent potentially tsunamigenic failure found on this survey is calculated to be >3700 years BP.

Seismic and sub bottom profiles, along with the slope morphology attained from swath imagery, identified several styles of failure. One style of failure relates to the sediment bedding planes in the Cainozoic sediment wedge, and the second style relates to the critical dynamics of the seaward face of volcanic highs, basement slope and sediment thickness. Taking these factors into consideration and assessing the location of significant un-failed sediment accumulations, a preliminary prediction can be made about the location of high risk areas for future slides. Five areas were identified as zones of potential future failure which display incipient failure features, sediment accumulation and slope undercutting. These include:

- A 10 km-long area off Newcastle between 300-1000 m water depth.
- A 7 km-long area off the northern Illawarra region between 1150-1550 m.
- A 3.7 km long by 5.3 km wide area off Sugarloaf Point between 900-1300 m.
- A large 50 km long area between the Hawkesbury River and Norah Head between 400-1500 m.
- A 10 km long by 5 km wide region off Sugarloaf Point.

While preliminary, these data provides a good overview of the nature of sediment slumping on the continental shelf. To ensure these findings are robust additional phases of work are required. These include a more comprehensive swath program infilling the areas not covered in the survey and a greater number of core profiles, and longer core profiles that penetrate the unfailed surface in order to tie down the ages of the failures. Geoscience Australia is well placed to carry out this work and to extend the insights to other locations around the Australian margin.

7. Acknowledgements

We thank Master Ian Taylor and all the ship's crew for their expert persistent handling of the RV *Southern Surveyor* in often challenging circumstances. We thank the GA staff particularly the Field and Engineering Support group, without whom this marine survey would not have been such a success. We are grateful to Fred Kroh and Mike Sexton who provided valuable help with attribute analysis and seismic processing and are indebted to the Sediment Lab staff and Jonathan Edwards for timely processing of sediments. The authors express their appreciation to the reviewers Dr Phil O'Brien and Dr Graham Logan, for their valuable comments.

8. References

- Alder, J.D., Hawley, S., Maung, T.U., Scott, J., Shaw, R.D., Sinelnikov, A. and Kouzmina, G., 1998. Prospectivity of the offshore Sydney Basin: a new perspective. *The APPEA Journal*, **38**, 68-91.
- Andrews, J., Lawrence, M. and Nilsson, C., 1980. Observations of the Tasman Front. *Journal of Physical Oceanography*, **10**, 1854–1869.
- Atkinson J. H. and Bransy P. L., *The Mechanics of Soils: An introduction to critical state soil mechanics*. 1978, McGRAW-HILL, University Series in Civil Engineering, ISBN 0-07-084077-6.
- Bickford, G., Heggie, D., Birch, G.F., Jenkins, C., Ferland, M.A., Keene, J.B. and Roy, P.S., 1992. *Preliminary Results of AGSO RV Rig Seismic Survey 112 Leg B: Offshore Sydney Basin Continental Shelf and Slope Geochemistry, Sedimentology and Geology*. Australian Geological Survey Organisation Record 1993/5, Canberra. 121pp.
- Borissova, I., Moore, A., Sayers, J., Parums, R., Coffin, M.F., and P.A. Symonds, 2002. *Geological Framework of the Kerguelen Plateau and adjacent Ocean Basins*. Geoscience Australia Record 2002/05, Canberra. 120pp.
- Boyd, R. and shipboard crew. 1999. *Cruise Report RV Franklin 15/98, Marine Stratigraphy and Sedimentology of the Northern NSW and SE Queensland Shelf*. University of Newcastle, 128p.
- Boyd, R., Ruming, K. and Roberts, J.J., 2004. Geomorphology and surficial sediments on the southeast Australian continental margin. *Australian Journal of Earth Sciences*, **51**, 743-764.
- Browne, I., 1994. Seismic stratigraphy and relict coastal sediments off the east coast of Australia. *Marine Geology*, **121**, 81-107.
- Bryant, E.A., Young, R.W. and Price, D.M., 1992. Evidence of tsunami sedimentation on the southeastern coast of Australia. *Journal of Geology*, **100**, 753-765.

- Chaytor, J.D. and Huftile, G.J., 2000. *Faulting in the Newcastle area and its relationship to the 1989 M5.6 Newcastle earthquake*. Dams, fault scarps and earthquakes; proceeding of a conference held by the Australian Earthquake Engineering Society, Australia, 2000. p. 9.0-9.5.
- Colwell, J.B., Coffin, M.F. and Spencer, R.A., 1993. Structure of the southern New South Wales continental margin, southeastern Australia. *BMR Journal of Australian Geology and Geophysics.*, **13**, 333-343.
- Colwell, J B and Roy, P S. 1983. *Description of subsurface sediments from the east Australian continental shelf ("Sonne" cruise SO-15)*. Bureau of Mineral Resources, Geology and Geophysics Record 1983/21, Canberra. 65pp.
- Conolly, J.R., 1969. Western Tasman Sea Floor. *New Zealand Journal of Geology and Geophysics*, **12**, 310-343.
- Davies, P.J., 1979. Marine geology of the continental shelf off southeastern Australia. *BMR Bulletin*, **195**, 51pp.
- Daytona Energy and Bounty Oil and Gas, 2001. Offshore Clarence-Moreton: An overlooked basin with petroleum potential? *PESA News, NSW Supplement*, October/November 2001, 20-21.
- DiCaprio, L.J., Muller, D., Gurnis, M., and A. Goncharov, *in press*. The structure and history of the Norfolk Basin, SW Pacific. *Geochemistry Geophysics Geosystems*.
- Dugan, B., and Flemings, P. B., 2000, Overpressure and fluid flow in the New Jersey Continental Slope: Implications for Slope Failure and Cold Seeps, *Science*, **289**, 288-291.
- Eldholm, O., Thiede, J., and Taylor, E., 1987. *Proceedings of the Ocean Drilling Program, Initial Reports*, vol. 104. College Station, Texas.
- Ferland, M.A., Roy, P.S. and Murray-Wallace, C.V., 1995. Glacial lowstand deposits on the outer continental shelf of southeastern Australia. *Quaternary Research*, **44**, 294-299.
- Godfrey, J.S., Cresswell, G.R., , Golding, T.J., Pearce, A.F. and Boyd, R. 1980. The separation of the East Australian Current. *Journal of Physical Oceanography*. V. 20, No. 3, 430-440.

- Greene, H.G., Murai, L.Y., Watts, P., Maher, N.A., Fisher, M.A., Paull, C.E., and Eichhubl, P., 2006. Submarine landslides in the Santa Barbara Channel as potential tsunami sources. *Natural Hazards and Earth System Sciences*, **6**, 63–88.
- Hayes, D.E. and Ringis, J., 1973. Seafloor spreading in the Tasman Sea. *Nature*, **243**, 454-458.
- Head K.H. (1986) Manual of soil laboratory testing, Volume 3, Pentech Press.
- Heggie, D. 1993. *Preliminary results of AGSO RV Rig Seismic Survey 112: Offshore Sydney Basin continental shelf and slope geochemistry, sedimentology and geology*. AGSO Record 1993/5, 121pp.
- Hodgins, B., 1995. *Cainozoic seismic stratigraphy of the continental shelf off Newcastle*. BSc Honours thesis, Department of Geology, University of Newcastle, (unpublished).
- Hubble, T.C.T., Packham, G.H., Hendry, D.A.F. and McDougall, I., 1992. Granitic and monzonitic rocks dredged from the southeast Australian continental margin. *Australian Journal of Earth Sciences*, **39**, 619-630.
- Hubble, T.C.T. and Jenkins, C.J., 1984. *Sediment samples and cores from the southern New South Wales upper continental slope*. University of Sydney Ocean Sciences Institute Report 8. 34pp.
- Huftile, G.J., Van Arsdale, R. and Boyd, R., 1999. *Pleistocene faulting offshore Newcastle, New South Wales*. Proceedings of the 1999 Conference, Australian Earthquake Engineering Society, Sydney. Paper 17, 1-5.
- Jenkins, C.J. and Keene, J.B., 1992. Submarine slope failures of the southwest Australian continental slope: a thinly sedimented margin. *Deep-Sea Research I*. **39**, 121-136.
- Jones, H.A., Davies, P.J. and Marshall, J.M., 1975. Origin of the shelf-break off southeast Australia. *Journal of the Geological Society of Australia*, **22**, 71-78.

- Jones, H.A., Lean, J. and Schlüter, H.-U., 1982. Seismic reflection profiling off the east coast of Australia, Newcastle to Cape Hawke. *Geologisches Jahrbuch*. **D56**, 69-75.
- Lane, J and Heggie, D., 1993. *Physical properties and bulk chemical composition of continental shelf and slope sediments of Australia*. Australian Geological Survey Organisation Record 1993/7, 86pp.
- Larsen, H.C., *et al.*, 1994. *Proceedings of the Ocean Drilling Program*, Initial Reports, vol. 152. College Station, Texas.
- McLachlan, A.. 2005. Standard Operating Procedure: Malvern Particle Size Analyser. GA Palaeontology and Sedimentology Laboratories unpublished internal document, SOP no. PMD-SED-SOP-2.
- Marshall, J F. 1980. Continental shelf sediments: southern Queensland and northern New South Wales. *BMR Bulletin*, **207**, 39pp.
- Marshall, J.F., 1979. The development of the continental shelf of northern New South Wales. *BMR Journal of Australian Geology and Geophysics*, **4**, 281-288.
- Maung, T. U, D. Alder, R. Shaw, and S. Hawley, 1997. *Offshore Sydney Basin*. Bureau of Resource Sciences, Petroleum Prospectivity Bulletin 1997/1. Canberra,
- Mernagh, T., Pyke, J., Taylor, P., Juodvalkis, A., McKenzie, G., 2007. Minerals Division Laboratory Methods (UG Lab methods 2.1). Geoscience Australia Minerals Laboratories, unpublished internal document.
- O'Brien, G W and Heggie, D T., 1990. *Organic carbon cycling and Quaternary phosphorite formation - East Australian continental margin (28 degrees-32 degrees S). Project 9131.03 sample locations and solid phase geochemical results*. Bureau of Mineral Resources, Geology and Geophysics Record 1990/45, Canberra. 109pp.
- Packham, G.H., 1983. *Morphology and acoustic properties of the N.S.W. slope with special references to the Coffs Harbour-Point Plommer and Montague Island-Green Cape area*. University of Sydney Ocean Sciences Institute Report 1.
- Planke, S., Symonds, P.A., Alvestad, E., and Skogseid, J., 2000. Seismic volcanostratigraphy of large-volume basaltic extrusive complexes on

- rifted margins. *Journal of Geophysical Research*, **105**, 19335-19351.
- Prior, D.B. and Coleman, J.M. 1980. Sonograph mosaics of submarine slope instabilities, Mississippi Delta. *Marine Geology*, **36**, 227–239.
- Quilty, P.G., Shafik, S., Jenkins, C.J., and Keene, J.B., 1997. An Early Cainozoic (Paleocene) foraminiferal fauna with *Fabiania* from offshore eastern Australia. *Alcheringa*, **21**, 299-315.
- Reid, J., 1986. On the total geostrophic circulation of the South Pacific Ocean: flow patterns, tracers, and transports. *Progress in Oceanography*, **16**, 1–61.
- Retallack, G.J., 1999, Postapocalyptic greenhouse paleoclimate revealed by earliest Triassic paleosols in the Sydney Basin, Australia: Geological Society of America Bulletin, **111**, 52–70.
- Ridgway, K. R. and Godfrey, J. S., 1994. Mass and heat budgets in the East Australian Current: a direct approach. *Journal of Geophysical Research*, **99**, 3231–3248.
- Ridgway, K. R. and Godfrey, J. S., 1997. Seasonal cycle of the East Australian Current. *Journal of Geophysical Research*, **102**, 22921-22936.
- Ringis, J., 1972. *The Structure and History of the Tasman Sea and Southwest Australian Margin*. PhD thesis, University of NSW, 338pp.
- Roberts, D.G., Backman, J., Morton, A.C., Murray, J.W., and Keene, J.B., 1984. Evolution of volcanic rifted margins: synthesis of Leg 81 results on the west margin of Rockall Plateau. *Initial Reports of Deep Sea Drilling Project*, vol. 81, 883-911.
- Roy, P.S. and Thom, B.G., 1981. Late Quaternary marine deposition in New South Wales and southern Queensland – an evolutionary model. *Journal of the Geological Society of Australia*. **28**, 471-189.
- Satake, K. and Kato, Y., 2001. The 1741 Oshima-Oshima eruption: extent and volume of submarine debris avalanche. *Geophysical Research Letters*, **28**, 427-430.
- Scheibner, E., and Basden, H., 1998. Geology of NSW, Synthesis, Vol. 2, Geological Evolution. Geological Survey of NSW, Memoir Geology, 13, 2.

- Shaw, R.D., 1978. Sea-floor spreading in the Tasman Sea: a Lord Howe Rise – eastern Australia reconstruction. *Australian Society of Exploration Geophysics*, **9**, 75-81.
- Shirley, J., 1964. An investigation of the sediments on the continental shelf of New South Wales, Australia. *Journal of the Geological Society of Australia*, **11**, 331-341.
- Short, A.D. and Trenaman, N.L., 1992. Wave climate of the Sydney region, an energetic and highly variable ocean wave regime. *Australian Journal of Marine and Freshwater Research*, **43**, 765-791.
- Stewart, R. and Alder, D. 2001 (editors) New South Wales Petroleum Potential. *Bulletin: New South Wales, Coal and Petroleum Geology Branch*.
- Symonds, P.A., Planke, S., Frey, O., and Skogseid, J., 1998. Volcanic evolution of the western Australian continental margin and its implications for basin development. *In The Sedimentary Basins of Western Australia 2. Proceedings of the PESA Symposium*, Eds. P.G. and R.R. Purcell, Perth, 33-54.
- Tappin, D.R., Matsumoto, T., Watts, P., Satake, K., McMurtry, G.M., Matsuyama, M., Lafoy, Y., Tsuji, Y., Kanamatsu, T., Lus, W., Iwabachi, Y., Yeh, H., Matsumoto, Y., Nakamura, M., Moihoi, M., Hill, P., Crook, K., Anton, L., and Walsh, J.P., 1999. Sediment slump likely caused the 1998 Papua New Guinea tsunami. *EOS Transactions of the American Geophysical Union*, **80**, 329, 334, 340.
- Troedson, A.L. and Davies, P.J., 2001. Contrasting facies patterns in subtropical and temperate continental slope sediments: inferences from east Australian late Quaternary records. *Marine Geology*, **172**, 265-285.
- Vail, P.R. and Mitchum, R.M., 1977. Seismic stratigraphy and global changes of sea level, 1, Overview. *Memoirs of the American Association of Petroleum Geologists*, **22**, 51-52.
- Young, R.W. Bryant E.A. and Price D.M., 1996. Catastrophic wave (tsunami?) transport of boulders in southern New South Wales, Australia. *Zeitschrift fur Geomorphologie*, **40**, 191-207.

9. Appendices

9.1. APPENDIX A: AVAILABILITY OF SURVEY DIGITAL DATA

Below is a list of survey data and products that can be requested for each data type. Data can be made available upon request, at cost of transfer. For further information on accessing digital data acquired during the survey contact: ausgeodata@ga.gov.au

9.1.1. Sub-bottom Profile Data

Sub-bottom profile data was collected using a TOPAS PU98 Parametric sub-bottom profiler. This data is in the raw form that can be read using TOPAS software and also in processed data in SEG-Y format. Sub-bottom profile (TOPAS) deliverables include:

- Data volume: ~80GB depending on format selected;
- Raw TOPAS internal format (no filtering or scaling) – requires Kongsberg TOPAS software to read but has the advantage of allowing data processing for specific attributes (amplitude, frequency and phase);
- Processed SEG-Y data – 32 bit IEEE format with filtering and time variant scaling applied.

9.1.2. Multi-beam Data

Multi-beam data was collected using a Kongsberg Simrad EM 300 multi-beam echo sounder with a nominal frequency of 30 kHz. This data was processed with Caris software. EM300 Swath data deliverables include:

- Data volume: ~5 to 50GB depending on format selected;
- Raw EM300 format data, which is an open-file format but has not been processed or despiked;
- Generic Sensor Format (GSF) with beam indexed amplitude, this is the reflectivity component of the multi-beam. Note, this is fully processed and despiked data;
- Caris HDGS format which contain all processed despiked data;
- X,Y,Z files as extracted from GSF data, which provides bathymetric at high resolution for use in a GIS. Note, these are fully processed and despiked data

9.2. APPENDIX B: VIDEO COMMENTARY

Location: Sydney/Illawarra Region

Site: Across the side scarp of the upper Bulli Slide

Water Depth: Ranging from 1370 to 1620 m (refer Figure 4.4).

Time on video	Sedimentary features	Biota
3:29:45	Faun coloured bioturbated sediments, with scattered white echinoderms, small burrows. Some of the burrows have spatially associated mounds ~3 – 5 cm and < 1 m apart. Conical burrows are recent (they have not been infilled)	small red fish,
3:30:27	Unconsolidated sediment cloud and seafloor Sediments are unconsolidated (3.30.27) Burrows ~5cm diameter, medium density in the viewing frame spacing of the burrows are ~10 - 15 cm apart	
3:30:47		Solitary sessile (?) organisms - sea whips (?) eel (?)
3:31:20	Soft unconsolidated bioturbated light coloured sediments	Areas of white thin armed echinoderms (3.31.20) in areas of fewer burrows
3:32:17	Mounded burrows	
3:32:37	algal (?) growth on the sediments growing upwards as small stalks (?)	
3:33:26		Fish near substrate and white echinoderm
3:33:49	subdued sea floor, occasional burrows	
3:34:53	occasional burrows on fairly lat	scattered white

	sea floor	echinoderm
3:35:05	burrows	White echinoderm
3:35:23		several small fish (small ~3 - -5 cm) swimming just above the substrate
3:36:34		soft coral (?) emergent from the substrate
3:37:45	Substrate showing history of bioturbation and thin covering veneer of more recent fine unconsolidated material	
3:38:15	Burrow and mounds, and soft coral (?)	
3:38:21	Burrows	
3:38:24		Single fish near substrate
3:39:11	extensive burrows	
3:39:20		Sea whip
3:39:48	lightly bioturbated seds with some mounds	Close-up sea whip, and larger fish above the whip
3:39:55		Fish
3:40:00		Fish
3:40:03		Close-up sea whip
3:40:48	Lightly bioturbated soft sediments	Echinoderm light coloured and more compact than the other encountered so far.
3:42:51	Lightly bioturbated (burrows) soft sediments	
3:44:21		Comb jelly (?)
3:54:31	Apparent slope / gradient in the sea floor, soft substrate has algal (?) cover in places, and some burrow and mounds (~5cm high / deep)	2 independent small fish
3:55:03	small mounded burrows	small Black fish

3:59:17		Starfish and soft coral (?)
3:55:59	Algal (?) covered sediments burrows and mounds.	small fish on sea floor
4:01:08		close-up of jellyfish
4:01:47		Eels?
4:02:06		Sponge (on far left of screen) and eel / algae?
4:03:02		swimming Decapod (shrimp?)
		Echinoderm brittle star (?)
	Mounded bioturbated sediments, appears to be on a slope due to the camera angle.	
4:05:32	Bivalve. No current at seabed.	
4:05:49	Largest burrows observed at this video transect (~15cm).	
4:06:08	Mounded bioturbated sediments, appears to be on a slope due to the camera angle.	


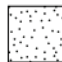




9.3. APPENDIX C: VISUAL CORE LOGS

Core Log Legend






Fossils

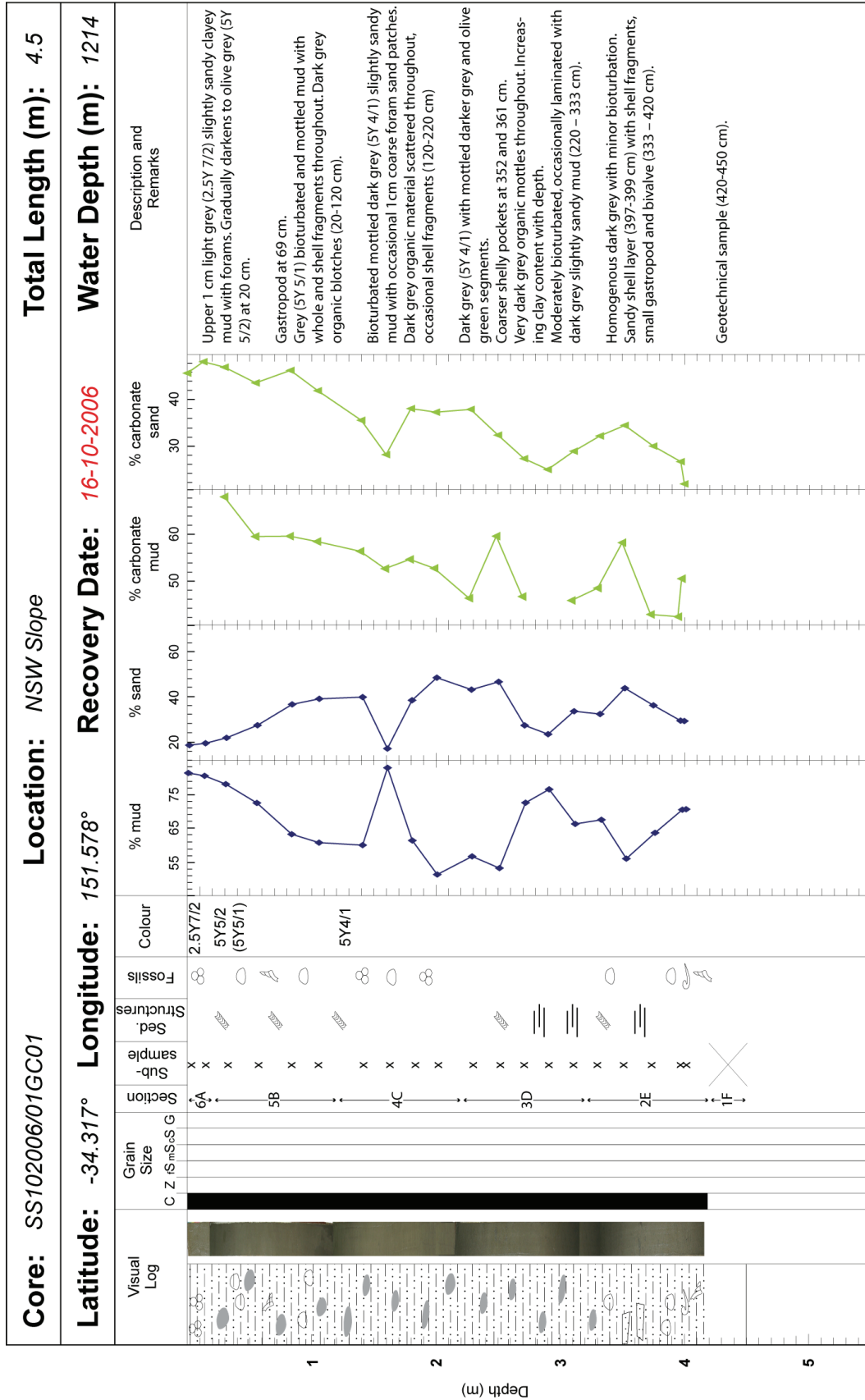
	Shell fragment
	Bivalve
	Foraminifera
	Gastropod
	Pteropod
	Echinoderm
	Worm tube

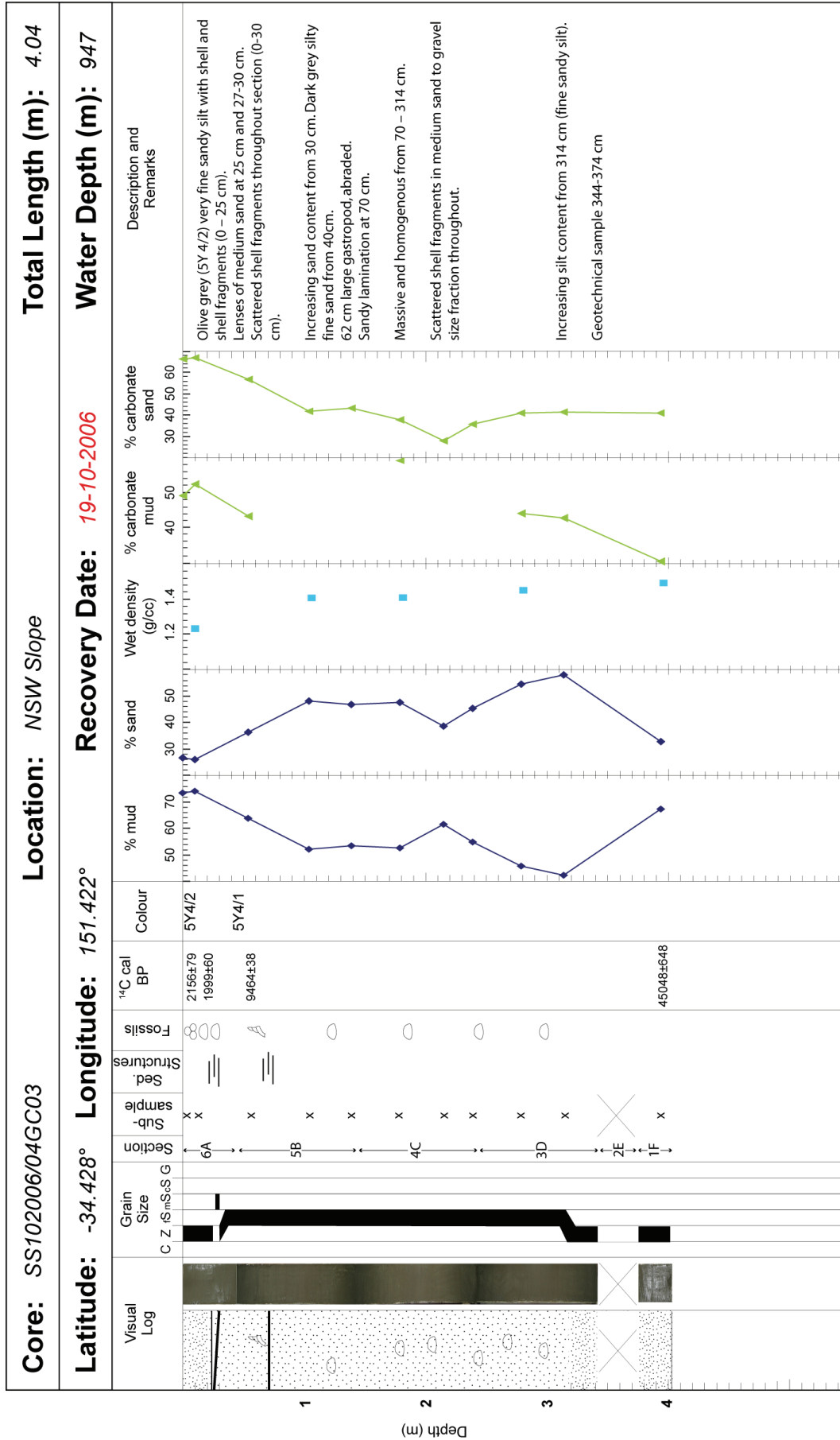
Lithology

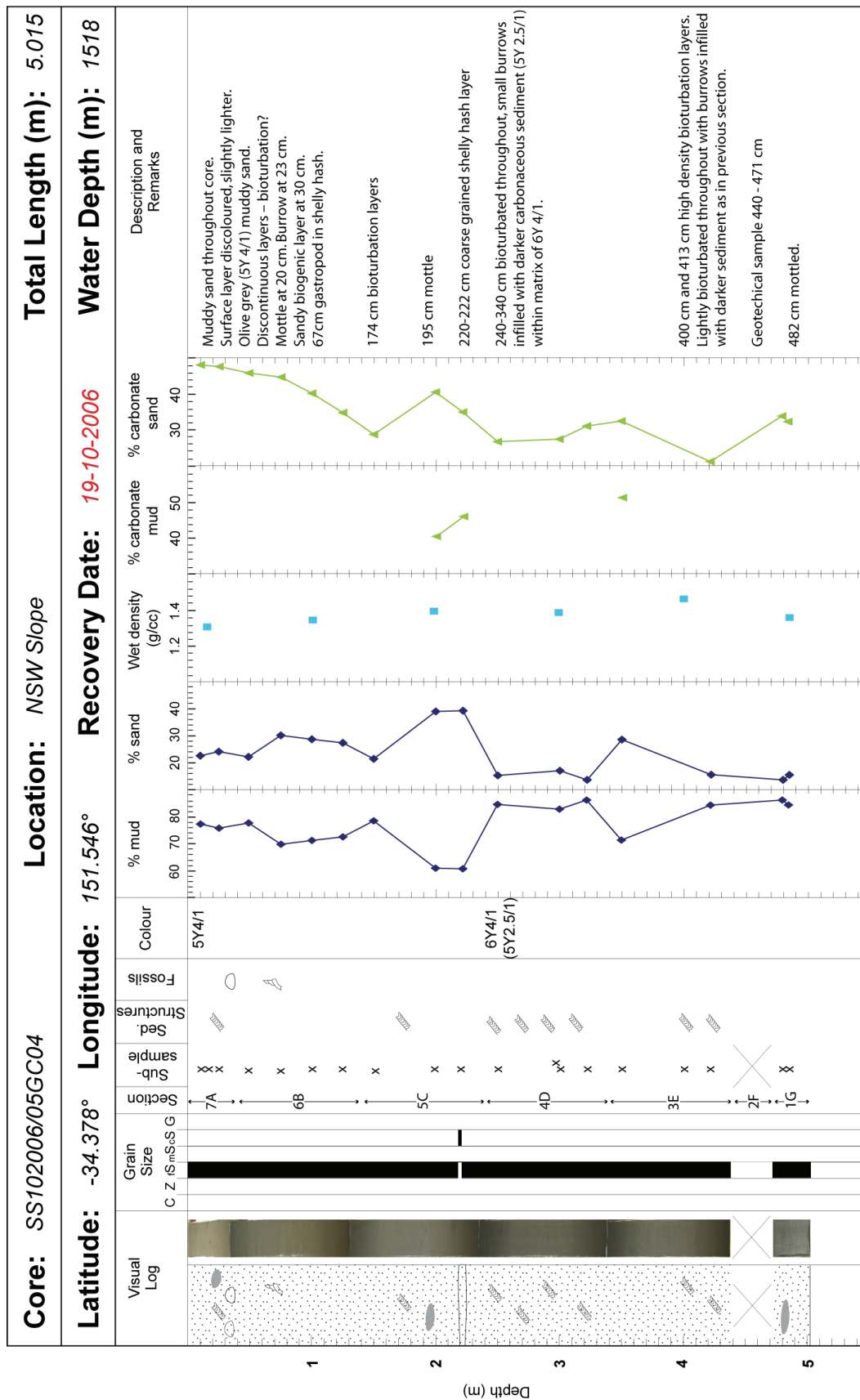
	Clay
	Silt
	Sandy mud
	Fine sand
	Medium sand
	Coarse sand

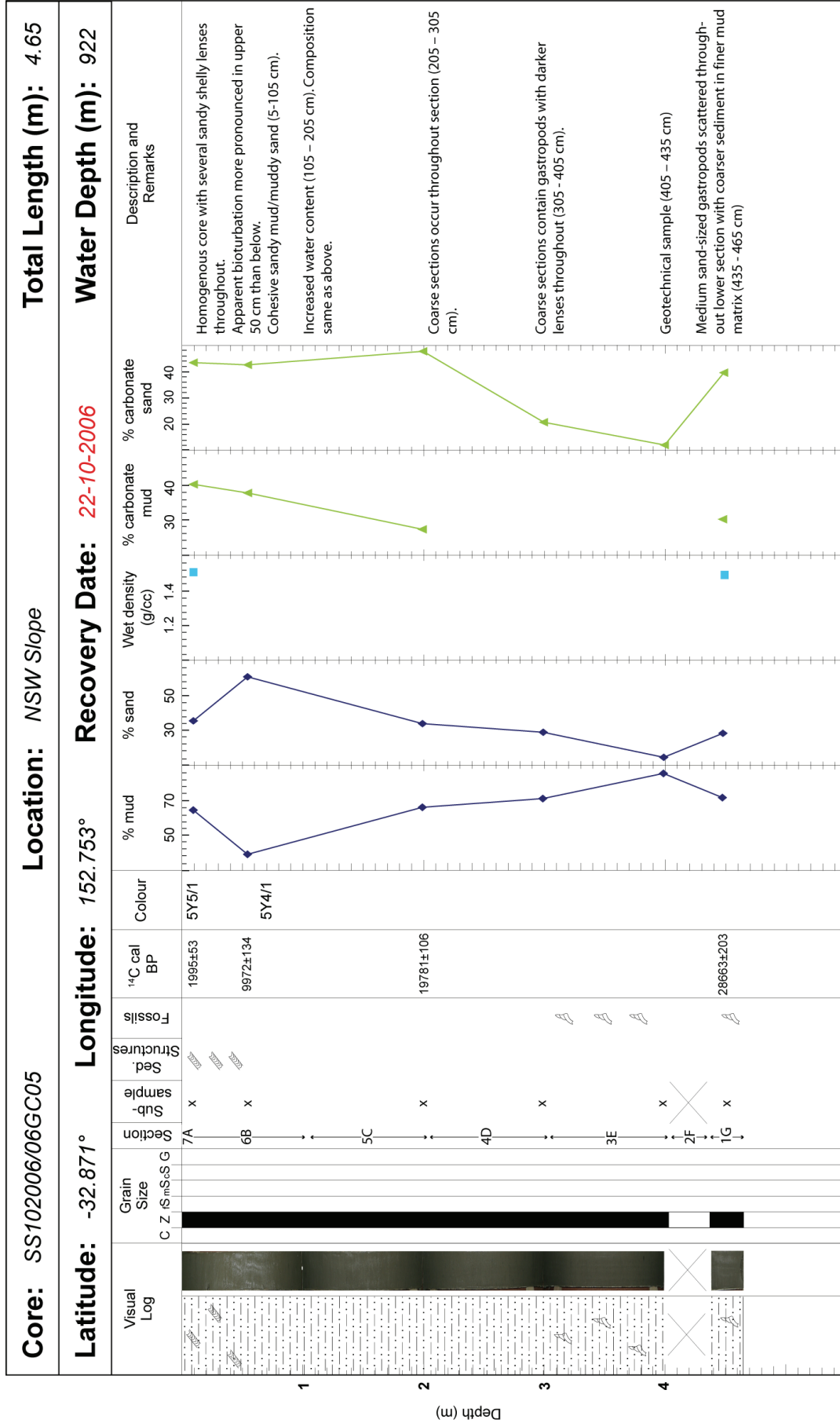
Sedimentary Features

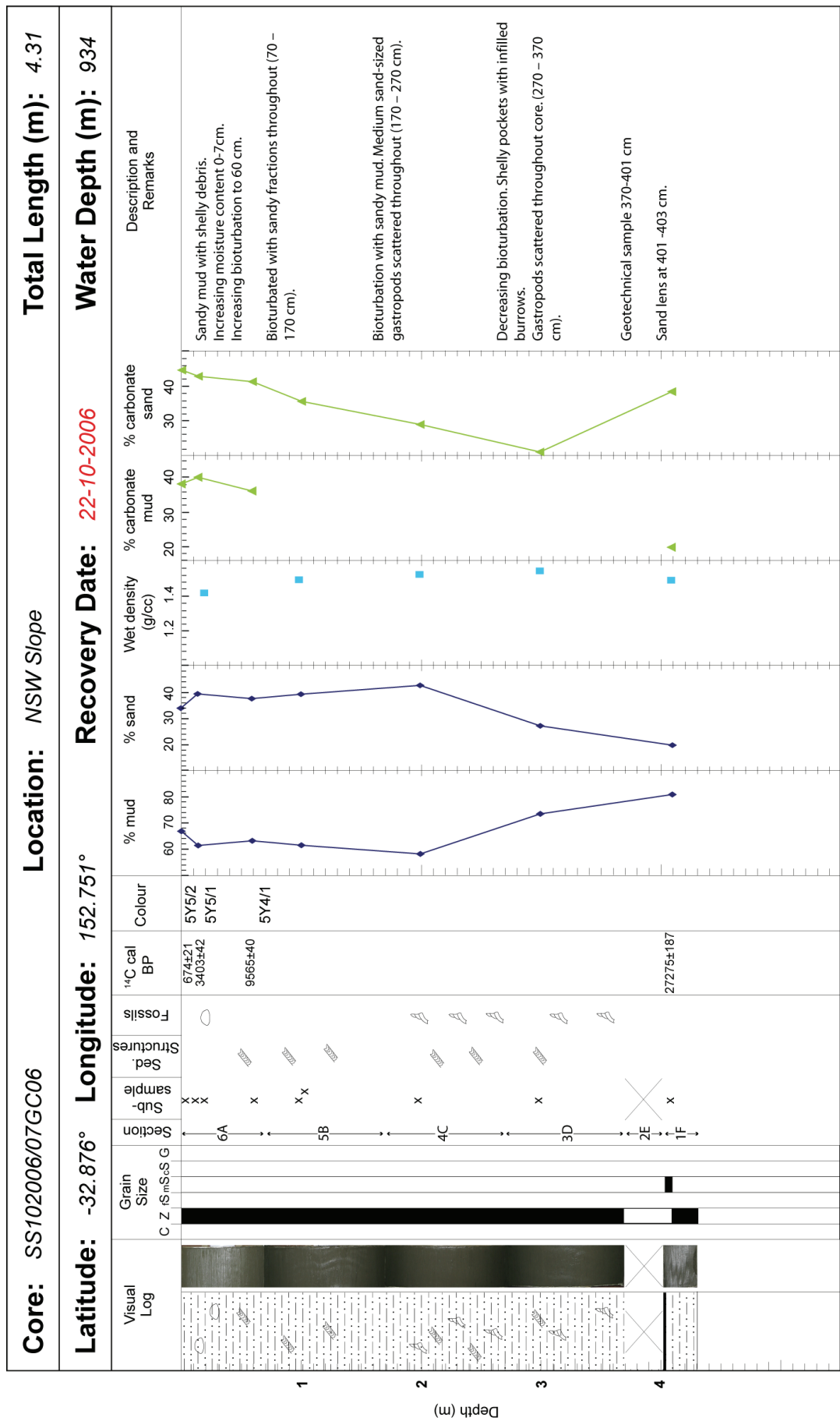
	Wood
	Laminations
	Bioturbation
	Organic streak
	Mottle

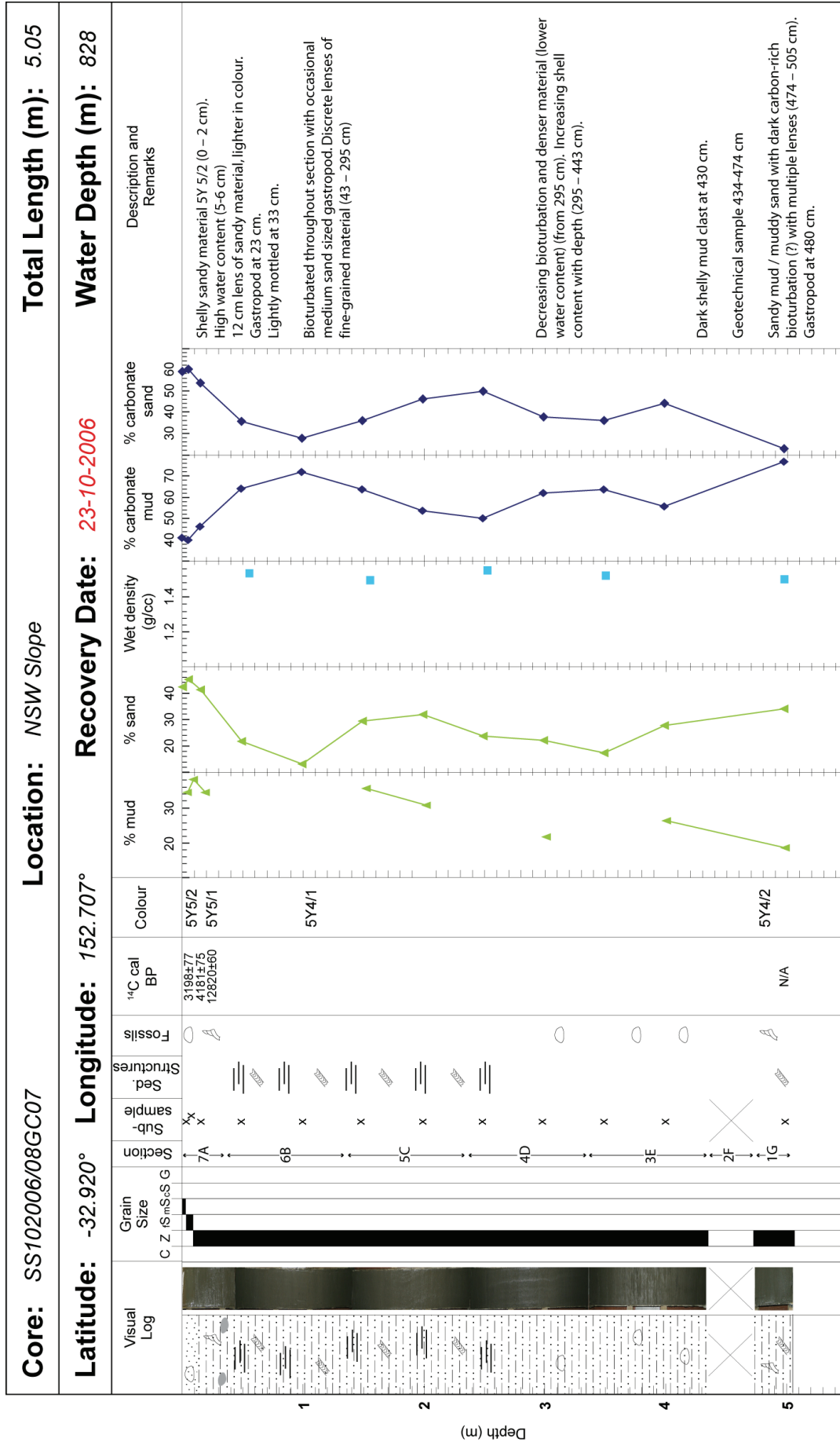


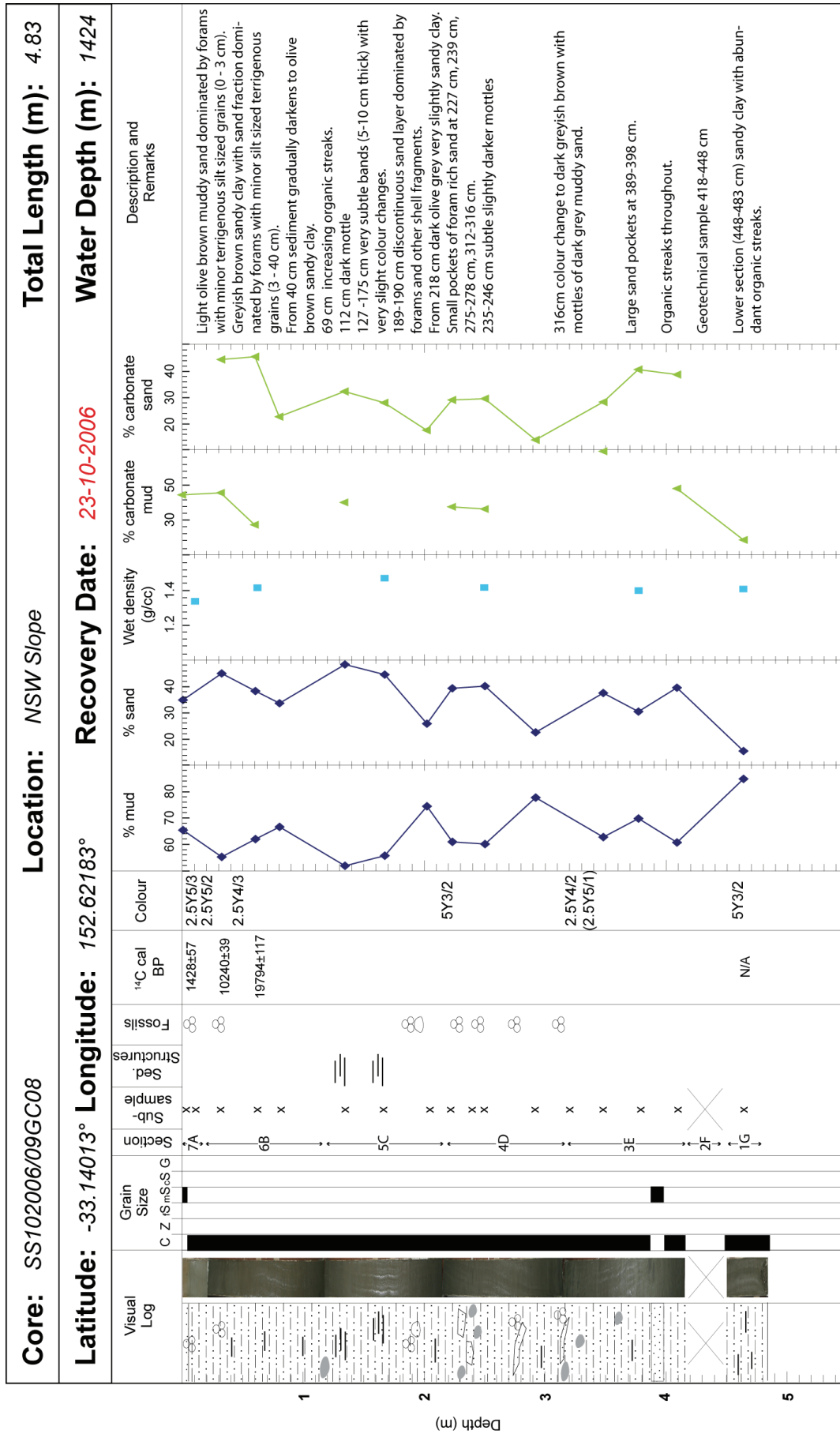


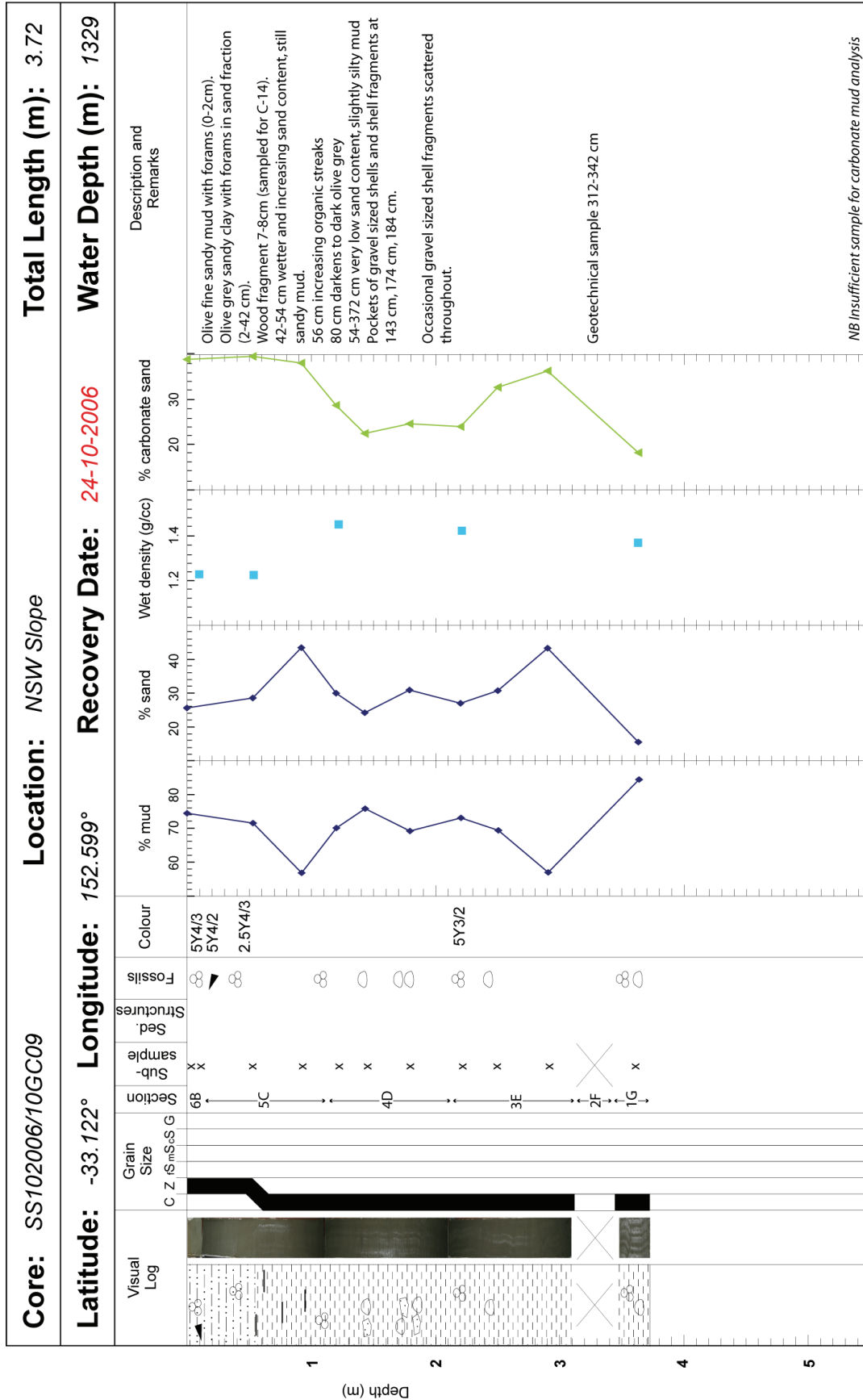


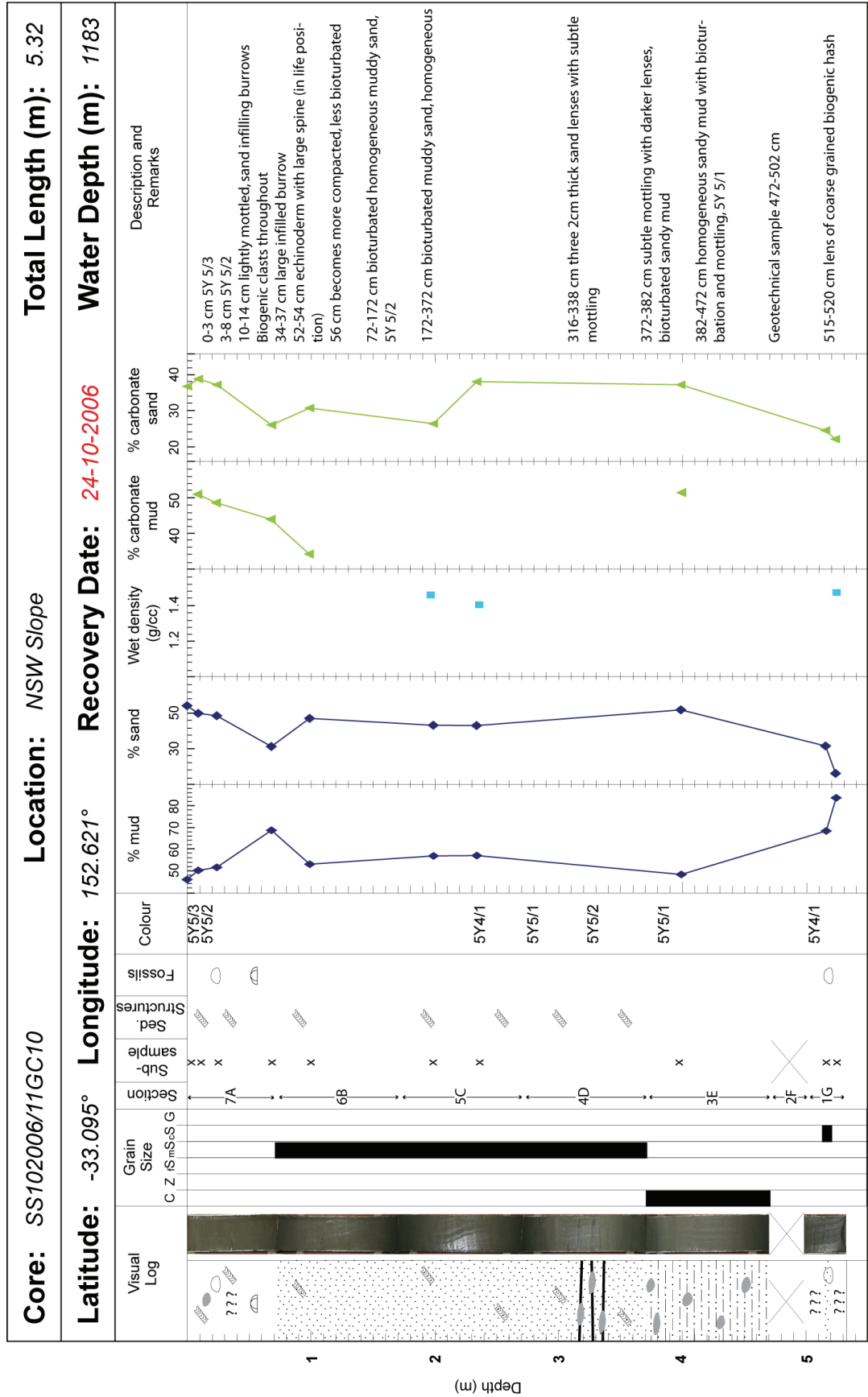


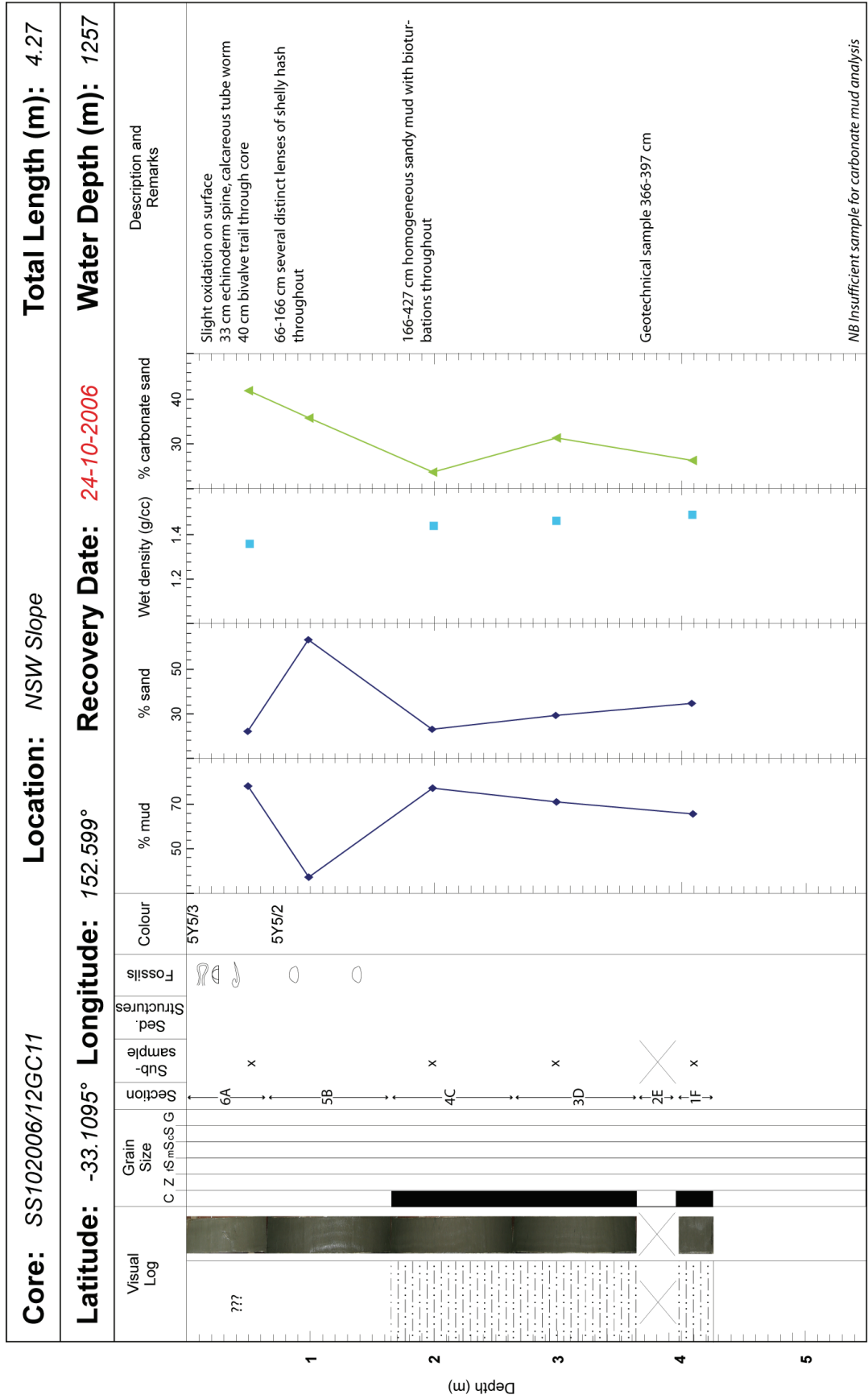


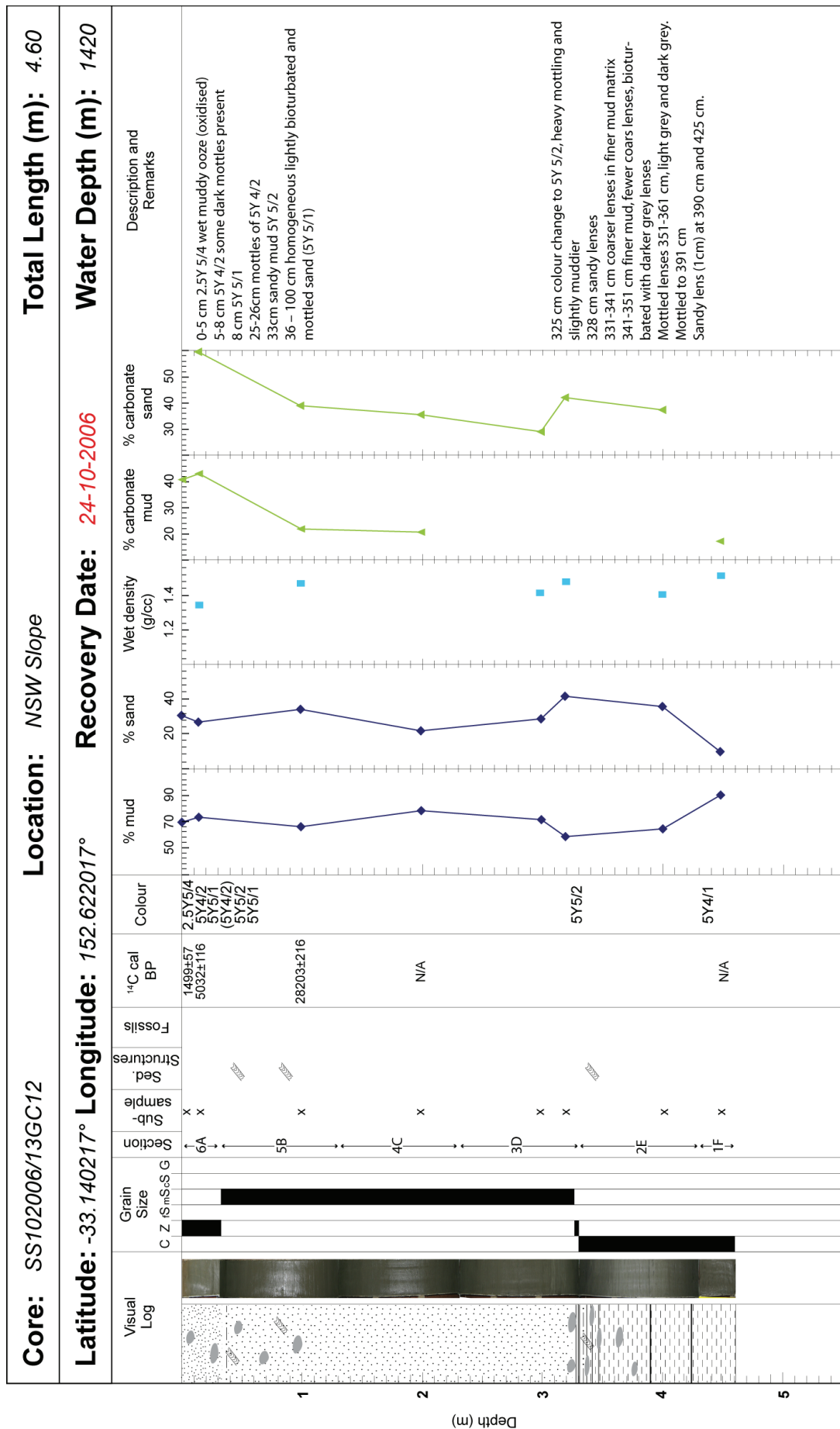


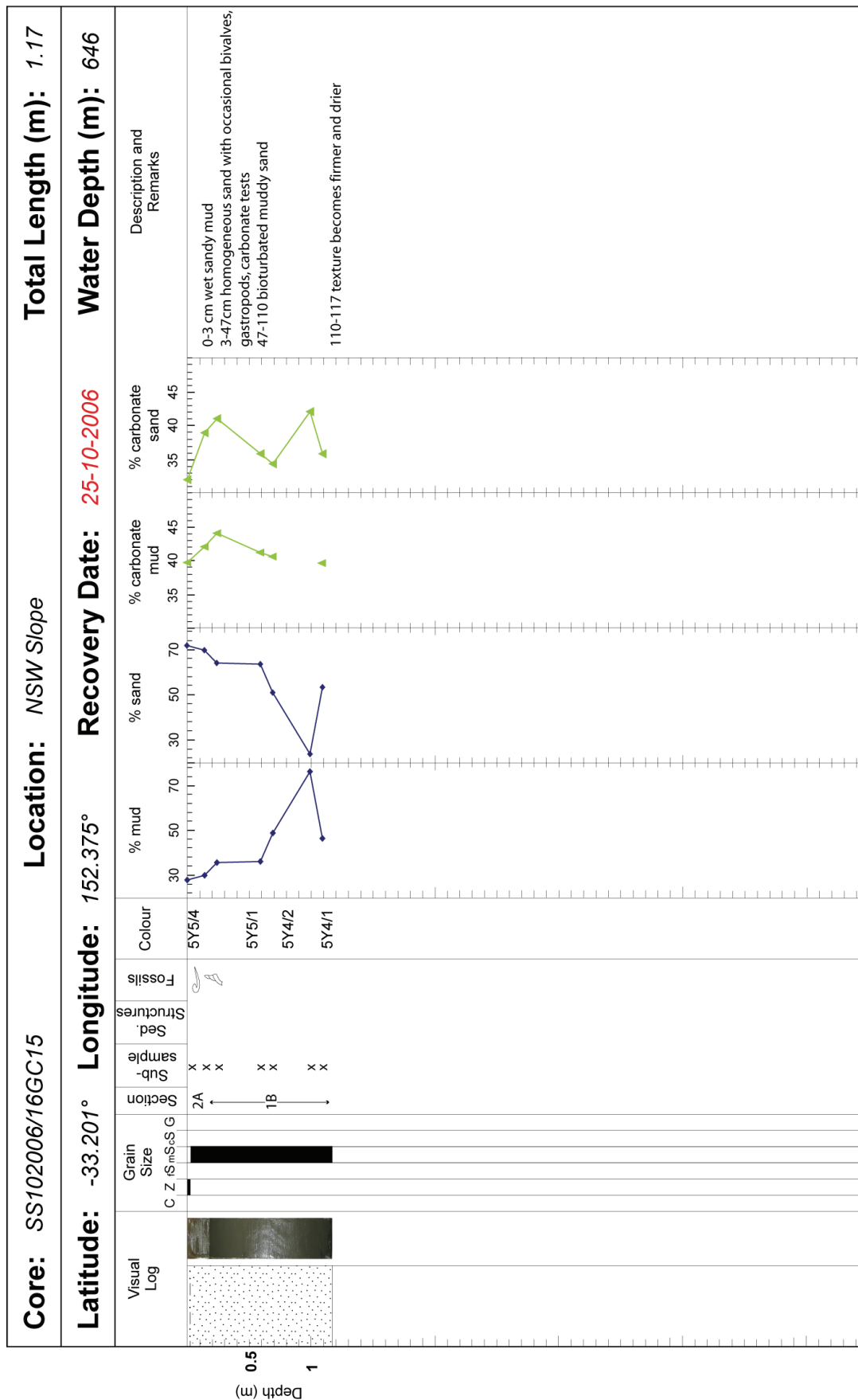












9.4. APPENDIX D: XRD AND PIMA RESULTS

Sample	XRD results (approximate weight %)					PIMA MINERALS (TSG default identification of 2 most abundant mineral groups with diagnostic absorption features in infrared range)		Lab results (weight %)				Density (grams/cubic centimetre)		
	Quartz	Calcite	Aragonite	Halloysite/ Accessory Minerals		Mineral 1	Mineral 2	Gravel	Sand	Mud	CaCO ₃	Porosity	Wet Density	Dry Density
05GC04 400-402cm	33	35	3.7	16	Muscovite, Albite, Sodium Chloride, Orthoclase	Kaolin	Organic Matter	-	-	-	-	38.46	1.46	1.76
05GC04 485-487cm	28	36	4.4	21	Muscovite, Albite, Sodium Chloride, Orthoclase	Kaolin	-	0.12	12.73	87.15	34.4	41.31	1.36	1.62

03GC02 288-290cm	41	28	6	14	Muscovite, Albite, Sodium Chloride	Kaolin	-	0	30.97	69.03	32.1	36.75	1.38	1.61
04GC03 279-281cm	39	30	12	9	Albite, Orthoclase, Sodium Chloride	Carbonate	Kaolin	0	52.82	47.18	40.4	36.76	1.45	1.72
04GC03 394-396cm	41	31	9	8	Muscovite, Albite, Sodium Chloride	Carbonate	Kaolin	0	37.94	62.06	33.1	36.91	1.49	1.79
07GC06 298-300cm	39	25	7	17	Muscovite, Albite, Sodium Chloride	Kaolin	-	0	20.97	79.03	25.2	38.93	1.54	1.89
07GC06 408-410cm	38	22	7	18	Muscovite, Albite, Sodium Chloride, Orthoclase	Carbonate	Kaolin	0	17.63	82.37	22.8	35.26	1.48	1.76
06GC05 448-450cm	35	24	13	11	Muscovite,	Kaolin	-	0.11	24.61	75.28	31.6	35.35	1.49	1.77

					Albite, Sodium Chloride									
10GC09 362-364cm	37	22	4	21	Muscovite, Albite, Sodium Chloride, Orthoclase	Kaolin	-	0	10.71	89.29	17.9	36.26	1.37	1.58
12GC11 298-300cm	30	33	11	11	Muscovite, Albite, Sodium Chloride	Kaolin	-	0	19.95	80.05	32.3	38.68	1.46	1.76
12GC11 408-410cm	41	27	8	10	Muscovite, Albite, Sodium Chloride	Kaolin	-	0	29.21	70.79	25.9	34.82	1.48	1.75
09GC08 241-242cm	40	34	7	12	Albite, Sodium chloride	Carbonate	Kaolin	-	-	-	-	-	-	-
09GC08 292-293cm	40	21	2	22	Albite, Muscovite, Sodium	Kaolin	-	0.00	16.67	83.33	15.9	-	-	-

					chloride,									
09GC08 321-322cm	27	51	3	12	Albite, Sodium Chloride	Kaolin	Carbonate	-	-	-	-	-	-	-
09GC08 377-379cm	23	55	3	12	Albite, Sodium Chloride	Kaolin	Carbonate	0.00	24.53	75.57	43.3	-	-	-

As part of the compositional sediment analysis, infrared absorption spectra were collected for 15 samples using a Portable Infrared Mineral Analyser (PIMA). Infrared analysis has the potential to produce mineralogy information more efficiently than traditional analyses (e.g. XRD/XRF, Carbonate Bomb), but is rarely used on marine samples. Sediment samples collected during this survey provided an opportunity to compare PIMA data with results of a suite of other compositional analyses, and assess the potential of this method to produce quantitative mineral information for marine sediments. Only preliminary results produced in The Spectral Geologist (TSG) software (default identification of 2 most abundant mineral groups) are quoted in this report. More detailed interpretation of spectra and comparison to results of other analyses are in progress.

9.5. APPENDIX E: GEOTECHNICAL DATA

Undertaken by the University Of Sydney School Of Civil Engineering on behalf of Geoscience Australia.

TEST RECORD T659
SHEAR TESTING OF MARINE SEDIMENTS

May 2007

9.5.1. 1. INTRODUCTION

This report contains the results of laboratory testing carried out on samples recovered from offshore NSW as part of geotechnical investigation of submarine slides on the continental shelf. The tests have been carried out by the Centre for Geotechnical Research at the University of Sydney under contract #10002 with the University's Business Liaison Office. Core samples were provided by Geoscience Australia from the sites of submarine slides identified by scanning.

The report contains the results of four anisotropically compressed and sheared undrained (CK_oU) triaxial tests to determine undrained strengths and friction angles relevant to first time slides, and four cyclic shear box tests performed to determine the residual friction angle. The test procedures generally followed the methods outlined by Head (1986).

9.5.2. TEST EQUIPMENT AND PROCEDURE

9.5.3. 2.1 Equipment

The triaxial test equipment is shown in [Appendix 5E.A](#). It consists of a conventional triaxial cell with an internal load cell for accurate measurement of the stress state. The equipment is fully computer controlled. Measurements are made of cell pressure, pore pressure, deviator load, axial displacement and volume change.

9.5.4. 2.2 Procedure

2.2.1 Triaxial Tests

The samples were trimmed to size, approximately 49.5 mm diameter by 110 mm high, and set-up in the triaxial cell. Porous disks were placed at each end to facilitate drainage. An isotropic stress of between 10 and 50 kPa was applied and the specimens allowed to drain and reach equilibrium. The sample was then saturated by raising cell pressure and back pressure together until the back pressure reached 200 kPa. The specimen was then left for at least 24 hours to allow dissolution of any remaining air bubbles.

During the compression stage of the tests the cell pressure was ramped up at a steady rate from 5 to 18 kPa/day. This rate was selected by estimating the coefficient of consolidation from the initial cell pressure application, and then using this in a numerical analysis of one-dimensional consolidation to estimate the rate of stress increase that would ensure the excess pore pressures did not exceed 30 kPa. To enforce one-dimensional conditions (on average) the axial stress was adjusted to maintain equal axial and volumetric strains. When the axial stress had reached the required level the cell pressure was held constant while continuing to maintain equal axial and volume strains. When the rate of straining had reached a slow value an undrained shear test was performed. The drainage taps were closed, and the specimens loaded at a rate of 0.003mm/min.

Some unintentional departures from this procedure occurred, and the influence of these are considered below in interpreting the results.

Shear Box

The core specimens were trimmed to fit into the shear box (87 mm diameter and typically 40 mm thick). The vertical stress was increased in stages to a value of 200 kPa. At this point several fast cycles of shearing were carried out to create a well defined shear plane. The specimen was then subjected to two slow cycles to determine the residual friction angle. The normal stress was then increased to 500 kPa and the series of fast and slow cycles repeated. On completion of the tests the specimen was unloaded and samples for moisture content determination taken from the vicinity of the shear plane.

9.5.5. 2. RESULTS

2.1 Triaxial Tests

Figures 1 to 3 summarise the main outcomes of the triaxial tests. Salient data from these tests are including in Table 1, and individual test responses are shown in Appendix 5E.B. Figure 1 shows the relationship between void ratio and mean effective pressure, p' . In producing this plot a specific gravity of 2.75 was assumed, because this appeared to give the best agreement between volume changes and changes in moisture content during the tests. Values of initial and final moisture contents are given in Table 1. Figure 1 shows that specimen 07GC06 has a higher compressibility than the other three specimens. This specimen also had a significantly lower coefficient of consolidation, indicating that this specimen was more fine-grained than the others. During the compression phase of the test on specimen 07GC06 the ratio of axial strain to volume strain was 1.35, rather than the intended ratio of 1, and this will have resulted in the specimen being closer to failure than in-situ. Further difficulties were encountered with this specimen because of the large strains which resulted in the axial displacement transducer going out of range and computer control being lost when the mean effective stress reached 100 kPa. The test was restarted, but because the deformations were not known precisely the estimated undrained strength and friction angle from this specimen are less reliable.

The kink in the void ratio, mean effective stress response for specimen 10GC09 was a consequence of reducing the rate of stress increase during compression.

An important observation from Figure 1 is that all the specimens are essentially normally consolidated, and show no evidence of past stresses greater than those currently acting in-situ.

Figure 2 shows the stress paths in a plot of deviator stress, q , versus mean effective stress, p' . It was expected that during the compression phase of the tests the ratio of effective radial stress to effective vertical stress (and ratio q/p') would reach a constant value because the ratio of axial to volume strains was kept constant. Apart from specimen 07GC06 this did not occur. This may be a consequence of the rate of loading being too fast. That the

rate was too fast is also suggested by the effective stress paths for specimens 2 to 4. These three specimens all showed considerable ongoing strain when the radial stress was held constant towards the end of the compression stage (this can be seen from the change in slope of the effective stress path). In enforcing the constant strain ratio further, increases in axial and deviator stress occurred. Data from the initial stress application would suggest that most of the ongoing straining is due to creep. The radial stress was held constant for at least 2 days before commencing the undrained shearing stage. Despite the wait, significant creep strains were still occurring when shearing commenced, and these will have influenced the undrained shear responses. Because of the test control algorithm the soil responses during the creep phase were different to those expected in-situ when creep occurs. In-situ the axial stress stays constant, and the radial stress would need to reduce to maintain one-dimensional conditions, and this in turn would lead to unloading and a reduction in creep. The continuing creep also results in further compression which increases the undrained strength, as this is fundamentally a function of the void ratio. A consequence of this behaviour is that the ratio of undrained strength to effective vertical stress (s_u/σ'_v) will increase. It follows that the undrained strength for a given effective vertical stress (depth of burial) should be greater than indicated by the data in this report.

Figure 2 shows that during undrained shearing the effective stress paths move to the left towards an ultimate frictional failure, indicated by the black line in Figure 2. Very little, if any, increase in deviator stress occurs once undrained shearing commences, and the peak undrained strength occurs at very small strains. The ultimate frictional resistance indicated by the black line in Figure 2 corresponds to a ratio q/p' ($= M$) = 1.68. Other specimens had slightly lower values as indicated in Table 1 and Appendix 5E.B. These correspond to effective friction angles in the range from 37° to 41° .

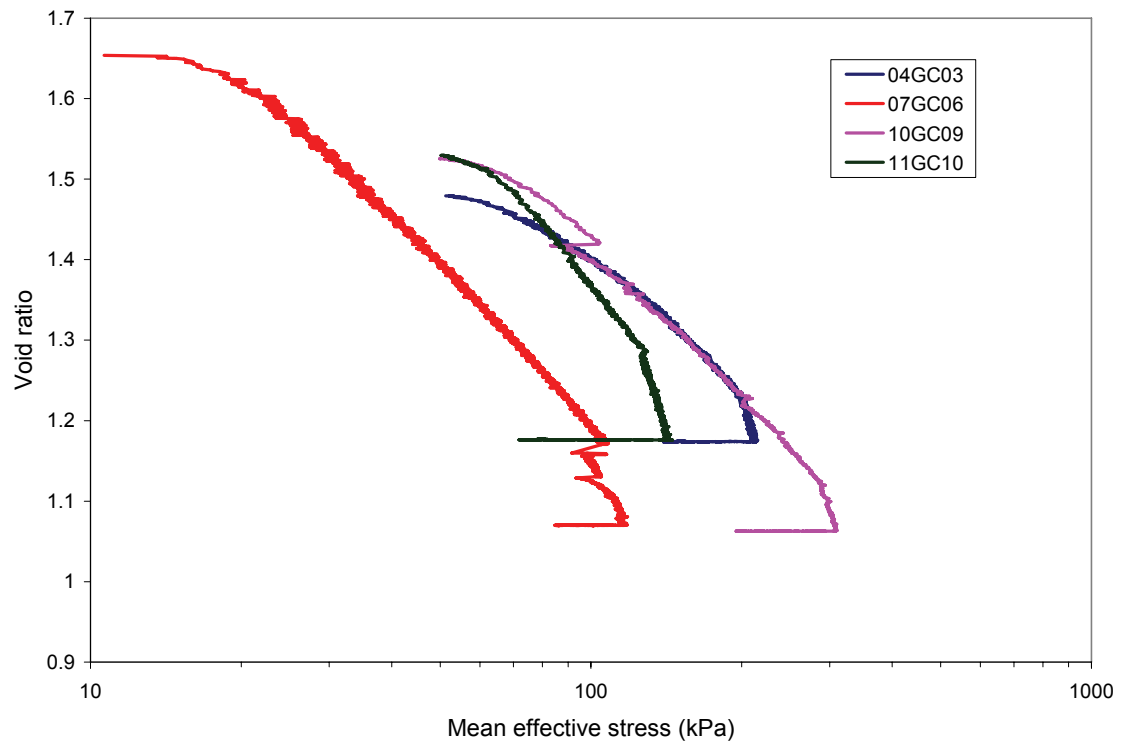


Figure 1: Compression responses (Void ratio, e , versus Mean effective stress, p')

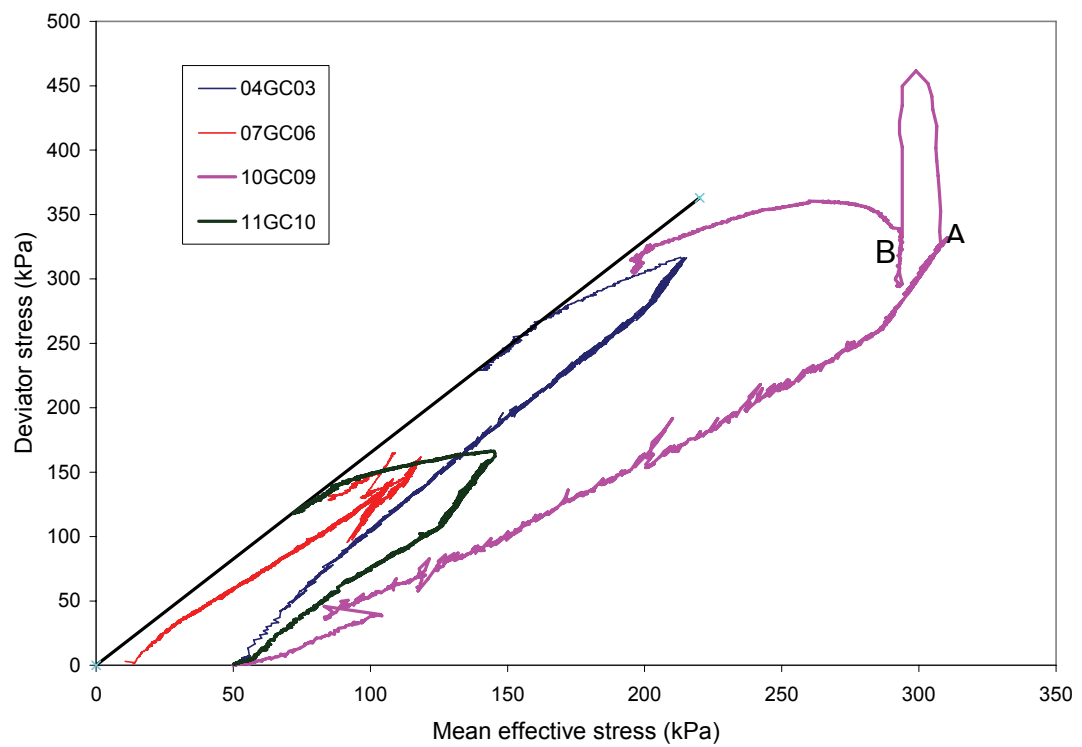


Figure 2: Effective stress paths (Deviator stress, q , versus Mean effective stress, p')

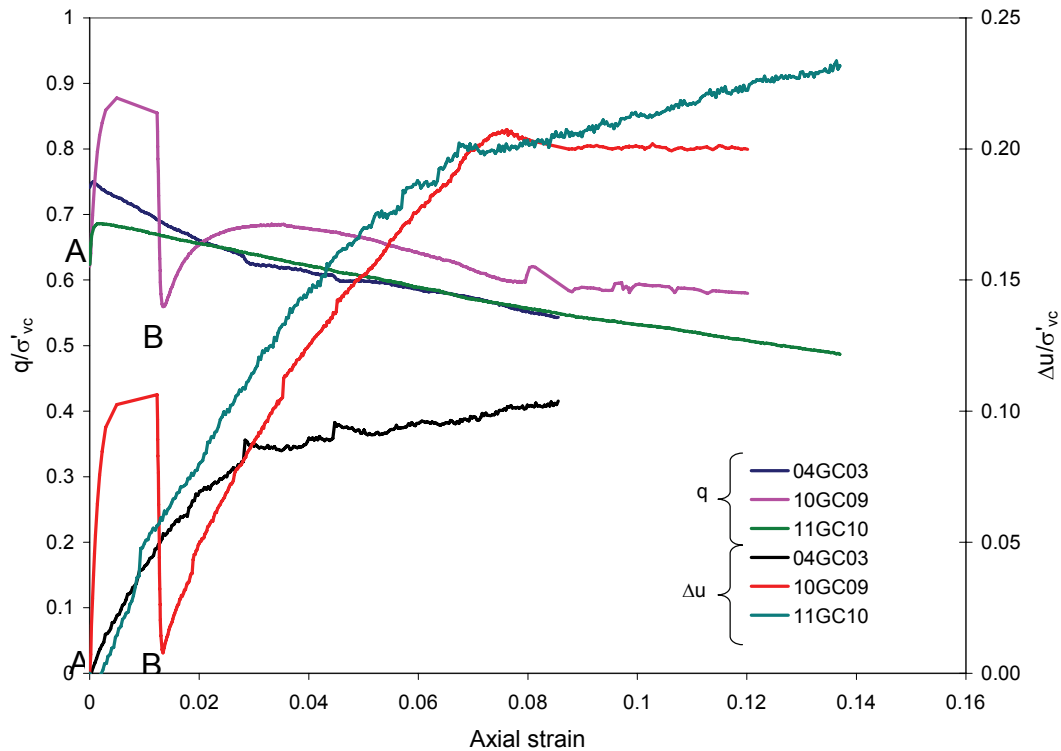


Figure 3: Undrained shear responses

Figure 3 shows that the undrained strengths normalised by the effective vertical stress at the start of shearing, σ'_{vc} , are similar, as would be expected for normally consolidated specimens of similar properties. The higher normalised strength at small strains in test 2 was a consequence of a fast rate of loading that was applied for a few seconds at the start of shearing. During this period of fast loading no excess pore pressures were measured by the pore pressure transducer, which was located externally to the cell. Many studies have shown that the pore pressures are underestimated by external transducers when fast loading rates are used, and to enable the plots to be more reasonable, values of pore pressure have been assumed between points A and B in figures 2 and 3 and in [Figure B2 in Appendix 5E.B](#). Note that this assumed response only affects the pore pressure and mean effective stress; it does not affect the deviator stress (strength).

Table 1: Summary of test data

Specimen Number	Moisture contents (%)		Axial Effective Stress at start of shear, σ'_{vc} (kPa)	Undrained strength, s_u (kPa)	M	ϕ' (°)	ϕ'_r (°)
	Initial	Final					
07GC06	55.1	38.9	200	82.5	1.5	36.9	30.8
10GC09	61.8	38.7	520	225/180	1.6	39.2	33.8
11GC10	59.9	42.8	250	83	1.6	39.2	29.9
04GC03	52.7	42.7	420	155	1.68	41.0	37.3

2.2 Shear Box results

Figure 4 shows a summary of the residual strength measurements for the four specimens. Values of the residual friction angle (assuming $c_r = 0$) are shown in Table 1. Detailed results are shown in Appendix 5E.C. It may be noted that there is little difference between the fast and slow rates of shearing and there is no evidence of any reduction in friction angle with accumulation of displacement. The shear box results indicate significantly lower residual strengths than the ultimate strengths measured in the triaxial tests. However, as there is no evidence of a reduced residual strength for these specimens it is believed that the difference in the numbers is an artefact of the shear box configuration. The interpretation of the shear box requires an assumption about soil behaviour, i.e. that $\phi' = \tan^{-1} (\tau/\sigma)$. There has been some debate about this assumption in the literature, and it is generally observed that the shear box gives slightly lower (safe/conservative) values of friction angle. It may also be noted from Fig. 4 that the residual friction angle appears to increase slightly as the stress level decreases. This may be contributing to the difference between the triaxial and shear box values as the ultimate frictional state is reached in the triaxial tests at lower stress levels than in the shear box tests.

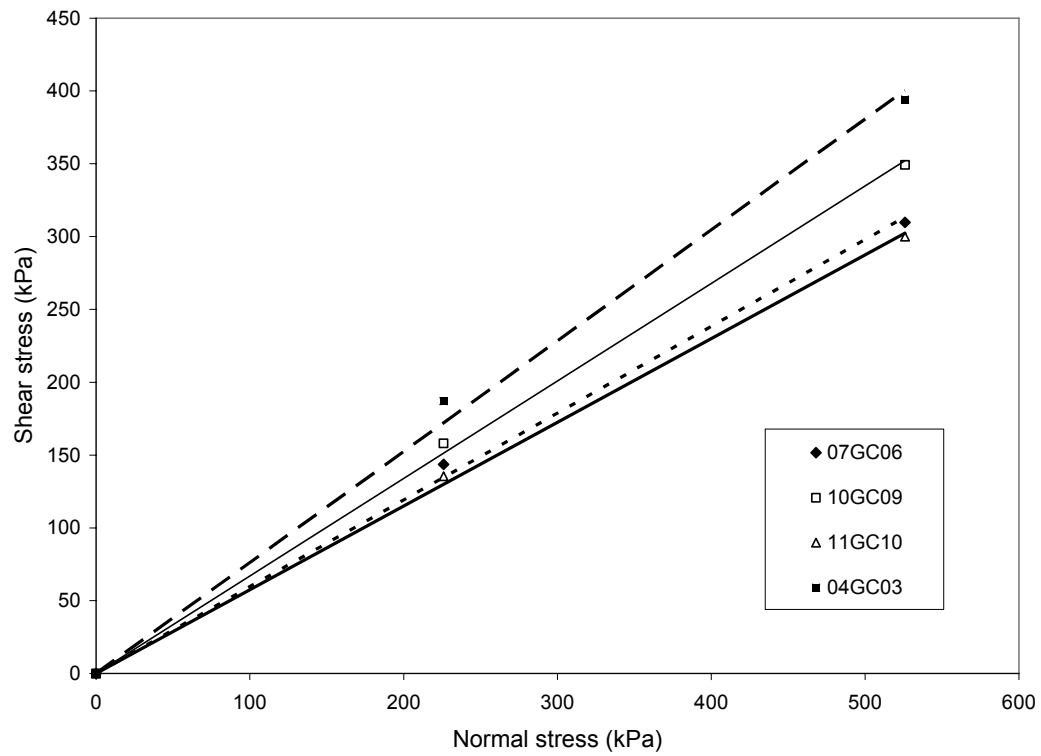
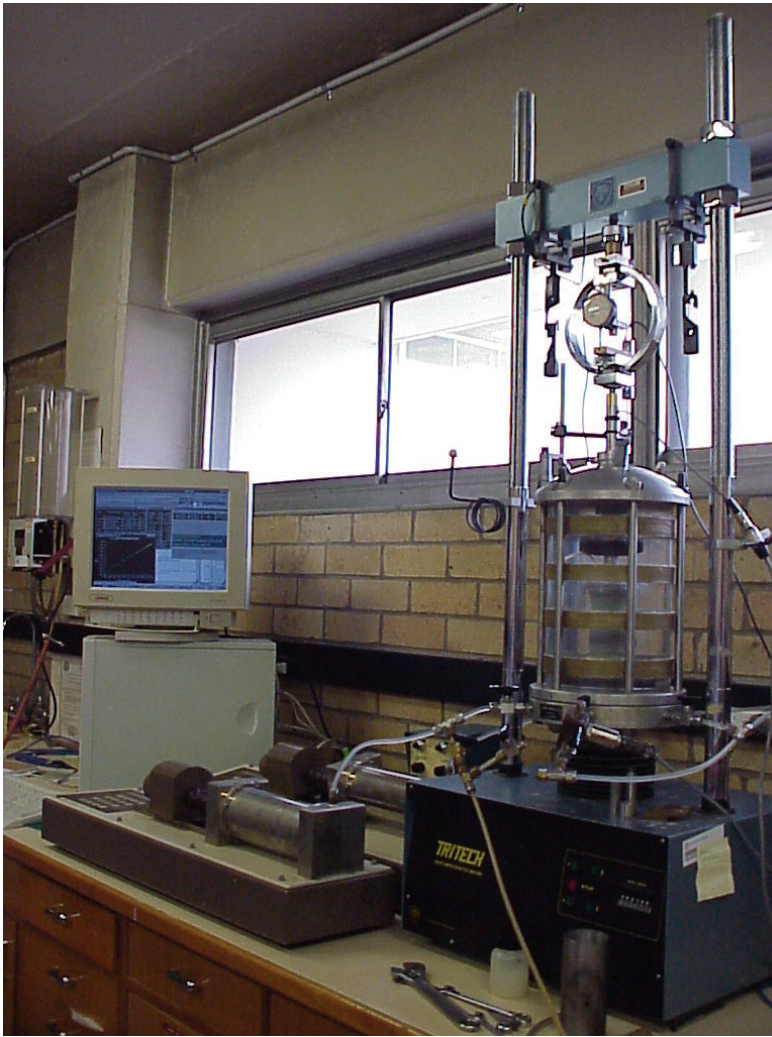


Figure 4 Residual strength envelopes

Head K.H. (1986) Manual of soil laboratory testing, Volume 3, Pentech Press

APPENDIX 5E.A



Photograph of Triaxial Apparatus

APPENDIX 5E.B

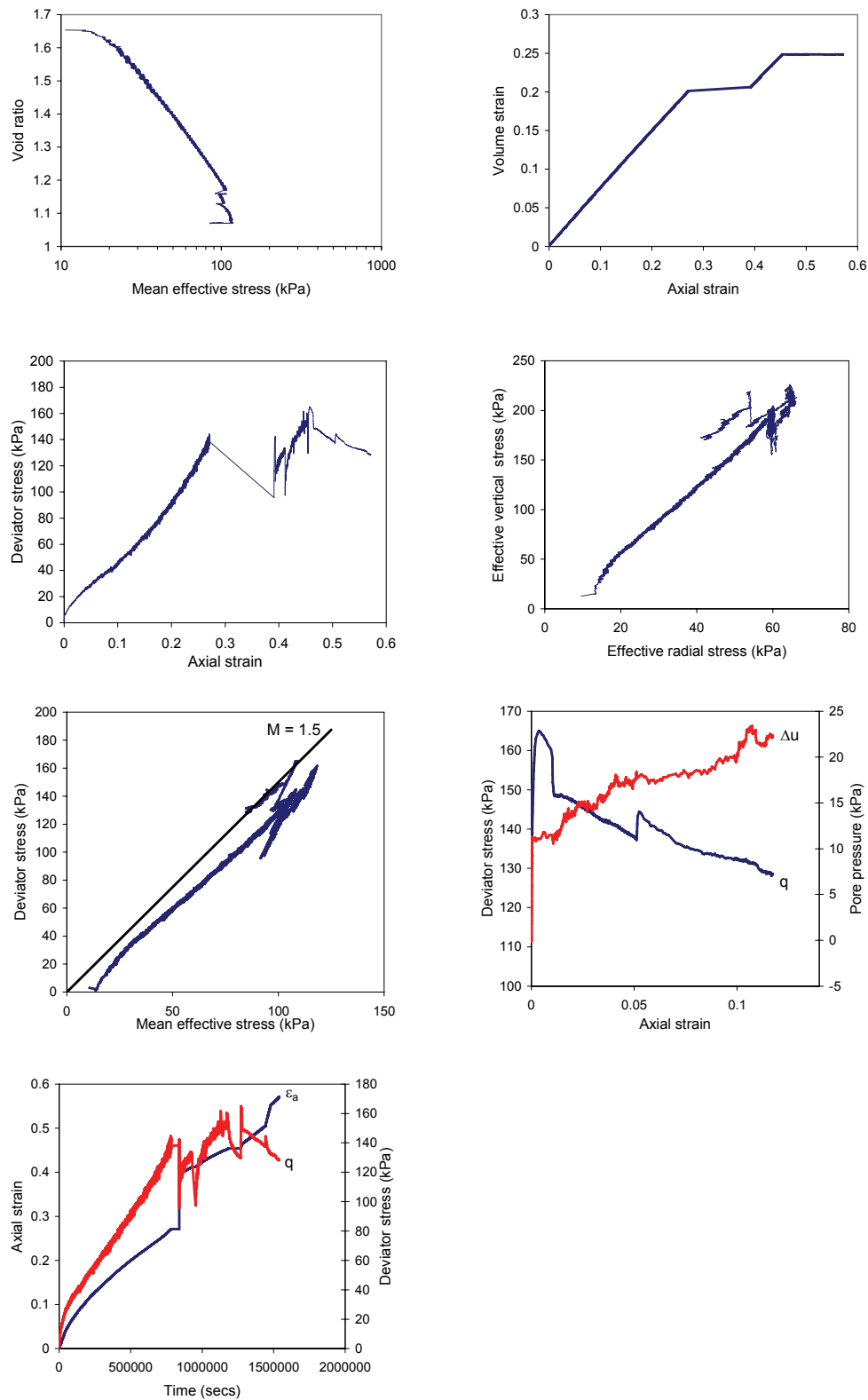


Figure 5E1: Triaxial test results, Specimen 07GC06

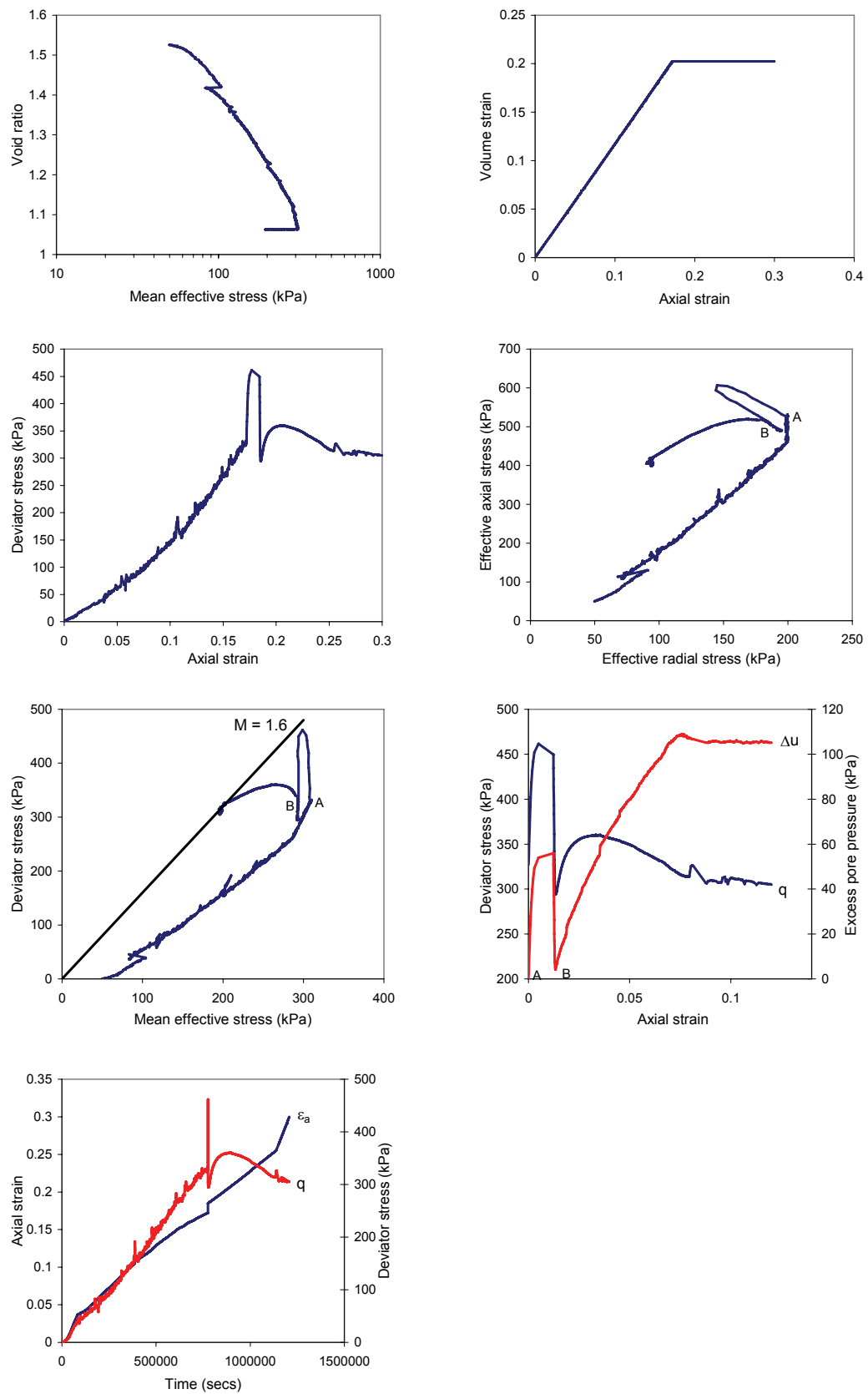


Figure 5E 2: Triaxial results Specimen 10GC09

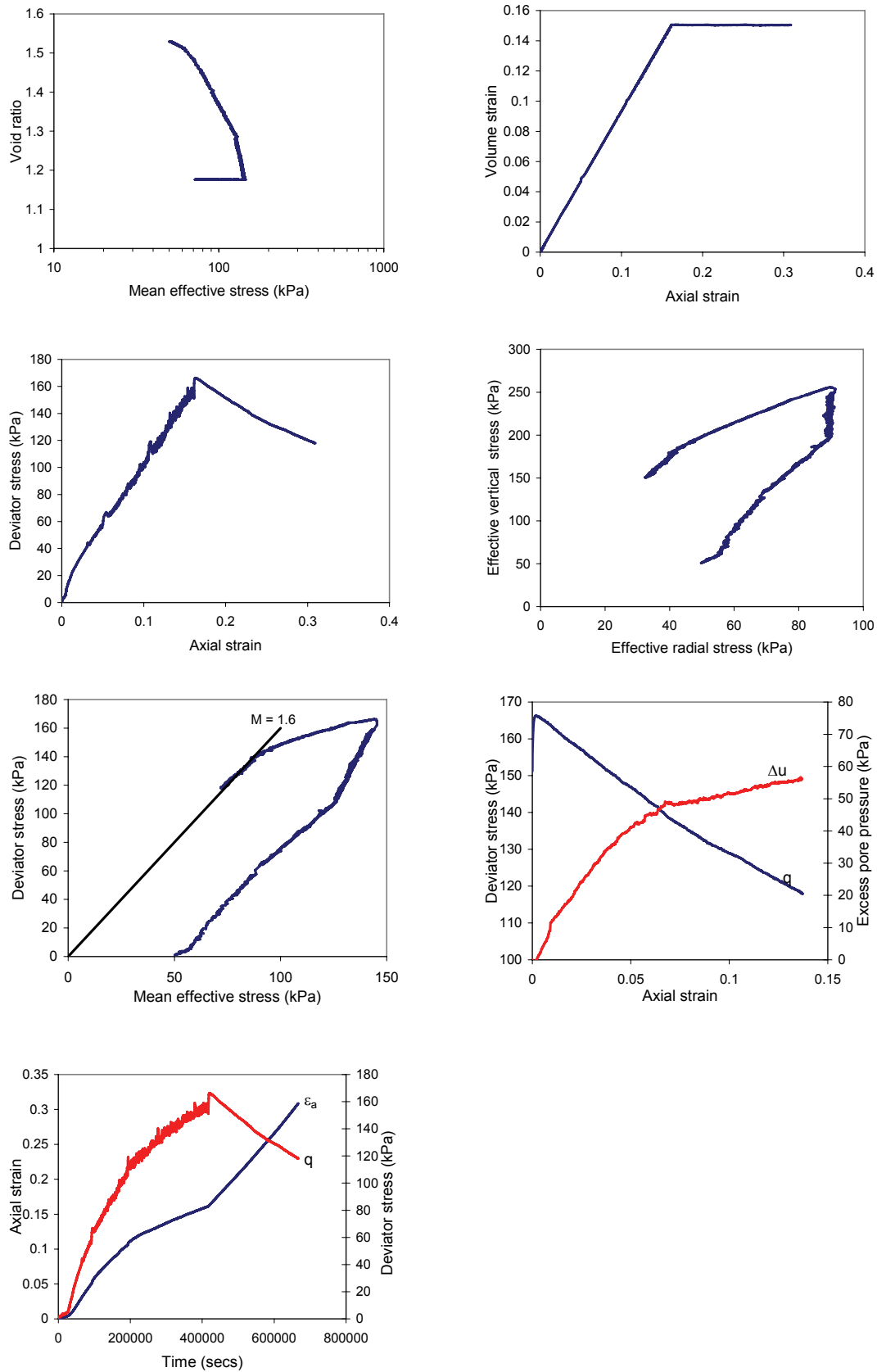


Figure 5E 3: Triaxial test results, Specimen 11GC10

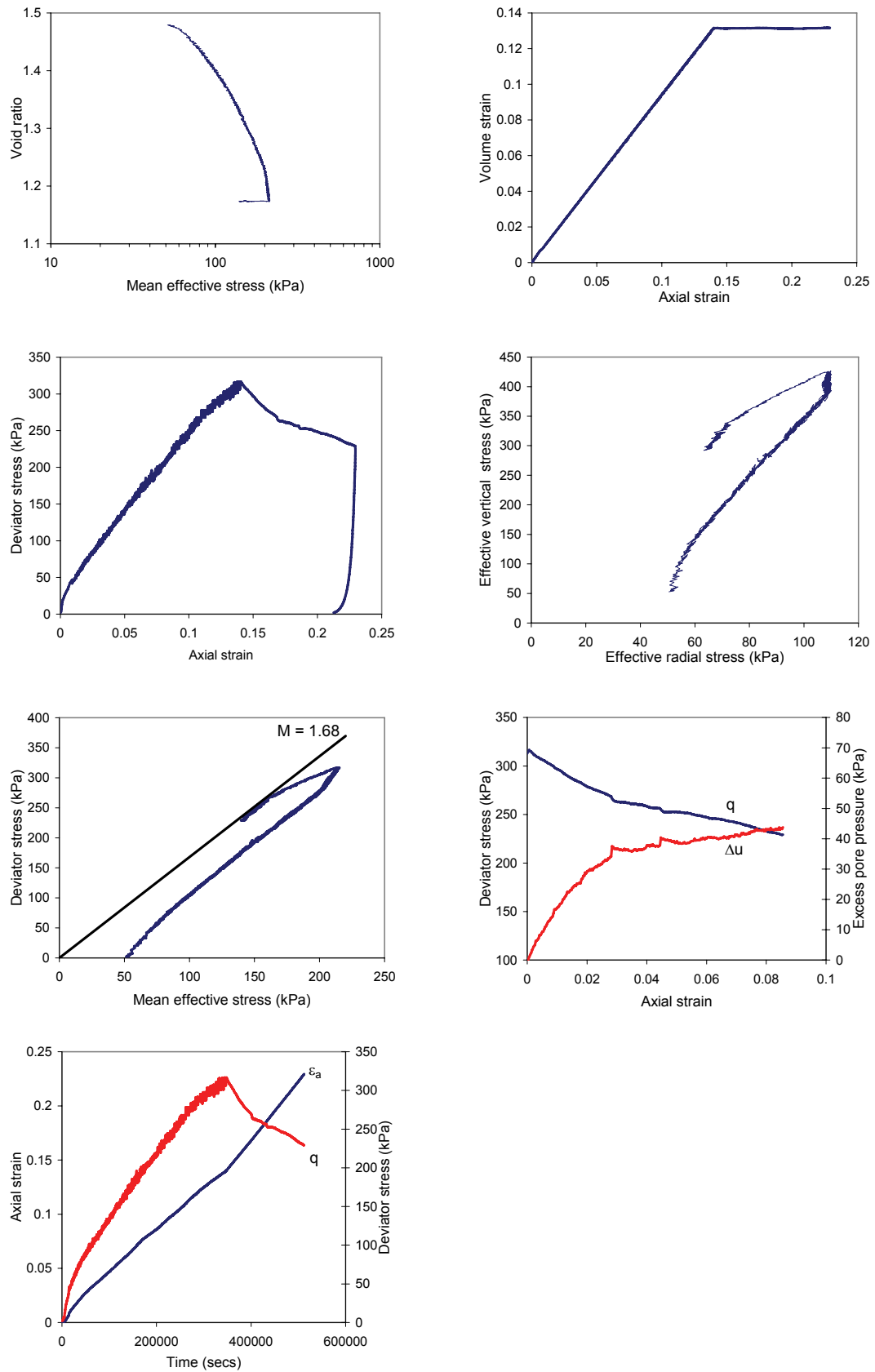
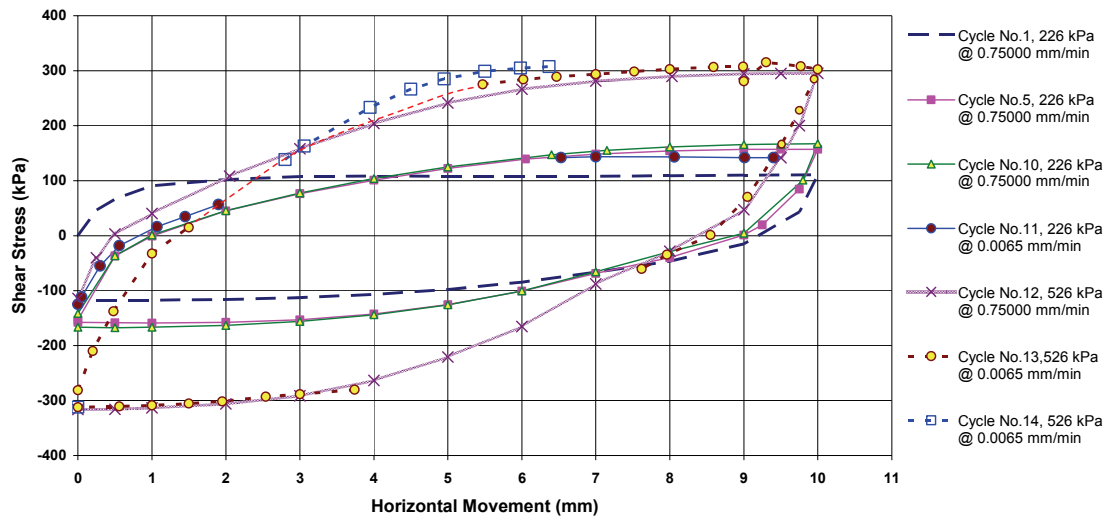


Figure 5E 4: Triaxial test results, Specimen 04GC03

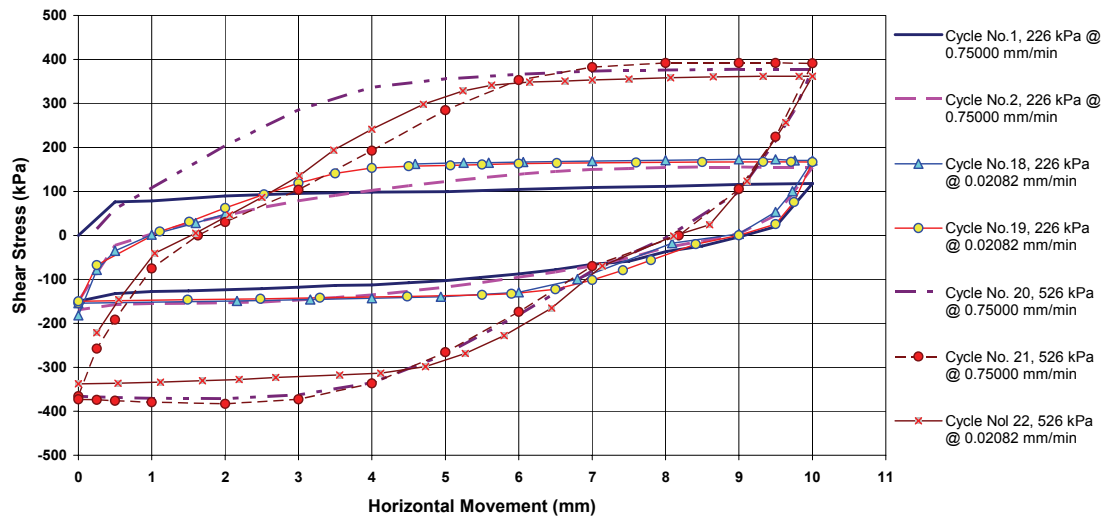
APPENDIX 5.C

SHEAR BOX RESULTS

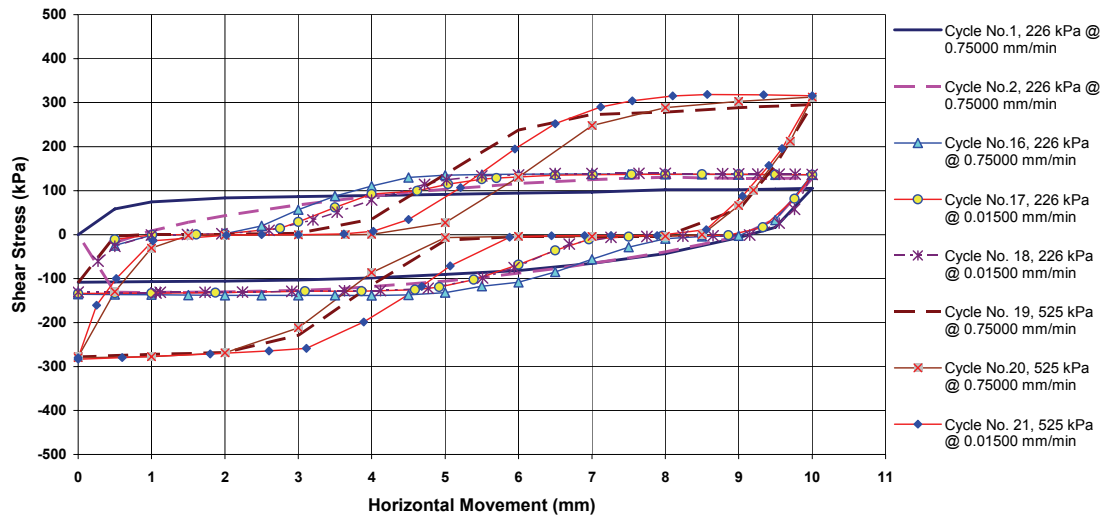
Direct Shearbox Test
T1(Sample 07GC06)



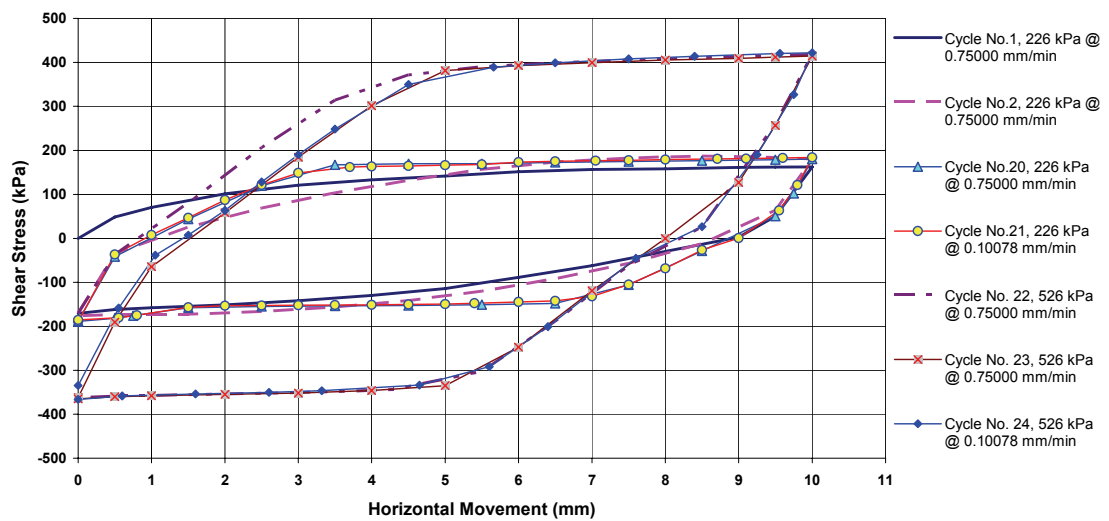
Direct Shearbox Test
T2 (Sample 10GC09)



Direct Shearbox Test T3 (Sample 11GC10)



Direct Shearbox Test T4 (Sample 04GC03)



9.6. APPENDIX F: RADIOMETRIC DATA

Sample Name	Depth	$\delta^{13}\text{C}$ (‰)	Radiocarbon Age	$\delta^{14}\text{C}$ (‰)	$\Delta^{14}\text{C}$ (‰)	Percent Modern	Description	Cal age range	Cal age (BP)	Cal error
SS102006/03GC02 0-2cm	1	1.4	1880 ± 30 BP	-171 ± 2.9	-214.1 ± 2.7	78.59 ± 0.27	forams	1372-1475	1423.5	51.5
SS102006/03GC02 10-11cm	10.5	1.3	3879 ± 30	-353.7 ± 2.3	-387.2 ± 2.2	61.28 ± 0.22	forams	3794-3909	3851.5	57.5
SS102006/03GC02 48-49cm	48.5	1	13438 ± 45	-803.5 ± 1.1	-813.6 ± 1	18.64 ± 0.1	forams	15228-15528	15378	150
SS102006/03GC02 288-289cm	288.5	0.5	47800 ± 1600	-997.3 ± 0.5	-997.4 ± 0.5	0.26 ± 0.05	forams	NA		
SS102006/04GC03 0-1cm	0.5	1.4	2561 ± 30	-238.3 ± 2.6	-278 ± 2.5	72.2 ± 0.25	forams	2183-2293	2238	55
SS102006/04GC03 10-11cm	10.5	1.3	2450 ± 30	-228 ± 2.7	-268 ± 2.5	73.2 ± 0.25	forams	2031-2141	2086	55
SS102006/04GC03 54-55cm	54.5	0.8	8840 ± 35	-651.9 ± 1.5	-669.6 ± 1.4	33.04 ± 0.14	forams	9464-9524	9494	30
SS102006/04GC03 394-395cm	394.5	0.7	40770 ± 690	-993.5 ± 0.6	-993.8 ± 0.5	0.62 ± 0.05	forams	NA		
SS102006/06GC05 9-10cm	9.5	1.4	2448 ± 25	-227.6 ± 2.6	-267.8 ± 2.4	73.22 ± 0.24	forams	2035-2135	2085	50
SS102006/06GC05 54-55cm	54.5	1.4	9264 ± 35	-669 ± 1.5	-686.5 ± 1.4	31.35 ± 0.14	forams	10038-10056	10047	9
SS102006/06GC05 199-200cm	199.5	0.5	17059 ± 60	-874.9 ± 1	-881.2 ± 0.9	11.88 ± 0.09	forams	19594-19675	19634.5	40.5
SS102006/06GC05 448-450cm	449	0.4	24340 ± 120	-949.5 ± 0.7	-952 ± 0.7	4.8 ± 0.07	forams	NA		
SS102006/07GC06 0-1cm	0.5	1.4	1136 ± 25	-90.5 ± 3	-137.8 ± 2.8	86.22 ± 0.28	forams	654-707	680.5	26.5
SS102006/07GC06 14-15cm	14.5	1.6	3590 ± 30	-329.6 ± 2.3	-364.8 ± 2.2	63.52 ± 0.22	forams	3433-3536	3484.5	51.5
SS102006/07GC06 59-60cm	59.5	1.4	9028 ± 35	-659.5 ± 1.5	-677.2 ± 1.4	32.28 ± 0.14	forams	9619-9792	9705.5	86.5
SS102006/07GC06 409-410cm	409.5	0.1	23110 ± 100	-941.2 ± 0.8	-944.1 ± 0.7	5.59 ± 0.07	forams	NA		
SS102006/08GC07 0-1cm	0.5	1.6	3405 ± 30	-314 ± 2.4	-350 ± 2.2	65 ± 0.22	forams	3236-3331	3283.5	47.5
SS102006/08GC07 5-6cm	5.5	1.9	4204 ± 30	-378.7 ± 2.2	-411.5 ± 2.1	58.85 ± 0.21	forams	4237-4360	4298.5	61.5
SS102006/08GC07 15-16cm	15.5	1.2	11336 ± 45	-744.6 ± 1.5	-757.8 ± 1.4	24.22 ± 0.14	forams	12855-12908	12881.5	26.5
SS102006/08GC07 498-500cm	499	1	>50000	-999.2 ± 0.5	-999.3 ± 0.5	0.07 ± 0.05	forams	NA		
SS102006/09GC08 0-1cm	0.5	1.6	1951 ± 30	-177.8 ± 2.9	-221 ± 2.8	77.9 ± 0.28	forams	1438-1545	1491.5	53.5
SS102006/09GC08 32-33cm	32.5	1.4	9498 ± 40	-678.8 ± 1.6	-695.6 ± 1.5	30.44 ± 0.15	forams	10268-10407	10337.5	69.5
SS102006/09GC08 60-61cm	60.5	1	17070 ± 70	-875 ± 1.1	-881.4 ± 1	11.86 ± 0.1	forams	19593-19676	19634.5	41.5
SS102006/09GC08 464-465cm	464.5	0.1	52500 ± 2900	-998.5 ± 0.5	-998.6 ± 0.5	0.14 ± 0.05	forams	NA		

Sample Name	lat	long	water depth	core length (m)	Cal age range (BP)	% mud range	% sand range	Variation in Wet density (gm/cm ³)	% carbonate mud range	% carbonate sand range
GC01	-34.317	151.578	1214	4.5	§	47-82	17-52		21-49	42-69
GC02	-34.461	151.435	1194	3	1359 / 15183	40-81	19-60	0.26	27-54	42-59
GC03	-34.428	151.422	947	4.04	2156 / 45048	43-74	26-57	0.26	28-52	41-67
GC04	-34.378	151.546	1518	5.015	§	65-88	Dec-35	0.15	21-48	41-51
GC05	-32.871	152.753	922	4.65	1995 / 28663	50-90	Oct-50	0.01	Dec-38	40-48
GC06	-32.876	152.751	934	4.31	674 / 27275	53-82	18-47	0.13	20-38	38-45
GC07	-32.92	152.707	828	5.05	3198 / 12820	36-78	22-64	0.06	13-38	22-45
GC08	-33.14	152.621	1424	4.83	1428 / 19794	52-83	17-48	0.14	14-41	33-62
GC09	-33.122	152.599	1329	3.72	§	60-89	Nov-40	0.23	18-40	50.5 - *
GC10	-33.095	152.621	1183	5.32	§	50-88	Dec-50	0.07	18-41	34-51
GC11	-33.109	152.599	1257	4.27	§	71-84	16-29	0.13	24-42	#
GC12	-33.14	152.622	1420	4.6	1499 / 28203	60-91	Sep-40	0.17	17-43	36-60
GC15	-33.201	152.374	648	1.17	§	28-78	22-72	§	32-42	40-44

X = dated sediment

*=single

measurement

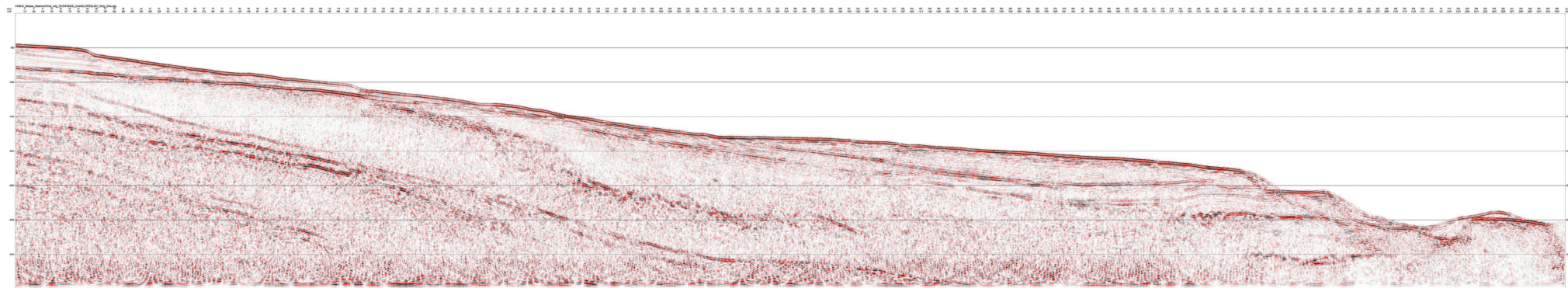
= insufficient

volumes

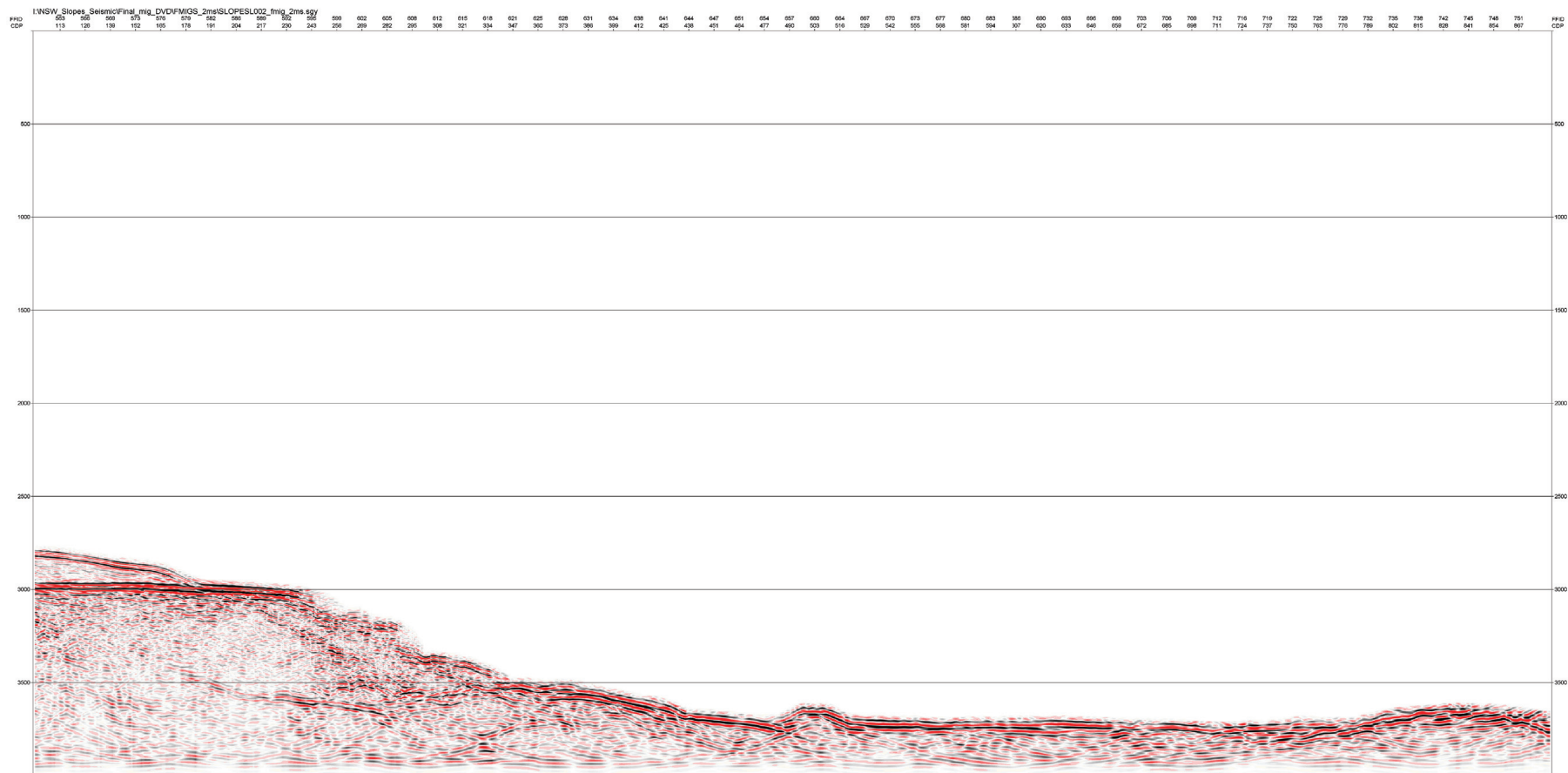
§ = not analysed

9.7. APPENDIX G: SEISMIC DATA

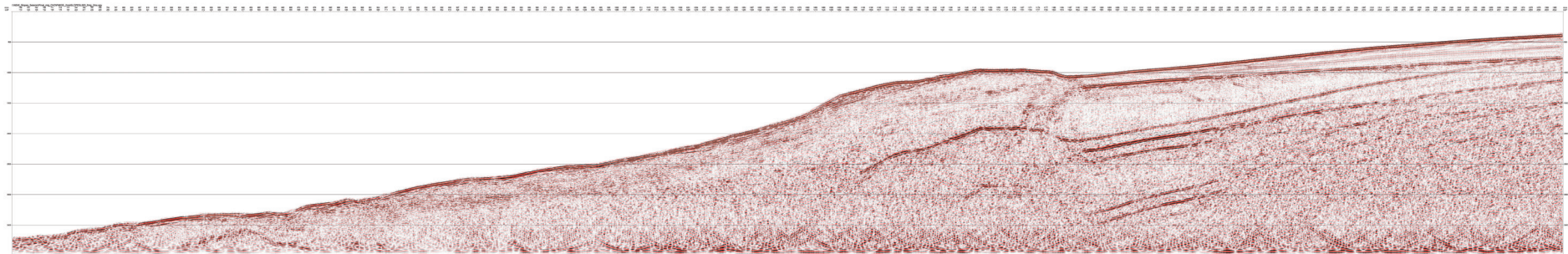
All of the following seismic images can be expanded for detailed scientific interrogation



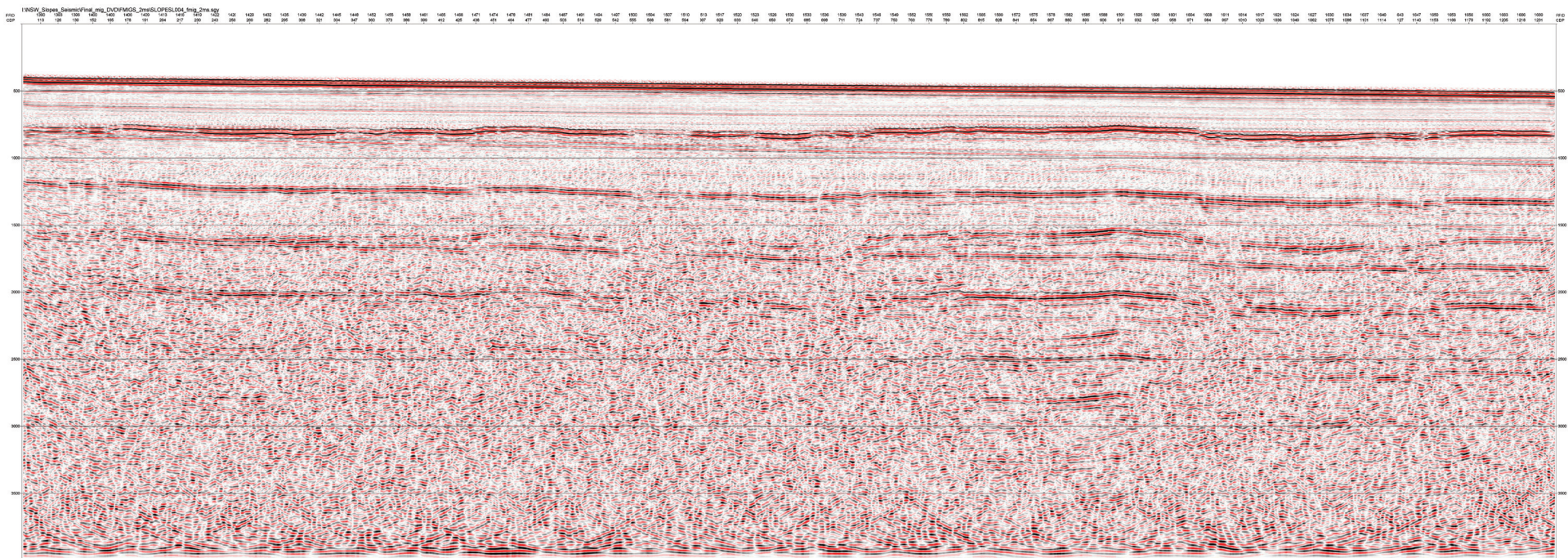
Seismic Line SS 10 2006/01



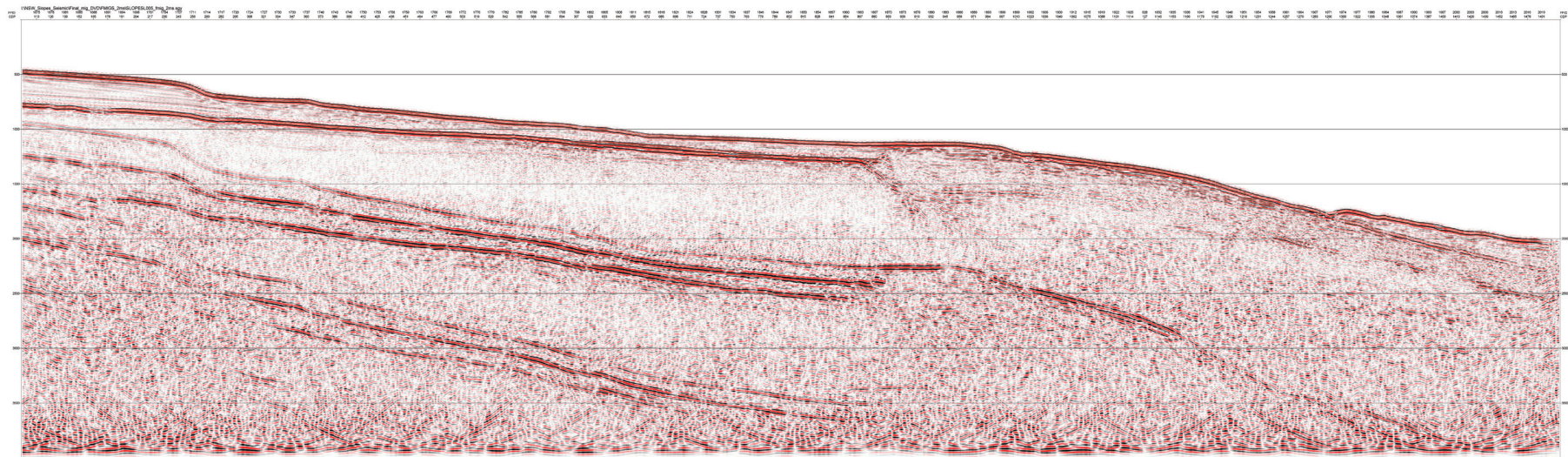
Seismic Line SS 10 2006/02



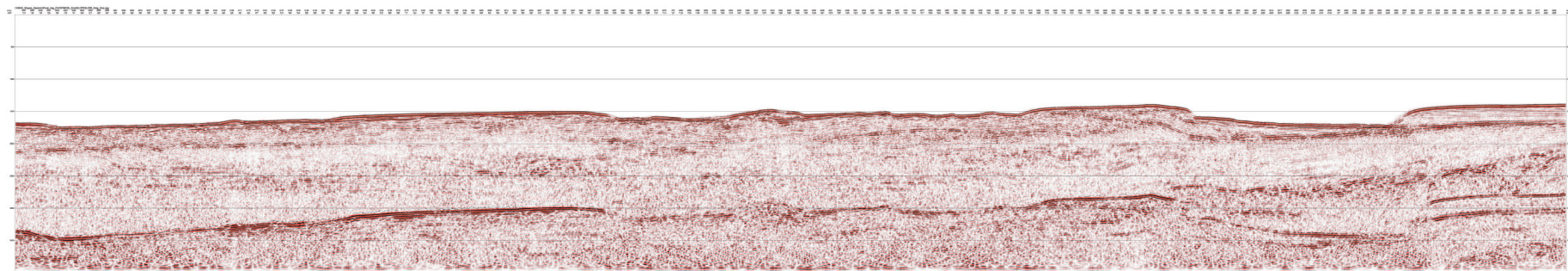
Seismic Line SS 10 2006/03



Seismic Line SS 10 2006/04



Seismic Line SS 10 2006/05



Seismic Line SS 10 2006/06

Instructions for the CD-ROM

NSW Continental Slope Survey - Post Cruise Report

This CD-ROM contains the above-titled Report as Record 2008/14.pdf

View this .pdf document using Adobe Acrobat Reader (click Adobe.txt for information on readers)

Click on: Record 2008/14.pdf to launch the document.